Coupling of mechanical deformation and electromagnetic fields in biological cells

Mehdi Torbati and Kosar Mozaffari

Department of Mechanical Engineering, University of Houston, Houston, Texas 77204, USA

Liping Liu

Department of Mathematics and Mechanical and Aerospace Engineering, Rutgers University, New Jersey 08854, USA

Pradeep Sharma[*]

Departments of Mechanical Engineering, Physics, and the Materials Science and Engineering Program, University of Houston, Houston, Texas 77204, USA

(published 6 May 2022)

The cell, as the most fundamental unit of life, is a microcosm of biology in which the confluence of nearly all aspects of classical physics (mechanics, statistical physics, condensed matter, and electromagnetism) plays out. This leads to a rich and complex emergent behavior that determines the entire gamut of biological functions. Specifically, at the cellular scale, mechanical forces and deformations are inextricably linked to electrical fields (and, to a lesser degree, magnetic fields). This in turn is responsible for phenomenology such as cell-cell communication, morphological evolution, cell fusion, self-assembly, cell fission, magnetoreception, endocytosis, and adhesion, among others. From the viewpoint of biomedicine, cellular response to the combined influence of electrical, magnetic, and mechanical fields has applications in cancer treatment, targeted transfer of medicine, gene therapy, and wound amelioration. As an example of the profound influence of the combined electrical-mechanical coupling, one needs to take cognizance only of the operation of ion channels that form the basis for our sensing system (such as hearing, sight, and tactile sense). The coupled mechanical and electromagnetic behavior of a cell is a highly interdisciplinary endeavor and this review provides a distillation of both the theoretical underpinnings of the subject and the pertinent biological interpretation. The key developments pertaining to this topic are reviewed, a unified mathematical framework that couples nonlinear deformation and electromagnetic behavior as germane for soft biological entities is summarized, gaps in current knowledge are pointed out, and the central issues that are pertinent to future research are commented upon.

CONTENTS

[*] psharma@central.uh.edu

I. INTRODUCTION

Consider the following observations: (i) An electrical field may be used to create transient pores in a cell to precisely inject pertinent genetic material or drug molecules for genetic therapy and personalized medicine (Tsong, 1989; Weaver and Chizmadzhev, 1996; Gehl, 2003; Kar et al., 2018). (ii) Some animals have such a sophisticated ability to detect magnetic fields (Blakemore, 1975; Lohmann, 1991; Wu and David Dickman, 2012; O'Neill, 2013) that they not only can infer north-south directionality (Johnsen and Lohmann, 2005b; Wiltschko and Wiltschko, 2005; Wiltschko, 2012) but also possess a "low-resolution Global Positioning System" that allows them to ascertain their actual location (Wiltschko and Wiltschko, 1972, 2003; Lohmann and Lohmann, 2006; Lohmann, Lohmann, and Putman, 2007; Lohmann, 2010). (iii) The hair cells in the mammalian auditory system use a complex electromechanical transduction mechanism that permits (in humans) a frequency discrimination of 1/30th of a piano semitone, an auditory range of 3 orders of magnitude, and the capability of handling millionfold variations in sound amplitude (Martin and Hudspeth, 2001; Deng, Liu, and Sharma, 2014a; Hudspeth, 2014; Deng et al., 2019). These three observations are just a few of many that underscore the significance of the combined effects of deformation and electromagnetic fields on biological cells and the implications of these effects.

Figure 1 graphically highlights much of the phenomenology as well as applications that relate to the central theme of this review. It is instructive to examine some of these applications in more detail. One of the defining physical characteristics of a cell is its extreme mechanical "softness," i.e., its propensity to mechanically deform. This necessarily implies that even modest electrical fields are able to induce pronounced mechanical forces on the cell and the subcellular structures. In other words, deformation and/or mechanical forces are inextricably linked with electrical field effects. A cell exposed to an electrical field therefore can exhibit a rich spectrum of morphological changes that have been well documented in experiments (Dimova et al., 2009). It is worthwhile to make a special mention of the cell membrane, which is complicit in several interesting aspects of cellular reaction to electrical and magnetic fields. The typical cell membrane is just a few nanometers thick and consists primarily of phospholipid molecules and embedded proteins. The membrane is dielectric in nature and is the envelope through which cells and organelles interact with their environment. In particular, cellular membranes serve as the

"gatekeepers" for the cells and vesicles and, through ion channels, facilitate the transport of chemicals, mechanical and electrical signaling, transduction, and adhesion. Imposed electrical fields, due to the so-called Maxwell stress effect or electrostriction,[1] can cause thinning of the membrane and consequently generate mechanical tension in the plane of the cell membrane. The in-plane tension can potentially impact the operation of ion channels, although this notion is still rather speculative (Gullingsrud and Schulten, 2004; Reeves et al., 2008; Schmidt and MacKinnon, 2008). Likewise, the bending of membranes can lead to the generation of electrical fields due to a phenomenon called *flexoelectricity*, which has been speculated to cause [in addition to impacting the operation of ion channels (Petrov et al., 1993; Petrov, 2002)] dynamical instabilities in the oscillation of hair cells, which play a critical role in the hearing mechanism (Deng et al., 2019).

While modest exogenous electric fields will merely deform the cell as a whole and cause thinning of the membrane, increased intensity can lead to a form of instability that opens up pores in the membrane structure (Gehl, 2003). This phenomenon of *electroporation*, which was alluded to earlier, is of interest from a fundamental science viewpoint due to its status as an essential intermediate step in biological processes such as fusion. Following the formation of nanoscale pores in the cell membrane, depending on the precise nature of the applied electric field, the cell either can survive by resealing the pores (reversible electroporation) or can fail to recover its homeostasis (irreversible electroporation). In particular, reversible electroporation may be used to transport chemical species into the cell (Tsong, 1989; Gothelf, Mir, and Gehl, 2003; Kar et al., 2018), while irreversible electroporation has found applications in cancer cell treatment (Lee, Thai, and Kee, 2010; Thomson, 2010). If electroporation is simultaneously exercised on two adjoining cells, short intense electrical pulses may catalyze cell fusion (*electrofusion*) (Zimmermann, 1982). Cell fusion is a critical step in a number of biological processes, such as embryogenesis (Oren-Suissa and Podbilewicz, 2007), the differentiation of muscle cells (Sampath, Sampath, and Millay, 2018), therapy for organ transplantation (Sullivan and Eggan, 2006), and other processes (Harris, 1970). The key electromechanical reaction pathways that lead to electrofusion are rich and still a topic of active research. We remark as an aside that cell electroporation and electrofusion triggered by lightning has been suggested to be instrumental in the gene transfer of prokaryotes during evolution (Kotnik, 2013). Electromechanics also appears to regulate volume in a class of tissue cells, which is critical for phenomena such as cell growth (Yellin et al., 2018).

Although the theoretical treatment of magnetic effects has significant parallels with the handling of electrical fields, the effect of magnetic fields on biological cells is more subtle and arguably more controversial. The key difference between the two, despite a close mathematical similarity, lies in the fact

---

[1]The Maxwell stress effect and electrostriction are two physically distinct electromechanical mechanisms, although they are mathematically identical. We discuss the distinction in Sec. II, but for the purpose of discussion there is no loss of generality in using them interchangeably.
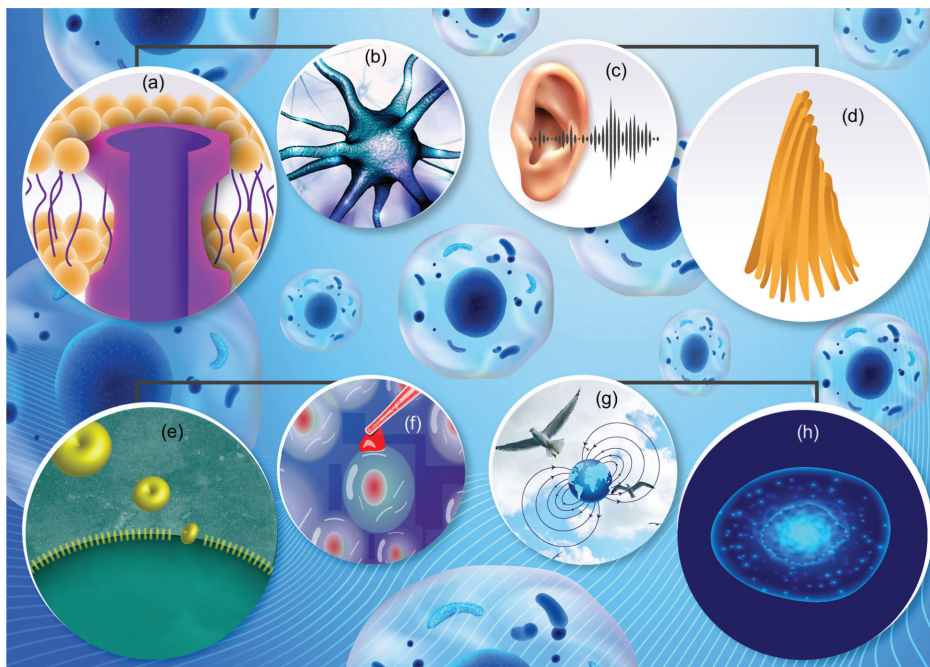
FIG. 1.   The combined effect of deformation and electro-magnetic fields on biological cells manifests in myriad ways: (a) operation of ion channels, (b) impact on our nervous system, (c) the hearing mechanism, (d) dynamics of auditory hair cells, (e) cellular electroporation, (f) its applications in cell fusion and drug delivery, and (g),(h) magnetoreception in selected animals.

that all materials have a dielectric permittivity that is different from the vacuum (and hence are polarizable). In sharp contrast, with the exception of a few, most natural materials have a magnetic permeability that is the same as the vacuum (and hence are not magnetizable). In other words, most materials are transparent to magnetic fields and mechanisms analogous to the Maxwell stress effect or electrostriction (namely, *magnetostriction*) tend to be nonexistent or negligible. That said, the magnetic field can couple with deformation if the intercellular region is filled with a ferrofluid and/or is in the presence of ferrite particles that may appreciably enhance the magnetic permeability of the cell or its membrane. The origins of the well-studied phenomenon of magnetoreception in animals [see Johnsen and Lohmann (2005b) and references therein], which is tantalizing and has recently also been speculated about in humans (Wang *et al.*, 2019), remains an enduring mystery and a somewhat controversial subject. Accordingly, in this review the nuanced discussion of magnetic field coupling with deformation and its interaction with biological cells is discussed separately from that of electric fields.

An understanding of the coupled effects of mechanical deformation and electromagnetic effects on biological cells requires a highly multidisciplinary approach: applied mathematics, biology, nearly all of classical physics,[2] and continuum mechanics. Therein lies both the richness and the complexity

of the subject. In particular, when one is contending with the soft mechanical nature of the cells and cell membranes, nonlinear continuum mechanics must be invoked. Large deformations therefore also require being cognizant of instabilities and bifurcations that are exhibited by cellular structures. A single review cannot be simultaneously rigorous and comprehensive enough to do justice to the complex subject matter discussed here. Our aspirations are therefore modest. We target the uniqueness of our review at an emphasis on a physics-based understanding of the subject matter predicated on a unifying theoretical treatment that attempts to tie the various subtopics to a single setting. In addition, we guide the reader, using simple (sometimes even toy) examples, to the basics of each subtopic and then in that context present the state of the art in the pertinent literature. We do not focus on experimental methods and details of the extensive experiments conducted on the theme of our review. We invoke the key experimental findings selectively when, aided by the relevant theoretical underpinning, the results enhance our understanding of a particular phenomenon. This is not to imply that we cede less importance to experiments, rather that we have limited the scope of our review to a physics-based interpretation as opposed to pure phenomenology. To elaborate on the scope of the review, it is germane to mention that modeling of the combined deformation and electromagnetic effects may proceed on several fronts: classical molecular dynamics, Monte Carlo, coarse-grained atomistic simulations, or a field theoretic partial differential equation–based approach, among many other variations thereof. Consistent with our earlier stated goals, we are agnostic to the methodology *per se* and emphasize the approach that best facilitates the development of intuition

---

[2]Although we do not discuss the role of quantum mechanics here, the intersection of quantum effects in a biological context is a rapidly evolving field; see Lambert *et al.* (2013), Marais *et al.* (2018), McFadden and Al-Khalili (2018), Cao *et al.* (2020), and references therein.

about the subject matter. Accordingly, simple analytical models and continuum theories are overemphasized.

Given the breadth of the topic of this review, we must understandably omit some topics. The electrophoretic response of biological cells (Mehrishi and Bauer, 2002), defined as their motion relative to the solution due to the effect of a spatially uniform electric field, provides information about the electrical and mechanical properties of the cell surface (Mehrishi and Bauer, 2002; Kremser, Blaas, and Kenndler, 2004) and also has applications in cell motility (Ross, 2017). The technique has also been implemented for cell separation. However, owing to the complexity of the basic science behind the technique from a biological and physical point of view, it is used mostly to separate biomolecules rather than cells (Bhagat *et al.*, 2010). Indeed, the electrophoretic response of biomolecules has gained much interest due its application in DNA separation (Carle, Frank, and Olson, 1986; Kaji *et al.*, 2004) and detecting protein–nucleic acid interactions (Hellman and Fried, 2007). Since electrophoresis is relatively less relevant in cells, we exclude this topic, although we discuss *dielectrophoresis* in detail. Exposure of a biological cell to electromagnetic fields can affect not only the cell in its entirety and its lipid membrane but also the subcellular organelles and the biomolecules. For instance, it has been shown that an electric field can manipulate the microtubules (Stracke *et al.*, 2002; Jia *et al.*, 2004; Van den *et al.*, 2006; Chafai *et al.*, 2019) and actin filaments (Riveline *et al.*, 1998) of the cytoskeleton, which are the main regulators of the shape and structure of biological cells. It has also been suggested that the proteins can undergo conformational changes under the effect of an electromagnetic field (Laurence *et al.*, 2000; Mancinelli *et al.*, 2004; English and Mooney, 2007; English, Solomentsev, and O'Brien, 2009). Similar effects can occur for other kinds of biomolecules, such as enzymes (Zhao and Yang, 2010), peptides (Toschi *et al.*, 2009; Todorova *et al.*, 2016; Liang, Cheng, and Wang, 2018), and DNA molecules (Heng *et al.*, 2005). These effects are beyond the scope of this review. Further, for the majority of the phenomena discussed in this review, there are molecular-level and electrochemical descriptions that may provide additional insights into the underlying mechanisms. An example of such a description is electroporation, where a lipid membrane is exposed to microsecond and millisecond pulsed electric fields. Evidence indicates that exposure of a lipid membrane to these pulses results in the generation of reactive oxygen species and induces oxidative damage of unsaturated lipids that are correlated with membrane permeability (Gabriel and Teissie, 1994; Boonnoy *et al.*, 2015). Molecular dynamics simulations suggest that during electroporation the pulsed electric field, in addition to increasing membrane permeability, can affect membrane proteins and create conductive pores in the voltage-sensor domains of voltage-gated ion channels (Rems *et al.*, 2020), which serve as a gating mechanism of ion channels where the electric field may affect the conformational change of the protein structure of the channel. Evidently, this mechanism is extremely sensitive to the *p*H level of the extracellular medium and acidification reduces the magnitude of the ion-channel current (Trapani and Korn, 2003). The solution *p*H itself is a major contributor to the behavior of biological processes that involve lipid membranes. The *p*H levels of extracellular and intracellular fluids are ∼7.4 and ∼7, respectively. However, biological membranes can be exposed to environments with different *p*H values that for apical membranes of gastric surface mucus cells in a mammalian stomach can be as low as < 1 to 6 and still keep their integrity (Barreto and Lichtenberger, 1992). This has inspired researchers to investigate the interaction between biological membranes and hydroxide ions and protons to understand mechanisms that allow cells to maintain their structures in such environments. These studies include the effect of change in the *p*H level on the lateral phase separation (Smaby, Muderhwa, and Brockman, 1994; Furuike *et al.*, 1999), membrane interfacial tension (Harlos, Stümpel, and Eibl, 1979; Petelska and Figaszewski, 2002), ionic penetration to nanopores (Buyukdagli, Manghi, and Palmeri, 2011), and membrane mechanics and electrostatics (Zhou and Raphael, 2007). We deliberately avoid delving into more details about the previously mentioned effects indicated, primarily due to the limitation of continuum theories in describing the complexity of intermolecular interactions. For further information, see Kotnik *et al.* (2019) and related works.

While it is not easily possible to use simple theoretical methods and continuum theories to provide molecular-level descriptions of biological processes such as the gating mechanism of ion channels and lipid-protein interactions, there are other microscopic-level computational approaches that can be employed. A popular and increasingly important approach to interrogating biophysical phenomena is via atomistic simulations. Indeed, atomistic methods (in the form of coarse-grained molecular dynamics, Monte Carlo, or all-atom calculations) have been used in nearly all the topics that we cover in this review, electroporation (Böckmann *et al.*, 2008; Delemotte and Tarek, 2012; Kotnik *et al.*, 2019), ion transport (Gurtovenko and Vattulainen, 2005; Peter and Hummer, 2005), and gating mechanisms in ion channels (Maffeo *et al.*, 2012; Flood *et al.*, 2019), among others. Despite the large number of studies on ion channels using molecular dynamics simulations, there are several limitations that relate to the availability of an atomic-resolution structure of the ion channel, the development of an accurate force field, and the computational limitation inherent in molecular dynamics approaches to handling large size scales and long timescales that are relevant to biophysical phenomena. The insights that have been recorded in works on atomistic simulations can be important, but given our stated goals we cite only a few such works and only when warranted by the context.

This review is organized as follows. In Sec. II, we present a unified theoretical framework that allows a facile inclusion of electrical fields and nonlinear deformation in a single variational setting and permits the identification of the key electromechanical coupling mechanisms relevant for soft and biological matter. Specifically, we also outline how the theories typically used in the biophysical literature (such as the Helfrich formulation of membranes) follow from the three-dimensional equations of electricity when specialized to slender (thin) objects. Our exposition also allows for an easy extension in the subsequent sections, where magnetic effects are discussed. Section II is an important starting point for the
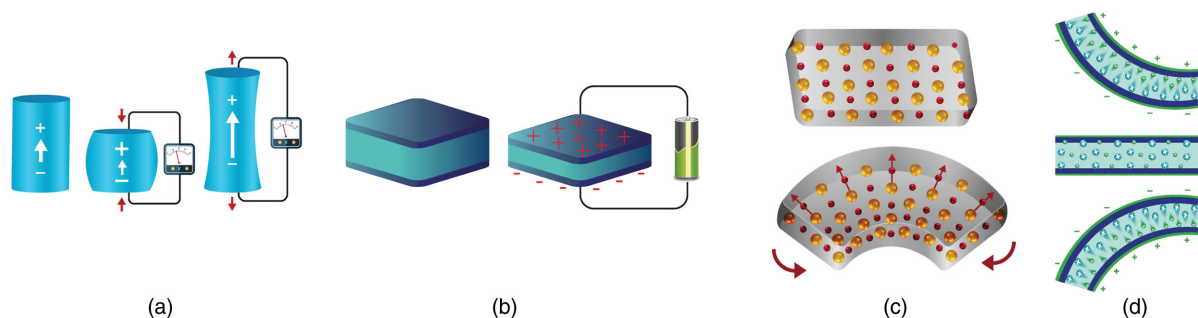
FIG. 2.   Various mechanisms of electromechanical coupling. (a) Piezoelectricity. A direct linear coupling between uniform mechanical strain (or stress) and electrical field (or polarization) usually present only in certain crystalline dielectrics that lack centrosymmetry. (b) Maxwell stress or electrostriction. A universal phenomenon present in all materials that refers to the deformation due to the electrostatic forces developed on the opposing electrodes under the application of an electric field. (c) Flexoelectricity. A universal phenomenon present in all dielectrics that refers to the notion that nonuniform deformation (such as bending) can induce electrical fields in any material by a rearrangement of atoms and consequently charge distribution (even those that are nominally nonpiezoelectric). (d) Ionic diffusion. Under the action of an electrical field, ions preferentially migrate toward one of the electrodes, thus causing a time-dependent deformation. Conversely, mechanical stresses can alter the electrochemical potential and thus provide the driving force for diffusion.

conceptual understanding of the key equations underpinning the relevant phenomena that follow in later sections. In Sec. III, we present the motion of cells under electrical fields. In Sec. IV, we discuss deformation of cells, specifically the behavior of lipid membranes under electrical fields, and examine phenomena such as electrodeformation, electroporation, and electrofusion. Arguably one of the most well-documented fields of study has been the effect of electrical fields on ion channels; this topic is discussed in Sec. V along with the ramifications of voltage sensing in lipid membranes. In particular, we also present a case study illustrating how deformation coupling with electrical fields and ion channels can impact a sensory mechanism (hearing). As alluded to earlier, although magnetic fields can be mathematically treated in a manner similar to electrical fields, there are subtle differences that justify a separate section (Sec. VI) where we present both the mathematical framework necessary to understand magnetic coupling with cell deformation and the its implications, particularly the phenomenon of magneto-reception. We conclude in Sec. VII, where we highlight topics that defy the ready classification inherent in Sec. VI, mention those that are inadequately covered, and suggest topics that the interested reader may consider for further study.

II. THEORY OF ELECTRIC-FIELD-DEFORMATION INTERACTION IN CELLS

A. Mechanisms for electromechanical coupling

The mechanisms that mediate coupling between mechanical deformation and electrical fields could be one of the following (Fig. 2): (i) piezoelectricity, (ii) Maxwell stress or electrostriction, (iii) flexoelectricity, and finally (iv) ionic diffusion.

The first of them, piezoelectricity, is arguably the most well known in the materials physics community and perhaps the least relevant in the context of biological cells. As we further elaborate on in this section, piezoelectricity entails a linear relation between the development of electrical polarization in a material in response to a uniform deformation or stress (and vice versa). Only crystalline dielectrics that have a certain type of anisotropy (notably a lack of mirror symmetry) can exhibit this phenomenon and, accordingly, typically only a few mechanically hard, crystalline ceramics possess this property (Nowick, 2005). Given the lack of any crystalline order in biological cells and its constituents, the absence of conventional piezoelectricity is hardly surprising. Some soft matter that appears to be piezoelectric or even ferroelectric is a result of other mechanisms masquerading as piezoelectricity.[3]

The Maxwell stress effect and electrostriction are universal phenomena and are present in all dielectrics. Essentially, upon the application of an electric field, all bodies deform due to electrostatic forces that develop on the opposing electrodes. The Maxwell stress is proportional to E^2, where E is the applied electric field. This force is modest unless a large voltage difference is imposed and the mechanical stiffness of the material is small. This implies that only soft dielectrics such as elastomers and biological matter deform appreciably for practically feasible applied electric fields. A key distinction compared to piezoelectricity is that the Maxwell stress is a one-way coupling, and thus while an electric field will generate deformation a mechanical stress will not induce any electricity. In this review we do not distinguish between the Maxwell stress effect and electrostriction, since they are

---

[3]For instance, frozen dipoles and charges in sufficiently soft (and even amorphous, manifestly isotropic) materials, together with the action of Maxwell stress or electrostriction, can exhibit a piezoelectric-like behavior. Such materials are known as electrets (Neugschwandtner *et al.*, 2000; Bauer, Gerhard-Multhaupt, and Sessler, 2004; Liu *et al.*, 2012; Rahmati, Bauer, and Sharma, 2019; Apte *et al.*, 2020). Besides, apparent piezoelectricity can be promoted by novel material designs adopting gradual change in material properties or architected design at the microscopic level (Mbarki *et al.*, 2014; Grasinger, Mozaffari, and Sharma, 2021). Apparent piezoelectricity (or even ferroelectric behavior) at the tissue level is well known (Fukada and Yasuda, 1957; Lang, 2000; Liu *et al.*, 2012, 2014).

mathematically similar and this distinction does not impact the central message of our review.[4]

Piezoelectricity is a linear coupling between uniform mechanical strain (or stress) and an electrical field (or polarization). As stated earlier, only materials that have broken mirror symmetry in their microstructure are able to exhibit this effect. However, an inhomogeneous strain can locally break mirror symmetry. The coupling between strain gradients and polarization is the phenomenon of flexoelectricity (Tagantsev, 1986; Nguyen et al., 2013; Zubko, Catalan, and Tagantsev, 2013; Mao and Purohit, 2014; Ahmadpoor and Sharma, 2015; Krichen and Sharma, 2016). Much like electrostriction, and unlike piezoelectricity, flexoelectricity is a universal phenomenon and is present in all dielectrics. The coupling may be weak and the effect may be negligible; however, all insulators are capable of being polarized when subjected to strain gradients. This is of profound importance in the biological context (especially at the cellular level), where the noncentrosymmetry of the microstructure[5] is hard to come by (Petrov, 1975, 2002; Petrov and Mircevova, 1986; Raphael, Popel, and Brownell, 2000; Brownell et al., 2001; Rey, 2006; Spector et al., 2006; Gao et al., 2008; Breneman, Brownell, and Rabbitt, 2009; Breneman and Rabbitt, 2009; Sachs, Brownell, and Petrov, 2009; Abou-Dakka, Herrera-Valencia, and Rey, 2012; Liu and Sharma, 2013; Deng, Liu, and Sharma, 2014b; Ahmadpoor and Sharma, 2015; Deng et al., 2019; Mozzaffari, Ahmadpoor, and Sharma, 2021). For a biological membrane, flexoelectricity is simply the change in the dipole moment upon changes in the curvature: a convenient electromechanical coupling mechanism since biological membranes bend easily.

Ionic diffusion plays a crucial role in regulating cellular function. However, lipid bilayers are not permeable to ions and the ions cannot easily pass through the membrane by the normal diffusion process mediated by concentration gradients or, more broadly, differential chemical potential. For passing through, ions need a channel formed by special proteins that facilitate this action. These narrow channels allow the ions to pass through by normal diffusion without the resistance of the lipid bilayer. Mechanical deformation is well known to alter the electrochemical potential and thus can directly impact the diffusion process (Larche and Cahn, 1978; Larcht'e and Cahn, 1982; Hong et al., 2008; Anand, 2012; Di Leo, Rejovitzky, and Anand, 2014; Grazioli et al., 2019). In addition, diffusion of ions (driven by electrical fields) can cause a time-dependent deformation owing to the fact that ions migrate preferentially to one of the electrodes. For instance, the undulation of a membrane under the effect of an electric field may be enhanced by the unbalanced electric stress resulting from

the ion current in the membrane (Sens and Isambert, 2002). Because of this mechanism, a thin film containing mobile ions will typically bend under the influence of an electrical field. In an intriguing work (Harland et al., 2010), it was shown how ion transport may couple with mechanical deformation such that applied voltage may cause a bending of the lipid membranes. In that sense, Harland et al. (2010) provided a model to assess the contribution of ion diffusion to the mechanism of flexoelectricity. This concept is also used extensively in materials science to create so-called ionic polymer–metal composites and ionic gels to serve as actuators and sensors and includes biomedical applications such as artificial muscles (Shahinpoor, 1999; Bar-Cohen, 2004; Kim and Tadokoro, 2007; Park et al., 2008; Schneider, 2015).

B. A variational formulation of electrostatics

In this section, we outline an energetic formulation of the classical theory of electrostatics. This formulation is convenient for including additional physics such as bulk and surface elasticity, magnetism, and dissipative phenomena and naturally fits into the framework of continuum thermodynamics. In particular, the equilibrium states are determined by the principle of minimum free energy in isothermal processes, and non-equilibrium processes are dictated by the dissipation potential.

Notation.—Direct notation is employed for brevity and for transparency of physical interpretation whenever possible. Frequently, recognizing that many readers may be more familiar with the index notation, we also present translations in index form to illustrate details of the calculations. Tensors and vectors are denoted by bold symbols $\mathbf{e}$, $\mathbf{E}$, $\mathbf{m}$, etc., while scalars are denoted by ξ, ζ, etc. When the index notation is in use, the convention of summation over a repeated index is followed. The inner (or dot) product between matrices $\mathbf{A}$ and $\mathbf{B}$ of the same size $m \times n$ is defined as $\mathbf{A} \cdot \mathbf{B} := \mathrm{Tr}(\mathbf{A}^T \mathbf{B}) = (\mathbf{A})_{ij}(\mathbf{B})_{ij}$, the norm $|\mathbf{A}| = (\mathbf{A} \cdot \mathbf{A})^{1/2}$, and the tensor product $\mathbf{A} \otimes \mathbf{B}$ is the tensor such that, for any $\mathbf{C} \in \mathbb{R}^{m \times n}$, $(\mathbf{A} \otimes \mathbf{B})\mathbf{C} = (\mathbf{B} \cdot \mathbf{C})\mathbf{A}$. For a vector field $\mathbf{v}$, in index form the gradient operator $\nabla \mathbf{v}$ is equivalent to $(\mathbf{v})_{i,j}$ with i (j) the first (second) index. We denote by ∇, $\nabla\cdot$, and $\nabla\times$ the gradient, divergence, and curl of a field with respect to the spatial variables $\mathbf{y}$ in the current configuration.

We begin with a polarizable body occupying a domain $\Omega \subset \mathbb{R}^3$ with boundary $\partial\Omega$ as illustrated in Fig. 3(b). The body is in an ambient medium V with boundaries ∂V. For the moment we neglect deformation and assume that the thermodynamic state of the body is described by the polarization $\mathbf{p}$. Denote by $\mathbf{e}$ the electric field and by $\mathbf{d} = \epsilon_0 \mathbf{e} + \mathbf{p}$ the electric displacement. Using Maxwell's equations and in the absence of free charges, these fields satisfy[6]

$$\nabla \times \mathbf{e} = 0, \qquad \nabla \cdot \mathbf{d} = 0 \qquad \text{on } V. \tag{1}$$

---

[4]There is a subtle difference between the physical origins of the Maxwell stress effect and electrostriction. For further discussions on this topic, see Tian (2008), Zhao and Suo (2008), and Tian et al. (2012).

[5]Noncentrosymmetry is referred to as the lack of inversion symmetry in crystal structures. Consider an "arrow" originating at the geometric centroid of a crystal unit cell. In centrosymmetric crystals, the arrow will see an identical environment if it undergoes a mirror reflection.

[6]Since we later discuss deformations, for clarity we use lowercase letters $\mathbf{e}, \mathbf{d}, \mathbf{p}, \mathbf{h}, \mathbf{b}, \mathbf{m}$, etc., to represent electromagnetic quantities in the current configuration, whereas the corresponding quantities in the reference configuration are represented by uppercase letters such as $\mathbf{E}, \mathbf{D}, \mathbf{P}, \mathbf{H}, \mathbf{B}$, and $\mathbf{M}$.
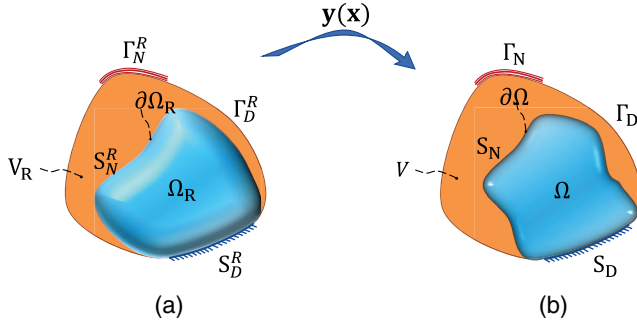
FIG. 3. Schematic of the electroelastic system with the pertinent boundary conditions in both reference and current configurations.

From Eq. (1), we see that there is a scalar field ξ, i.e., the electric potential, such that $\mathbf{e} = -\nabla\xi$.

We necessarily specify the boundary conditions on ∂V to determine the electric field. For example, let Γ_D and Γ_N be a partition of the boundary ∂V (i.e., $\Gamma_D \cap \Gamma_N = \varnothing$, $\Gamma_N \cup \Gamma_D = \partial V$), let ξ_b be the prescribed boundary potential, let $\mathbf{n}$ be the unit outward normal on ∂V, and assume that

$$\begin{aligned} \xi = \xi_b \quad &\text{on } \Gamma_D, \\ \mathbf{n} \cdot \mathbf{d} = 0 \quad &\text{on } \Gamma_N. \end{aligned} \tag{2}$$

Equations (1) and (2) can then be rewritten as the following boundary value problem for potential ξ:

$$\begin{aligned} \nabla \cdot (-\epsilon_0 \nabla\xi + \mathbf{p}\chi_\Omega) = 0 \quad &\text{in } V, \\ \xi = \xi_b \quad \text{on } \Gamma_D, \qquad \mathbf{n} \cdot \mathbf{d} = 0 \quad &\text{on } \Gamma_N, \end{aligned} \tag{3}$$

where $\chi_\Omega = 1$ on Ω, 0 otherwise. Further, if the dielectric property of the body Ω is specified (ϵ is the permittivity of the body),

$$\mathbf{p} = (\epsilon - \epsilon_0)\mathbf{e}, \tag{4}$$

upon inserting Eq. (4) into Eq. (3), we can uniquely determine the spatial electric field $-\nabla\xi$.

An alternative way to formulate electrostatic theory for a continuum body is to consider the energy of the system. For the applied boundary conditions (2), we identify the total free energy of the system as a functional of polarization $\mathbf{p}$:

$$\mathcal{F}[\mathbf{p}] = \mathcal{E}^{\text{elect}}[\mathbf{p}] + \mathcal{U}[\mathbf{p}] + W^{\text{ext}}[\mathbf{p}], \tag{5}$$

where the Maxwell equation (3) is enforced to determine ξ (as a nonlocal functional of $\mathbf{p}$) and

$$\begin{aligned} \mathcal{E}^{\text{elect}}[\mathbf{p}] &= \frac{\epsilon_0}{2} \int_V |\nabla\xi|^2, \\ \mathcal{U}[\mathbf{p}] &= \int_\Omega \psi(\mathbf{p}), \\ W^{\text{ext}}[\mathbf{p}] &= \int_{\Gamma_D} \xi_b \mathbf{n} \cdot \mathbf{d}. \end{aligned} \tag{6}$$

Physically, the term $\mathcal{E}^{\text{elect}}[\mathbf{p}]$ is the energy associated with the electric field on V, $\mathcal{U}[\mathbf{p}]$ is the energy of the polarizable

body Ω with $\psi(\mathbf{p})$ being the free-energy density, and $W^{\text{ext}}[\mathbf{p}]$ is the energy associated with the boundary devices for maintaining the boundary conditions (2). From thermodynamics, we claim that the equilibrium polarization of the body is determined by the principle of minimum free energy:

$$\min\{\mathcal{F}[\mathbf{p}] : \text{all admissible polarization } \mathbf{p}\}. \tag{7}$$

The variational principle (7) implies that the first variation of $\mathcal{F}[\mathbf{p}]$ must vanish for all admissible perturbation $\mathbf{p}_1$:

$$\delta\mathcal{F}[\mathbf{p}] := \left.\frac{d\mathcal{F}[\mathbf{p} + \varepsilon\mathbf{p}_1]}{d\varepsilon}\right|_{\varepsilon=0} = 0. \tag{8}$$

Using a calculus of the variations, we find that Eq. (8) implies that (Liu, 2013b)

$$\frac{\partial\psi}{\partial\mathbf{p}} + \nabla\xi = 0 \quad \text{in } \Omega \tag{9}$$

as the Euler-Lagrange equation, which can also be regarded as the constitutive relation between the local electric field and polarization.

Electrostatic theories for a variety of materials can be variationally formulated as previously described by choosing appropriate forms of the free-energy density function $\psi(\mathbf{p})$, including linear and nonlinear dielectrics and ferroelectric materials. For instance, to model linear dielectric materials we consider the free-energy density function ($\epsilon = \epsilon_0\epsilon_r$)

$$\psi(\mathbf{p}) = \tfrac{1}{2}a|\mathbf{p}|^2, \qquad a = \frac{1}{\epsilon_0(\epsilon_r - 1)}. \tag{10}$$

Using Eqs. (5) and (6), we write the total free energy of the system as

$$\mathcal{F}[\mathbf{p}] = \int_\Omega \left(\frac{1}{2}a|\mathbf{p}|^2 + \frac{\epsilon_0}{2}|\nabla\xi|^2\right) + \int_{\Gamma_D} \xi_b \mathbf{n} \cdot (-\epsilon_0 \nabla\xi + \mathbf{p}). \tag{11}$$

The variational principle (7) then implies Eq. (9) as a necessary condition, which is equivalent to the constitutive relation (4).

Compared to the conventional formulation based on the field equations and constitutive laws, the advantage of a variational formulation (7) includes the fact that new material models that account for general couplings can be incorporated into the framework by directly postulating the new free-energy density function $\psi = \psi$ (state variables). Moreover, constraints implied by the thermodynamics laws, frame indifference, and material symmetries can be conveniently enforced by restricting the form of the free-energy density function ψ.

There are alternative choices of the state variables and energy functionals for continuum electroelasticity in the literature that were reviewed by Liu (2014b) and references therein. Here we proceed with the polarization $\mathbf{p}$–based formulation since polarization is defined only on the body Ω (trivial in $V\backslash\Omega$) and the resulting variational problem is a minimization problem for the total free energy. Having a

minimum energy principle can facilitate stability analysis, which is one of the advantages of the **p**-based formulation.

C. Coupling of electrostatics with elasticity and the Maxwell stress

In this section, we consider the coupling between electrostatics and elasticity. To this end, we introduce an additional state variable, namely, the deformation. Let Ω_R (Ω) be the "reference configuration" before the deformation ("current configuration") of the body. V_R is similarly defined as the reference domain of the current domain V; see Fig. 3. A material point in reference (current) configuration is denoted by the Lagrangian coordinate $\mathbf{x} \in \Omega_R$ (Eulerian coordinates $\mathbf{y} \in \Omega$). The transformation $\mathbf{y} = \mathbf{y}(\mathbf{x})$ from the reference configuration to the current configuration is referred to as the deformation $\mathbf{y} : \Omega_R \to \Omega$. In addition, the displacement $\mathbf{u} : \Omega_R \to \mathbb{R}^3$ is defined as[7]

$$\mathbf{u}(\mathbf{x}) = \mathbf{y}(\mathbf{x}) - \mathbf{x}. \tag{12}$$

For clarity, we denote by ∇, $\nabla\cdot$, and $\nabla\times$ ($\nabla_\mathbf{x}$, $\nabla_\mathbf{x}\cdot$, and $\nabla_\mathbf{x}\times$) as the gradient, divergence, and curl of a field with respect to the spatial variables $\mathbf{y}$ in the current configuration (the material point variables $\mathbf{x}$ in the reference configuration). We denote by

$$\mathbf{F} = \nabla_\mathbf{x}\mathbf{y}, \qquad \mathbf{G} = \nabla_\mathbf{x}\nabla_\mathbf{x}\mathbf{y} = \nabla_\mathbf{x}\nabla_\mathbf{x}\mathbf{u}, \qquad J = \det\mathbf{F} \tag{13}$$

the deformation gradient, strain gradient, and Jacobian, respectively.[8] Since material points cannot interpenetrate, we require $J > 0$ everywhere.

In the presence of deformation, familiar field equations and physical quantities are usually defined on the current configuration with $\mathbf{y}$ being the spatial variables. On the other hand, the definition of strain must involve the reference coordinates $\mathbf{x}$, and variational calculations are much easier with functionals expressed as integrals over the reference configuration. Therefore, we frequently have to transform quantities between the reference configuration and the current configuration. Although they are standard in classical continuum thermodynamics, we now give an overview of some of the important transformations.

Let ξ, $\mathbf{v}$, and $\mathbf{T}$ be a scalar field, a vector field, and a tensor field, respectively. Here and subsequently, we adopt the convention $(\nabla_\mathbf{x}\mathbf{v})_{ij} = \partial v_i/\partial x_j = v_{i,x_j}$ for the vector field $\mathbf{v} = (v_i)$ and $(\nabla_\mathbf{x}\cdot\mathbf{T})_p = \partial T_{pk}/\partial x_k = T_{pk,x_k}$ for the tensor field $\mathbf{T} = (T_{pi})$. Upon a change of variables $\mathbf{y} \to \mathbf{x}$ and following the chain rule, we find that the gradients are related by

$$\xi_{,x_i} = \xi_{,y_k}y_{k,x_i} \quad \text{i.e.,} \quad \nabla_\mathbf{x}\xi = \mathbf{F}^T\nabla\xi,$$
$$v_{i,x_j} = v_{i,y_k}y_{k,x_j} \quad \text{i.e.,} \quad \nabla_\mathbf{x}\mathbf{v} = (\nabla\mathbf{v})\mathbf{F}. \tag{14}$$

----

[7]The displacement field in Eq. (12) can be written in index notation as $u_i = y_i - x_i$.

[8]The defined conventions in index notation are $F_{ij} = y_{i,j}$, $G_{ijk} = y_{i,jk} = u_{i,jk}$, and $J = \det(F_{ij})$.

In addition, for the Jacobian $J = \det\mathbf{F}$ and cofactor matrix $\text{cof}\mathbf{F} = J\mathbf{F}^{-T}$ we recall the identities

$$J_{,x_i} = J(\mathbf{F}^{-1})_{kl}(\mathbf{F})_{lk,x_i}, \qquad [J(\mathbf{F}^{-1})_{ki}]_{,x_k} = (\text{cof}\mathbf{F})_{ik,x_k} = 0.$$

Therefore,

$$\nabla \cdot \mathbf{v} = v_{i,y_i} = v_{i,x_k}(\mathbf{F}^{-1})_{ki} = \frac{1}{J}[J(\mathbf{F}^{-1})_{ki}v_i]_{x_k}$$
$$= \frac{1}{J}\nabla_\mathbf{x} \cdot (J\mathbf{F}^{-1}\mathbf{v}). \tag{15}$$

Similarly,

$$T_{pi,y_i} = T_{pi,x_k}(\mathbf{F}^{-1})_{ki} = \frac{1}{J}[J(\mathbf{F}^{-1})_{ki}T_{pi}]_{x_k}, \qquad \text{i.e.,}$$

$$\nabla \cdot \mathbf{T} = \frac{1}{J}\nabla_\mathbf{x} \cdot (J\mathbf{T}\mathbf{F}^{-T}). \tag{16}$$

In integral form we have, for any material volume element $\mathcal{P}_R \subset \Omega_R$ in the reference configuration and $\mathcal{P} = \mathbf{y}(\mathcal{P}_R)$ in the current configuration,

$$\int_\mathcal{P} \nabla \cdot \mathbf{v} d\mathbf{y} = \int_{\mathcal{P}_R} \nabla_\mathbf{x} \cdot (J\mathbf{F}^{-1}\mathbf{v})d\mathbf{x},$$
$$\int_\mathcal{P} \nabla \cdot \mathbf{T} d\mathbf{y} = \int_{\mathcal{P}_R} \nabla_\mathbf{x} \cdot (J\mathbf{T}\mathbf{F}^{-T})d\mathbf{x}. \tag{17}$$

Next we proceed to the precise definition of our thermodynamic system. For simplicity, we assume the following mechanical boundary conditions, which specify the mechanical interaction of the body with external forces (i.e., loading devices):

$$\mathbf{y} = \mathbf{y}_b \qquad \text{on } S_D^R,$$
$$\text{surface traction} = \mathbf{t}_b \quad \text{on } S_N^R, \tag{18}$$

where S_D^R, S_N^R is a subdivision of the boundary $\partial\Omega_R$, $\mathbf{t}_b : S_N^R \to \mathbb{R}^3$ is the surface traction or the applied force density per unit area in the reference configuration that is independent of the deformation $\mathbf{y}$, and $\mathbf{y}_b : S_D^R \to \mathbb{R}^3$ prescribes the positions of boundary S_D^R. Further, the electrostatic boundary conditions (2) are applied on the reference configuration:

$$\xi = \xi_b \qquad \text{on } \Gamma_D^R,$$
$$\text{surface charge density} = 0 \quad \text{on } \Gamma_N^R, \tag{19}$$

where the boundary potential $\xi_b : \Gamma_D^R \to \mathbb{R}$ is independent of the deformation $\mathbf{y}$.

As claimed in Sec. II.B, general electroelasticity models can be obtained by postulating reasonable forms of free-energy density functions ψ of the body. For general nonlinear electroelastic models that account for *piezoelectricity* and/or flexoelectricity, we can assume that the free energy contributed by the body is given by

$$\mathcal{U}[\mathbf{y}, \tilde{\mathbf{P}}] = \int_{\Omega_R} \psi(\nabla_\mathbf{x}\mathbf{y}, \nabla_\mathbf{x}\nabla_\mathbf{x}\mathbf{y}, \tilde{\mathbf{P}}), \tag{20}$$

where $\tilde{\mathbf{P}}(\mathbf{x}) = J(\mathbf{x})\mathbf{p}(\mathbf{y}(\mathbf{x}))$ is the polarization per unit volume in the reference configuration and $\psi : \mathbb{R}^{3\times3} \times \mathbb{R}^{3\times3\times3} \times \mathbb{R}^3 \to \mathbb{R}$ is the free-energy density of the material body that is specified later. As in Eq. (5), the total free energy of the system $\mathcal{F}[\mathbf{y}, \tilde{\mathbf{P}}]$ can then be written as

$$
\begin{aligned}
\mathcal{F}[\mathbf{y}, \tilde{\mathbf{P}}] &= \mathcal{U}[\mathbf{y}, \tilde{\mathbf{P}}] + \mathcal{E}^{\text{elect}}[\mathbf{y}, \tilde{\mathbf{P}}] + W^{\text{ext}}[\mathbf{y}, \tilde{\mathbf{P}}] \\
&= \int_{\Omega_R} \psi(\nabla_{\mathbf{x}}\mathbf{y}, \nabla_{\mathbf{x}}\nabla_{\mathbf{x}}\mathbf{y}, \tilde{\mathbf{P}})d\mathbf{x} + \int_V \frac{\epsilon_0}{2}|\nabla\xi|^2 d\mathbf{y} \\
&\quad + \int_{\Gamma_D} \xi_b \mathbf{n} \cdot \mathbf{d} d\mathbf{y} - \int_{S_N^R} \mathbf{t}_b \cdot \mathbf{y}(\mathbf{x})d\mathbf{x},
\end{aligned} \tag{21}
$$

where the last term is the potential energy of the external mechanical loading device associated with the boundary condition (18) and, as in Sec. II.B, the electric potential ξ is determined by Eq. (3) or, equivalently, by the reference configuration [see Eqs. (14) and (15)]

$$
\begin{aligned}
\nabla_{\mathbf{x}} \cdot \tilde{\mathbf{D}} &= 0, \qquad \tilde{\mathbf{D}} = \mathbf{F}^{-1}(-\epsilon_0 J\mathbf{F}^{-T}\nabla_{\mathbf{x}}\xi + \tilde{\mathbf{P}}) \quad \text{on } V_R, \\
\xi &= \xi_b \quad \text{on } \Gamma_D^R, \qquad\qquad \tilde{\mathbf{D}} \cdot \mathbf{N} = 0 \quad \text{on } \Gamma_N^R.
\end{aligned} \tag{22}
$$

In Eq. (22) $\mathbf{N}$ is the unit outward surface normal in the reference configuration.

A subtlety of electrostatics for a deformable body arises from the fact that the electric energy contributed by the field $\mathcal{E}^{\text{elect}}$ and external devices W^{ext} depend on the deformation $\mathbf{y}$ regardless of the material properties of the body. This is more evident upon rewriting the total free energy of the system (21) on the reference configuration via a change of variables $\mathbf{y} \to \mathbf{x}$ as

$$
\begin{aligned}
\mathcal{F}[\mathbf{y}, \tilde{\mathbf{P}}] &= \int_{\Omega_R} \psi(\nabla_{\mathbf{x}}\mathbf{y}, \nabla_{\mathbf{x}}\nabla_{\mathbf{x}}\mathbf{y}, \tilde{\mathbf{P}})d\mathbf{x} + \frac{\epsilon_0}{2}\int_{V_R} J|\mathbf{F}^{-T}\nabla_{\mathbf{x}}\xi|^2 d\mathbf{x} \\
&\quad + \int_{\Gamma_D^R} \xi_b \mathbf{N} \cdot \tilde{\mathbf{D}} d\mathbf{x} - \int_{S_N^R} \mathbf{t}_b \cdot \mathbf{y} d\mathbf{x}.
\end{aligned} \tag{23}
$$

The principle of minimum free energy then implies that the equilibrium state is determined by the variational principle

$$
\min\{\mathcal{F}[\mathbf{y}, \tilde{\mathbf{P}}] \text{ in Eq. } (23) : \text{all admissible } \mathbf{y} \text{ and } \tilde{\mathbf{P}}\}. \tag{24}
$$

By the calculus of variations, we arrive at the following Euler-Lagrange equations for the equilibrium state (Liu, 2014b):

$$
\begin{aligned}
\nabla_{\mathbf{x}} \cdot \left(\frac{\partial\psi}{\partial\mathbf{F}} - \nabla_{\mathbf{x}} \cdot \frac{\partial\psi}{\partial\mathbf{G}} + \tilde{\mathbf{\Sigma}}_{\text{MW}}^0 \right) &= 0 \quad \text{on } \Omega_R, \\
\frac{\partial\psi}{\partial\mathbf{P}} - \mathbf{E} &= 0 \quad\qquad \text{on } \Omega_R,
\end{aligned} \tag{25}
$$

where $\mathbf{E} = -\mathbf{F}^{-T}\nabla_{\mathbf{x}}\xi = -\nabla\xi$ is the electric field in Lagrangian coordinates $\mathbf{x}$ and

$$
\tilde{\mathbf{\Sigma}}_{\text{MW}}^0 = \mathbf{E} \otimes \tilde{\mathbf{D}} - \frac{\epsilon_0}{2}J|\mathbf{E}|^2\mathbf{F}^{-T} \tag{26}
$$

is the nominal *Maxwell stress*.

A few remarks are in order here regarding the Euler-Lagrange equations (25) and the Maxwell stress. First, the

electric and elastic properties of the material are entirely determined by the free-energy density function $\psi = \psi(\mathbf{F}, \mathbf{G}, \tilde{\mathbf{P}})$. In particular, from Eq. (25) we can identify $\partial\psi/\partial\mathbf{F}$ ($\partial\psi/\partial\mathbf{G}$) as the Piola-Kirchhoff stress (moment stress) in the classical nonlinear elasticity, whereas Eq. (25) prescribes how the polarization and electrical field are related inside the medium. Second, the extra term, i.e., the nominal Maxwell stress $\tilde{\mathbf{\Sigma}}_{\text{MW}}^0$, in the mechanical balance equation (25) precisely arises from the dependence of electric energies on the deformation $\mathbf{y}$. In the current configuration, using Eq. (16) the nominal Maxwell stress (26) is transformed into ($\mathbf{I} \in \mathbb{R}^{3\times3}$ is the identity matrix)[9]

$$
\mathbf{\sigma}_{\text{MW}}^0 = \frac{1}{J}\tilde{\mathbf{\Sigma}}_{\text{MW}}^0 \mathbf{F}^T = \mathbf{e} \otimes \mathbf{d} - \frac{\epsilon_0}{2}|\mathbf{e}|^2\mathbf{I}, \tag{27}
$$

which admits the usual physical interpretation of Cauchy stress in the current configuration; $\mathbf{\sigma}_{\text{MW}}^0\mathbf{n}$ represents the traction on an interface with unit outward normal $\mathbf{n}$.

The interpretation and implications of the Maxwell stress (27) can be seen from a more intuitive perspective. If a body in the current configuration admits smooth distributions of the charges (ρ) and dipoles ($\mathbf{p}$) and hence the local electric field $\mathbf{e} = -\nabla\xi$ and gradient of the electric field $\nabla\mathbf{e}$ are well defined everywhere by a solution to the Maxwell equation (3), then from the fundamental physics the electric force on these charges and dipoles can be expressed as

$$
\mathbf{f}_e = \rho\mathbf{e} + (\nabla\mathbf{e})\mathbf{p}. \tag{28}
$$

Indeed, by direct calculation we can verify that

$$
\nabla \cdot (\mathbf{\sigma}_{\text{MW}}^0) = \mathbf{f}_e, \tag{29}
$$

which is consistent with the mechanical balance equation (25). The direct implementation of Eq. (28) to account for mechanical effects of electrostatics, however, suffers from the discontinuity or unboundedness of the electric field at the defects, such as point charges or interfaces between two media.

In general, not all mechanical effects contributed by electrostatic interactions are reflected by the particular form of Maxwell stress (27). There are additional stress terms that depend on polarization due to the coupling between the deformation gradient and the polarization in the free-energy density $\psi = \psi(\mathbf{F}, \mathbf{G}, \tilde{\mathbf{P}})$. Even for the minimum model of electroelastic materials, i.e., ideal dielectrics where there is no direct coupling between strain and polarization and the permittivity of the medium is a deformation-independent constant ϵ, it can be shown that the free-energy density must be of the following form (Liu, 2014b):

$$
\psi(\mathbf{F}, \tilde{\mathbf{P}}) = \psi^{\text{elast}}(\mathbf{F}) + \frac{|\tilde{\mathbf{P}}|^2}{2J(\epsilon - \epsilon_0)}. \tag{30}
$$

The stress term $\partial\psi/\partial\mathbf{F}$ in Eq. (25) can then be written as

_____

[9]The Maxwell stress in Eq. (27) can be written in index notation as $(\sigma_{\text{MW}}^0)_{ij} = (1/J)(\Sigma_{\text{MW}}^0)_{ik}F_{jk} = e_i d_j - (\epsilon_0/2)e_k e_k \delta_{ij}$.

$$\frac{\partial \psi}{\partial \mathbf{F}} = \frac{\partial \psi^{\text{elast}}}{\partial \mathbf{F}} + \frac{\partial}{\partial \mathbf{F}}\left(\frac{|\tilde{\mathbf{P}}|^2}{2J(\epsilon - \epsilon_0)}\right)$$
$$= \frac{\partial \psi^{\text{elast}}}{\partial \mathbf{F}} - \frac{|\tilde{\mathbf{P}}|^2}{2J(\epsilon - \epsilon_0)}\mathbf{F}^{-T}.$$

It is more enlightening to identify the first term of this equation as the "mechanical stress." Meanwhile, combining the last term with the Maxwell stress in Eq. (25), we obtain

$$\tilde{\mathbf{\Sigma}}_{\text{MW}} = \mathbf{E} \otimes \tilde{\mathbf{D}} - \left(\frac{\epsilon_0}{2}J|\mathbf{E}|^2 + \frac{|\tilde{\mathbf{P}}|^2}{2J(\epsilon - \epsilon_0)}\right)\mathbf{F}^{-T}$$
$$= \mathbf{E} \otimes \tilde{\mathbf{D}} - \frac{\epsilon}{2}J|\mathbf{E}|^2\mathbf{F}^{-T}, \tag{31}$$

or equivalently in the current configuration,

$$\boldsymbol{\sigma}_{\text{MW}} = \frac{1}{J}\tilde{\mathbf{\Sigma}}_{\text{MW}}\mathbf{F}^T = \mathbf{e} \otimes \mathbf{d} - \frac{\epsilon}{2}|\mathbf{e}|^2\mathbf{I}, \tag{32}$$

where the last equality in Eq. (31) follows from the application of Eqs. (25) and (30): $\mathbf{E} = \tilde{\mathbf{P}}/J(\epsilon - \epsilon_0)$. The quantities $\tilde{\mathbf{\Sigma}}_{\text{MW}}$ and $\boldsymbol{\sigma}_{\text{MW}}$ are also referred to as the modified Maxwell stress in the literature.

Within each homogeneous phase of ideal dielectrics, by direct calculations we see that

$$\nabla \cdot (\boldsymbol{\sigma}_{\text{MW}}) = \nabla_{\mathbf{x}} \cdot (\mathbf{\Sigma}_{\text{MW}}) = 0. \tag{33}$$

Moreover, by the divergence theorem we have, for any nonhomogeneous sub-body $\mathcal{B} \subset V$ in the current configuration,

$$\int_{\mathcal{B}} \nabla \cdot \boldsymbol{\sigma}_{\text{MW}}dv = \int_{\partial\mathcal{B}} \boldsymbol{\sigma}_{\text{MW}}\mathbf{n}ds,$$

where $\mathbf{n}$ is the outward unit normal on $\partial\mathcal{B}$. Therefore, the mechanical force on the sub-body $\mathcal{B}$ with the boundary $\partial\mathcal{B}$ due to the Maxwell stress $\boldsymbol{\sigma}_{\text{MW}}$ can sometimes be replaced by a surface traction

$$\mathbf{t}_e = \boldsymbol{\sigma}_{\text{MW}}\mathbf{n} \qquad \text{on } \partial\mathcal{B}. \tag{34}$$

In practice, the minimum model of ideal dielectrics often suffices for most applications. Further, it is desirable not to repeat the lengthy variational calculations to extract the mechanical effect of electric interactions. Instead, we may directly extend the concept of Maxwell stress in Eqs. (31)–(33) and the surface traction interpretation in Eq. (34) to more general settings, including ac fields, fluids, and mediums with effects of electric screening. From this viewpoint, we take the Maxwell stress in Eqs. (31)–(33) and the surface traction formula (34) as the applied "electric forces" to a deformable body without resorting to the energetic interpretation discussed in this section.

D. Piezoelectricity and flexoelectricity

Most biological materials are approximately ideal dielectrics, meaning that the permittivity of the medium is a constant independent of the polarization and deformation.

Nevertheless, some biological materials may exhibit piezoelectricity and all biological materials are flexoelectric (Petrov, 2002). Piezoelectricity is a direct coupling between the strain and polarization. In the current framework, a minimum model of piezoelectricity can be obtained by postulating a free-energy density function of the following form:

$$\psi(\mathbf{F}, \tilde{\mathbf{P}}) = \psi^{\text{elast}}(\mathbf{F}) + (\mathbf{R}^T\tilde{\mathbf{P}}) \cdot \mathbb{B}(\mathbf{F}^T\mathbf{F} - \mathbf{I})$$
$$+ \frac{(\mathbf{R}^T\tilde{\mathbf{P}}) \cdot \mathbb{A}(\mathbf{R}^T\tilde{\mathbf{P}})}{2J}, \tag{35}$$

where, to recover the usual linear Hookean elasticity, we assume that ($\mathbb{C} \in \mathbb{R}^{3\times3\times3\times3}$ is the fourth-order elasticity tensor)[10]

$$\psi^{\text{elast}}(\mathbf{F}) = \tfrac{1}{8}(\mathbf{F}^T\mathbf{F} - \mathbf{I}) \cdot \mathbb{C}(\mathbf{F}^T\mathbf{F} - \mathbf{I}).$$

The rigid rotation matrix $\mathbf{R}$ is such that $\mathbf{F} = \mathbf{R}\mathbf{U}$ and $\mathbf{U} = (\mathbf{F}^T\mathbf{F})^{1/2}$ in the polar decomposition of nonsingular $\mathbf{F}$. The expression $\mathbf{F}^T\mathbf{F}$, i.e., the Cauchy-Green tensor, arises from the *principle of frame indifference*.

As a comparison to the model of ideal dielectrics (30), an additional coupling term between strain and polarization was introduced in Eq. (35). Moreover, the fourth-order elasticity tensor $\mathbb{C} \in \mathbb{R}^{3\times3\times3\times3}$, the third-order piezoelectricity tensor $\mathbb{B} \in \mathbb{R}^{3\times3\times3}$, and the second-order susceptibility tensor $\mathbb{A} \in \mathbb{R}^{3\times3}$ are all material constants and are assumed to be independent of deformation and polarization. Inserting Eq. (35) into the general Euler-Lagrange equations (25), we immediately obtain the governing equations for the minimum model of piezoelectricity. For a simplified linear theory, we assume small strain and polarization ($|\mathbf{F} - \mathbf{I}| = |\nabla\mathbf{u}| \sim |\tilde{\mathbf{P}}| \sim \varepsilon \ll 1$), keep only the leading-order terms, and arrive at the following boundary value problem (Liu, 2014b):

$$\nabla \cdot (\mathbb{C}\nabla\mathbf{u} + \mathbb{B}^T\mathbf{p}) = 0 \quad \text{in } \Omega,$$
$$\nabla\xi + \mathbb{B}\nabla\mathbf{u} + \mathbb{A}\mathbf{p} = 0 \quad \text{in } \Omega,$$
$$\nabla \cdot (-\epsilon_0\nabla\xi + \mathbf{p}) = 0 \quad \text{in } V,$$

with the boundary conditions

$$\xi = \xi_b \text{ on } \Gamma_D, \quad \mathbf{d} \cdot \mathbf{n} = 0 \text{ on } \Gamma_N,$$
$$\mathbf{u} = \mathbf{u}_b \text{ on } S_D, \quad (\mathbb{C}\nabla\mathbf{u} + \mathbb{B}^T\mathbf{p})\mathbf{n} = 0 \text{ on } S_N. \tag{36}$$

In Eq. (36) we no longer differentiate between the reference and current configurations for small strains.

As previously discussed, most biological materials are unlikely to possess the lower symmetry required to be piezoelectric. Because of the centrosymmetry, piezoelectricity is then absent because the coupling tensor $\mathbb{B}$ is of third order and has to vanish for centrosymmetric materials. Therefore, the leading direct coupling between deformation and polarization for centrosymmetric materials would be the coupling

---

[10]The elastic part of the energy density function in Eq. (35) can be written in index notation as $\psi^{\text{elast}}(F_{ij}) = (1/2)(F_{mi}F_{mj} - \delta_{ij}) \times \mathbb{C}_{ijkl}(F_{nk}F_{nl} - \delta_{kl})$.

between the strain gradient $\nabla\nabla\mathbf{y} = \nabla\nabla\mathbf{u}$ and the polarization $\tilde{\mathbf{P}}$. In parallel to Eq. (35), a minimum model of *isotropic* flexoelectricity can be obtained by postulating a free-energy density function of the following form:

$$\psi(\nabla\mathbf{y}, \nabla\nabla\mathbf{y}, \tilde{\mathbf{P}}) = \psi^{\text{elast}}(\nabla\mathbf{y}) + \frac{g}{2}|\Delta\mathbf{y}|^2$$
$$+ f\tilde{\mathbf{P}} \cdot \Delta\mathbf{y} + \frac{|\tilde{\mathbf{P}}|^2}{2J(\epsilon - \epsilon_0)}, \quad (37)$$

where f is the flexoelectric coupling constant, $\Delta(\cdot) = \nabla \cdot \nabla(\cdot)$ denotes the Laplace operator with respect to the Lagrangian coordinates, and the term $(g/2)|\Delta\mathbf{y}|^2$, with $g > 0$, is required for stability. Inserting Eq. (37) into the general Euler-Lagrange equations (25), we obtain the governing equations for the minimum model of flexoelectricity. For a simplified linear theory, we assume small strain and polarization $(|\mathbf{F} - \mathbf{I}| = |\nabla\mathbf{u}| \sim |\tilde{\mathbf{P}}| \sim \varepsilon \ll 1)$, keep only the leading-order terms, and arrive at the following boundary value problem (Liu, 2014b)[11] :

$$-\nabla \cdot (\mathbb{C}\nabla\mathbf{u}) + \Delta(g\Delta\mathbf{u} + f\mathbf{p}) = 0 \quad \text{in } \Omega,$$
$$\nabla\xi + f\Delta\mathbf{u} + 1/(\epsilon - \epsilon_0)\mathbf{p} = 0 \quad \text{in } \Omega, \quad (38)$$
$$\nabla \cdot (-\epsilon_0\nabla\xi + \mathbf{p}) = 0 \quad \text{in } V,$$

with, in addition to the first three conditions in Eq. (36), the boundary conditions

$$(\mathbb{C}\nabla\mathbf{u})\mathbf{n} - [\nabla(g\Delta\mathbf{u} + f\mathbf{p})]\mathbf{n} - \mathbf{t}_b = 0 \text{ on } S_N,$$
$$g\Delta\mathbf{u} + f\mathbf{P} = 0 \text{ on } \partial\Omega. \quad (39)$$

As before, we do not differentiate between the reference and current configurations for small strains in the previously mentioned boundary value problem for flexoelectricity. We note that flexoelectric coupling is size dependent and could be significant in thin nanosize structures. One of the examples where flexoelectricity is considerable is in biological membranes (discussed in Sec. II.E [Eq. (56)]).

E. Electroelasticity for biological membranes

Biological membranes are thin structures formed by lipid molecules with embedded proteins. These membranes are often referred to as fluidic membranes since, within the plane of the membrane, the lipid molecules can flow and are unable to sustain any static shear stress. Mechanically, fluidic membranes can be modeled as isotropic elastic shells that can resist bending and stretching (Phillips *et al.*, 2012). Electrically, fluidic membranes can be modeled as mediums that are both polarizable and conductive. We now describe how the electroelasticity theory in three dimensions described in Sec. II.D translates into electric and mechanical models for fluidic membranes.

[11]The index notation for Eq. (38) is given by $-(\mathbb{C}_{ijkl}u_{k,l})_{,j} + (gu_{i,jj} + fp_i)_{,kk} = 0$ in Ω, $\xi_{,i} + fu_{i,jj} + 1/(\epsilon - \epsilon_0)p_i = 0$ in Ω, and $(-\epsilon_0\xi_{,i} + p_i)_{,i} = 0$ in V.

For simplicity, we assume linear responses for ambient media surrounding a biological cell. That is, the electric displacement is given by

$$\mathbf{d} = \epsilon^{(i)}\mathbf{e},$$

where $i = \text{ext (int)}$ or m represents the medium on the exterior (interior) side of the unit vector $\mathbf{n}$ or the membrane itself and

$$\epsilon^{(i)} = \epsilon_d^{(i)} + \frac{\sigma^{(i)}}{i\omega}.$$

Here $\epsilon_d^{(i)}$ is the dielectric constant, $\sigma^{(i)}$ is the conductivity, and ω is the ac frequency.

We now specify the boundary value problem for determining the electric field in space and the associated Maxwell stress, which is pivotal for understanding the electromechanical coupling of cells. In the absence of external charges, the Maxwell equation implies that

$$\nabla \cdot \mathbf{d} = \nabla \cdot [-\epsilon(\mathbf{x})\nabla\xi] = 0 \quad \text{in } \mathbb{R}^3,$$
$$-\nabla\xi \to \mathbf{e}^e \quad \text{as } |\mathbf{x}| \to +\infty, \quad (40)$$

where the complex dielectric coefficient $\epsilon(\mathbf{x})$ takes the value of $\epsilon^{(i)}$ in the i phase and $\mathbf{e}^e$ is the external electric field far from the membrane.

It is sometimes convenient to simplify the three-phase model (40) using a two-phase model. In this model, the membrane is assumed to be simply a surface with zero thickness; the electrical effects of the membrane are then accounted for using the following jump conditions:

$$[\![\mathbf{d}]\!] \cdot \mathbf{n} = 0 \quad \text{on } \mathbb{S},$$
$$\mathbf{n} \cdot \mathbf{d} + k[\![\xi]\!] = \mathbf{p}_* \cdot \mathbf{n} \quad \text{on } \mathbb{S}, \quad (41)$$

where the complex constant k can be interpreted as the capacitance of the membrane per unit area and $[\![\xi]\!]$ is recognized as the transmembrane potential. If the membrane is actually of thickness t with dielectric constant $\epsilon_d^{(m)}$ and conductivity $\sigma^{(m)}$,

$$k = \frac{1}{t}\left(\epsilon_d^{(m)} + \frac{\sigma^{(m)}}{i\omega}\right).$$

In addition, the quantity $\mathbf{p}_*$ in Eq. (41) could be interpreted as the additional polarization that is not accounted for by the dielectric constant, such as the polarization due to piezoelectricity or flexoelectricity. In other words, the actual polarization on the membrane is given by

$$\mathbf{p} = \mathbf{p}_* - (\epsilon_d^{(m)} - \epsilon_0)[\![\xi]\!]\mathbf{n}/t. \quad (42)$$

Unlike solid materials, fluidic membranes admit an additional symmetry: the elastic energy of the membrane depends only on the current configuration, typically the mean and Gaussian curvature of the membrane. To describe the electroelastic states of the membrane shown in Fig. 4, we introduce a parametrization (or coordinate patch) $\mathbf{y}: U \to \mathbb{S}$, where $U \subset \mathbb{R}^2$ is a fixed set for parametrization. We denote by (x^1, x^2) the coordinates of points in U with respect to an
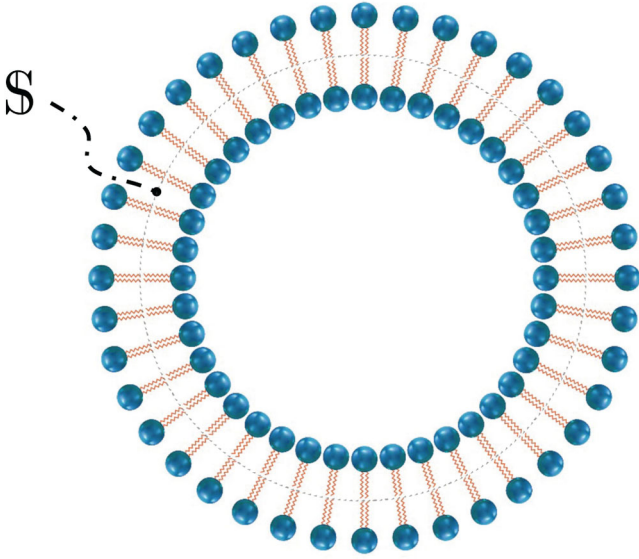
FIG. 4.   Schematic of a closed lipid vesicle with midsurface $\mathbb{S}$.

orthonormal basis, by $g_{\alpha\beta} = \mathbf{y}_\alpha \cdot \mathbf{y}_\beta$[12] the metric tensor (first fundamental form), by $G = \sqrt{\det(g_{\alpha\beta})}$ the surface Jacobian, and by

$$\mathbf{n} = \frac{\mathbf{y}_{,1} \times \mathbf{y}_{,2}}{|\mathbf{y}_{,1} \times \mathbf{y}_{,2}|}$$

the unit normal vector. In addition, the second fundamental form is defined as $K_{\alpha\beta} = \mathbf{n} \cdot \mathbf{y}_{,\alpha\beta}$. Further, at a point on the surface let $\mathcal{T}_\mathbf{n}$ be the tangential plane, let $\mathcal{P}_\mathbf{n} = \mathbf{I} - \mathbf{n} \otimes \mathbf{n}$ be the projection[13] from $\mathbb{R}^3$ into $\mathcal{T}_\mathbf{n}$, and let $\nabla_s(\cdot) = \nabla_\mathbf{x}(\cdot)\mathcal{P}_\mathbf{n}$ ($\nabla_s \cdot (\cdot) = \text{Tr}[\mathcal{P}_\mathbf{n}\nabla_\mathbf{x}(\cdot)\mathcal{P}_\mathbf{n}]$) be the surface gradient (divergence) operator (Mozaffari, Yang, and Sharma, 2020). We denote by $\mathbf{L}: \mathcal{T}_\mathbf{n} \to \mathcal{T}_\mathbf{n}$ and

$$\mathbf{L} = -\nabla_s \mathbf{n} \tag{43}$$

the Weingarten map,[14] and by

$$H = \tfrac{1}{2}\text{Tr}\mathbf{L}, \qquad K = \det \mathbf{L} \tag{44}$$

the mean curvature and Gaussian curvature, respectively.[15]

---

[12]The $\mathbf{y}_\alpha = \partial\mathbf{y}/\partial x^\alpha$ are the tangent vectors in the deformed (covariant) space (Deserno, 2015). Further, $g_{\alpha\beta}$ are the covariant components of the first fundamental form.

[13]The projection tensor in index notation is $(\mathcal{P}_\mathbf{n})_{ij} = \delta_{ij} - n_i n_j$.

[14]The Weingarten relation can be shown as $\mathbf{n}_{,\alpha} = -K_\alpha^\beta \mathbf{e}_\beta$, where $K_\alpha^\beta = K_{\alpha\gamma}g^{\gamma\beta}$ and $(g^{\alpha\beta}) = (g_{\alpha\beta})^{-1}$.

[15]The mean and Gaussian curvatures can be written as $H = (1/2)g^{\alpha\beta}K_{\alpha\beta}$ and $K = (1/2G^2)\varepsilon^{\alpha\beta}\varepsilon^{\lambda\gamma}K_{\alpha\lambda}K_{\beta\gamma}$, where $\varepsilon^{\alpha\beta}$ is the permutation tensor, i.e., $\varepsilon^{12} = -\varepsilon^{21} = 1$ and $\varepsilon^{11} = \varepsilon^{22} = 0$. As an example, assume a spherical surface of radius R with the position vector $\mathbf{y} = R\mathbf{e}_\mathrm{r}$ and the outward unit normal $\mathbf{n} = \mathbf{e}_\mathrm{r}$. The projection tensor is obtained as $\mathcal{P}_\mathbf{n} = \mathbf{e}_\theta \otimes \mathbf{e}_\theta + \mathbf{e}_\phi \otimes \mathbf{e}_\phi$, and from Eq. (43) the Weingarten map is $\mathbf{L} = -\nabla_s \mathbf{n} = -(1/R)(\mathbf{e}_\theta \otimes \mathbf{e}_\theta + \mathbf{e}_\phi \otimes \mathbf{e}_\phi)$ (Mozaffari, Yang, and Sharma, 2020). Therefore, the mean and Gaussian curvatures are obtained from Eq. (44) as $H = -1/R$ and $K = 1/R^2$.

For a fluidic membrane parametrized by $\mathbf{y} = \mathbf{y}(x^1, x^2)$ under the application of an electric field and mechanical surface forces $\mathbf{t}_b: \mathbb{S} \to \mathbb{R}^3$, the free energy of the membrane can be defined as

$$\mathcal{F}[\mathbf{y}] = \mathcal{U}[\mathbf{y}] + W^{\text{ext}}[\mathbf{y}], \tag{45}$$

where the elastic energy of the membrane is postulated as

$$\mathcal{U}[\mathbf{y}] = \int_\mathbb{S} \psi(H, K, \mathbf{p})da$$

and the potential energy due to the electric field and mechanical loading devices is given by

$$W^{\text{ext}}[\mathbf{y}] = -\int_\mathbb{S} (\mathbf{t}_b + \mathbf{t}_e) \cdot \mathbf{y}da.$$

Here, for brevity, we directly account for the mechanical effect of the electric field on the membrane using a surface traction

$$\mathbf{t}_e = [\![\boldsymbol{\sigma}_{\text{MW}}]\!]\mathbf{n} \equiv [\boldsymbol{\sigma}_{\text{MW}}|_+ - \boldsymbol{\sigma}_{\text{MW}}|_-]\mathbf{n}. \tag{46}$$

In addition to the membrane elastic energy, two physical constraints are frequently imposed on the admissible configurations $\mathbf{y}$ in the variational principle (49).

(C1)   *Local area conservation.*—The membrane, though deformable, has to conserve the area of each surface element; i.e., the surface Jacobian $G = G(x^1, x^2)$ is independent of variations of $\mathbf{y}$. This constraint can be accounted for by considering a Lagrange multiplier term

$$L_1[\mathbf{y}] = \int_\mathbb{S} \lambda da, \tag{47}$$

where λ can be interpreted as the local surface tension (it is not constant on the entire surface).

(C2)   *Enclosed volume conservation.*—If $\mathbb{S} = \partial\Omega$ is a close surface without an edge, the enclosed volume is typically assumed to be constant. This constraint can be addressed by considering a Lagrange multiplier term

$$L_2[\mathbf{y}] = p\int_\Omega dv. \tag{48}$$

The equilibrium configuration is determined by the principle of minimum free energy as follows:

$$\min\{\mathcal{F}[\mathbf{y}] \text{ in Eq. } (45): \text{all admissible } \mathbf{y}\}. \tag{49}$$

To derive the Euler-Lagrange equation associated with the previously mentioned variational principle, we consider variations of the surface $\mathbf{y} \to \mathbf{y}_\varepsilon = \mathbf{y} + \varepsilon\mathbf{v}$ and rewrite the surface integral in terms of the "reference" coordinates (x^1, x^2) as

$$\int_{\mathbb{S}} (\cdot) da = \int_{U} (\cdot) G dA.$$

Associated with the varied surface $\partial\Omega_\varepsilon$, to the first order the unit normal vector $\mathbf{n}_\varepsilon$, the mean curvature H_ε, the Gaussian curvature K_ε, and the surface Jacobian G_ε can be written as [see Biria, Maleki, and Fried (2013) for details][16]

$$\mathbf{n}_\varepsilon = \mathbf{n} - \varepsilon(\nabla_s \mathbf{v})^T \mathbf{n} + o(\varepsilon),$$

$$H_\varepsilon = H + \varepsilon[(2H^2 - K)v_\mathbf{n} + \tfrac{1}{2}\Delta_s v_\mathbf{n} + \nabla_s H \cdot \mathbf{v}_t] + o(\varepsilon),$$

$$K_\varepsilon = K + \varepsilon[2H(Kv_\mathbf{n} + \Delta_s v_\mathbf{n}) - \nabla_s \cdot (\mathbf{L}\nabla_s v_\mathbf{n} - 2v_\mathbf{n}\nabla_s H)$$
$$\qquad - 2v_\mathbf{n}\Delta_s H + \nabla_s K \cdot \mathbf{v}_t] + o(\varepsilon),$$

$$G_\varepsilon = G[1 + \varepsilon(-2Hv_\mathbf{n} + \nabla_s \cdot \mathbf{v}_t)] + o(\varepsilon), \qquad (50)$$

where $v_\mathbf{n}$ ($\mathbf{v}_t$) is the normal (tangential) components of vector field $\mathbf{v}$ and is given by

$$v_\mathbf{n} = \mathbf{v} \cdot \mathbf{n} \quad (\mathbf{v}_t = \mathbf{v} - v_\mathbf{n}\mathbf{n} = \mathcal{P}_\mathbf{n}\mathbf{v}).$$

Using the standard calculus of variations, we can now derive the associated Euler-Lagrange equations for the equilibrium configuration of the membrane $\mathbf{y} = \mathbf{y}(x^1, x^2)$ subject to the previously mentioned constraints (C1) and (C2). If the membrane is differentiable without an edge, we find the following governing equation for the equilibrium configuration:

$$\psi_H(2H^2 - K) + \tfrac{1}{2}\Delta_s\psi_H + 2\psi_K HK + 2\Delta_s(\psi_K H)$$
$$-\nabla_s \cdot (\mathbf{L}\nabla_s\psi_K) - 2(\nabla_s H) \cdot (\nabla_s\psi_K)$$
$$-2\psi_K\Delta_s H - 2H(\psi + \lambda) - (\mathbf{t}_e + \mathbf{t}_b) \cdot \mathbf{n} = p, \qquad (51)$$
$$\nabla_s\lambda + \mathcal{P}_\mathbf{n}(\mathbf{t}_e + \mathbf{t}_b) = \mathbf{0},$$

where $\psi_H = \partial\psi/\partial H$, $\psi_K = \partial\psi/\partial K$, and the first (second) equation corresponds to the balance of the total normal (tangential) force on any surface element. Moreover, in regard to Eq. (9) we postulate the constitutive relation

$$\mathbf{n} \cdot \frac{\partial\psi}{\partial\mathbf{p}} + [\![\xi]\!] = 0 \qquad \text{on } \partial\Omega, \qquad (52)$$

which, together with the mechanical equilibrium equation (51) and the Maxwell equations (40) and (41), forms a closed system that dictates the electroelastic behaviors of the membrane. For a systematic discussion of both the mechanical and electromechanical theory of membranes and a good review of the relevant literature, see Steigmann (1999), Biria, Maleki, and Fried (2013), and Deserno (2015).

To see the implication of this framework, we now specify the free-energy density function of the membrane. For a dielectric Helfrich-Canham membrane with a preferred mean curvature H_* (Helfrich, 1973b), we postulate that

$$\psi = \psi_{\text{HC}}(H, K, \mathbf{p})$$
$$= \tfrac{1}{2}\kappa_b(H - H_*)^2 + \kappa_g K + \tfrac{1}{2}a|\mathbf{p}|^2 + \lambda_*, \qquad (53)$$

where κ_b and κ_g are the bending moduli associated with the mean and Gaussian curvatures, respectively, $a = t/(e^{(m)} - \epsilon_0)$, and λ_* is the reference constant surface tension. Equation (51) can then be written as

$$\kappa_b(H - H_*)(2H^2 - K) + (\kappa_b/2)\Delta_s H$$
$$-2H(\psi - \kappa_g K + \lambda) - (\mathbf{t}_e + \mathbf{t}_b) \cdot \mathbf{n} = p, \qquad (54)$$
$$\nabla_s\lambda + \mathcal{P}_\mathbf{n}(\mathbf{t}_e + \mathbf{t}_b) = \mathbf{0},$$

and Eqs. (41), (42), and (52) imply the following interfacial conditions for the Maxwell equation (40):

$$[\![\mathbf{d}]\!] \cdot \mathbf{n} = 0 \qquad \text{on } \mathbb{S},$$
$$\mathbf{n} \cdot \mathbf{d} + k[\![\xi]\!] = 0 \quad \text{on } \mathbb{S}. \qquad (55)$$

The electroelastic membrane theory represented by Eqs. (40) and (41) and Eqs. (51) and (52) is geometrically nonlinear and coupled since the local electric field and Maxwell stress depend on the unknown surface configuration $\partial\Omega$. For a flexoelectric Helfrich-Canham membrane we assume that

$$\psi = \psi_{\text{HC}}(H, K, \mathbf{p}) + fH\mathbf{p} \cdot \mathbf{n}, \qquad (56)$$

where f is the flexoelectric constant. Upon repeating the variational calculation, we obtain the following mechanical equilibrium equations:

$$\kappa_b(H - H_*)(2H^2 - K) - Kf\mathbf{p} \cdot \mathbf{n} + (\kappa_b/2)\Delta_s H$$
$$+\tfrac{1}{2}f\Delta_s(\mathbf{p} \cdot \mathbf{n}) - 2H(\psi - \kappa_g K - fH\mathbf{p} \cdot \mathbf{n} + \lambda)$$
$$+f\nabla_s \cdot (H\mathbf{p}) - (\mathbf{t}_e + \mathbf{t}_b) \cdot \mathbf{n} = p, \qquad (57)$$
$$\nabla_s\lambda + fH\mathbf{L}\mathbf{p} + \mathcal{P}_\mathbf{n}(\mathbf{t}_e + \mathbf{t}_b) = \mathbf{0},$$

and Eqs. (41), (42), and (52) imply the following interfacial conditions for the Maxwell equation (40):

$$[\![\mathbf{d}]\!] \cdot \mathbf{n} = 0 \qquad \text{on } \mathbb{S},$$
$$\mathbf{n} \cdot \mathbf{d} + k[\![\xi]\!] = fH \quad \text{on } \mathbb{S}. \qquad (58)$$

Moreover, adopting the so-called Monge representation for surfaces, we can express the out-of-plane deformation in the membrane using a height function $h(\mathbf{x})$, where $\mathbf{x} = (x^1, x^2)$ is the position vector in the flat reference configuration.[17] Therefore, the position of the membrane in a deformed state can be expressed in the form of $(x^1, x^2, h(\mathbf{x}))$. The mean and Gaussian curvatures and the normal vector in Monge's gauge can be obtained as follows (Deserno, 2015)[18]:

---

[16]Alternatively, the surface gradient, surface divergence, and surface Laplacian can be expressed as $(\nabla_s f)_\alpha = g^{\alpha\beta}(\partial f/\partial x^\beta)$, $\nabla_s \cdot \mathbf{a} = (1/G)(\partial/\partial x^\alpha)(Ga^\alpha)$, and $\Delta_s f = (1/G)(\partial/\partial x^\alpha) \times [Gg^{\alpha\beta}(\partial f/\partial x^\beta)]$, where f and $\mathbf{a}$ are the arbitrary scalar and contravariant vector in the reference coordinates.

[17]This representation is valid only for surfaces without overhangs.
[18]Here we are working in two-dimensional space and $\nabla = [\partial/\partial x_1, \partial/\partial x_2]$, $\Delta = [\partial^2/\partial x_1^2, \partial^2/\partial x_2^2]$.

$$H = \nabla \cdot \left(\frac{\nabla h(\mathbf{x})}{\sqrt{1 + |\nabla h(\mathbf{x})|^2}} \right), \qquad K = \frac{\det[\nabla \nabla h(\mathbf{x})]}{[1 + |\nabla h(\mathbf{x})|^2]^2},$$

$$\mathbf{n} = \frac{(-\nabla h(\mathbf{x}), 1)}{\sqrt{1 + |\nabla h(\mathbf{x})|^2}}, \qquad J_h = \sqrt{1 + |\nabla h(\mathbf{x})|^2}. \qquad (59)$$

Upon linearization, by assuming that the deviation from the flat reference is small, i.e., $|\nabla h \ll 1|$, one can further simplify the mean and Gaussian curvatures in Eq. (59) as

$$H \simeq h_{11} + h_{22},$$
$$K \simeq \tfrac{1}{2}[(\Delta h)^2 - |\nabla \nabla h|^2] = h_{11} h_{22} - (h_{12})^2 \simeq 0. \qquad (60)$$

By imposing the linearized definitions of mean and Gaussian curvature in Eq. (60) and ignoring the spontaneous curvature, mechanical loadings, the surface, and the electrostatic effects, the equilibrium equations (57) can be further simplified as

$$\frac{\kappa_b}{2} \Delta(\Delta h) = 0, \qquad (61)$$

which is in good agreement with the familiar biharmonic differential equation used in the literature.

In this section, we directly present the translation of the three-dimensional theory of electroelasticity to membranes without any proof. It is important to note, however, that the rigorous derivation of the mathematical theory of membranes from its three-dimensional counterpart has indeed attracted much attention in the literature; see Friesecke, James, and Müller (2006), Deseri, Piccioni, and Zurlo (2008), Steigmann (2009, 2013, 2018), Edmiston and Steigmann (2011), Ogden and Steigmann (2011), Barham, Steigmann, and White (2012), and Roohbakhshan, Duong, and Sauer (2016). In our presentation of the theory of membranes, we are ignoring the tilt degrees of freedom, which under certain circumstances are important as well and can be readily incorporated into the framework described in this section (May, 2000; Zimmerberg and Kozlov, 2006; Rangamani and Steigmann, 2014; Deserno, 2015; Terzi and Deserno, 2017).

III. CELL MOTION UNDER AN EXTERNAL ELECTRIC FIELD

Manipulation of cells and vesicles, and specifically the control of their motion, is of critical importance in the biomedical sciences. For example, in the case of drug delivery, a drug carrying liposome must be placed in a specific location and prompted to release its content at a specific time (Sharma and Sharma, 1997; Mallouk and Sen, 2009; Kagan et al., 2010). Similarly, cells may be directed to fuse (Solovev et al., 2010), separate, or sort (Mehmet and Daniel, 2005; Xia et al., 2006; Chen et al., 2008). The use of electric field–based methods for cell manipulation and separation was found to have several advantages over conventional approaches that are based on size and density (Sato et al., 2006) or affinity (Fu et al., 1999). Electric field–based methods are faster and provide a higher resolution for treating small samples using noncontact devices. Among the different strategies to create motion in biological particles using an electric field,

dielectrophoresis is perhaps the most significant. Electrophoresis is also utilized but is specific to charged biological particles and the imposed electric field can be uniform and nonuniform. Dielectrophoresis, on the other hand, is a universal phenomenon and can also be applied to neutral particles, with the caveat that the imposed electric field must be inhomogeneous. In this section, we discuss the theory and physics of dielectrophoresis and electrorotation, which are widely used to achieve directed motion of biological cells.

A. Overview of dielectrophoresis and electrorotation

A neutral dielectric body polarizes when placed in an electric field. If the imposed external electrical field is uniform, while the body may deform and may be in a state of stress, the net force on the body will be zero and no motion will ensue. However, a spatially nonuniform electric field will induce a net force on the polarized body and create a directional motion. This phenomenon is called dielectrophoresis (DEP) (Pohl, 1951); see Fig. 5. When a dielectric body is placed in a rotating electric field, a torque is exerted on its surface that induces rotation in a process referred to as electrorotation. The magnitude and direction of the DEP force depend on the dielectric properties of the body, and thus may be used to distinguish cells. Indeed, the phenomenon of DEP was initially used to develop a method for biological cell separation (Pohl and Hawk, 1966). Over the last few decades, several other technologies based on DEP have been developed for a variety of applications, including characterization of the dielectric properties of biological membranes and cell interior (Gagnon, 2011), separation of cells of different types and manipulation of DNA molecules (Jones, 2003), trapping of cells between electrodes (Gray et al., 2004), sorting of the cells using traveling wave DEP (Cheng et al., 2009; Hughes, 2016; Karle et al., 2016), and assessment of cell viability (Zhang et al., 2020). A large body of literature exists on the aforementioned developments (Pethig, 2010), which have been reviewed extensively in recent years. We highlight the following reviews on cell manipulation, separation and detection (Gagnon, 2011; Yang, 2012; Devi et al., 2014), the application of DEP in stem cell research (Pethig et al., 2010), and the diagnosis of cancer and other diseases (Adekanmbi and Srivastava, 2016; Chan et al., 2018).

From a theoretical standpoint, the vast majority of the literature favors an approach called effective moment method (EMM) for computing DEP forces and torques (Jones, 1979; Wang et al., 1994) and using the resulting insights to either design cellular motion or interpret the results of relevant experiments. This approach approximates the charge accumulation on the surface of the polarized dielectric body by a set of multipoles and then computes the Coulombic interaction of the multipoles with the external electric field. The EMM, although a simplification, is expedient (especially if only the lowest-order dipole contribution is retained) due to closed-form expressions, and is especially suitable when the dielectric body is much smaller than the electrodes. With such an approximation, the dielectric body is then simply approximated as a sphere to calculate the DEP force and torque. Thus, local field effects are neglected, with the electrical signature
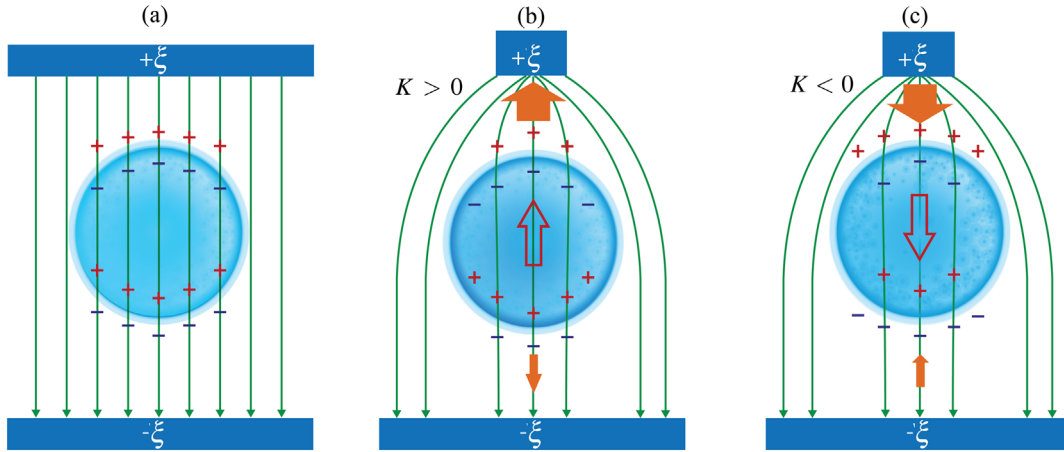
FIG. 5.   The basic premise underpinning dielectrophoresis. (a) Polarization of a body in a uniform electric field results in a neutral body with zero net exerted force. (b) Polarization of the body in a nonuniform electric field. Here the cell is more polarizable than the surrounding liquid ($\varepsilon_d^{(c)} > \varepsilon_d^{(l)}$) and it moves toward the region with a strong electric field [positive DEP (pDEP)]. (c) Polarization of the body in a nonuniform electric field where the cell is less polarizable than the surrounding liquid ($\varepsilon_d^{(c)} > \varepsilon_d^{(l)}$) and it moves toward the region with a weak electric field [negative DEP (nDEP)].

determined solely by the multipoles. Recent developments in the biomedical sciences and associated technologies have increasingly relied on microscale and nanoscale devices, where the scale of the dielectric body is comparable to the electrode and thus the local field on the body may significantly affect the results (Hughes, 2000; Freer *et al.*, 2010). Therefore, a more rigorous approach in a multipole approximation of the body may be required in those instances. Moreover, analytical solutions for higher-order moments are available only for spherically shaped bodies (Stratton, 2007; Yang and Lei, 2007). However, it has also been shown that the results of a spherical approximation are not reliable in many cases (Nili and Green, 2014). Higher-order multipoles instead need to be solved using numerical methods to approximate the response of different shapes (Green and Jones, 2007; Ogbi *et al.*, 2012; Nili and Green, 2014). This requirement somewhat reduces the advantage of the EMM approach. In all these cases, the method is still limited to an electric field that is rotationally symmetric along the symmetry axis of the body.

An alternative approach to calculate the DEP force and torque is based on the rigorously formulated theory (presented in Sec. II) based on the use of the Maxwell stress tensor, which is referred to in the literature as the Maxwell stress tensor (MST) method (Wang, Wang, and Gascoyne, 1997). While the MST approach is comprehensive and accurate, it may be computationally expensive and almost always requires a numerical solution. Currently, there are several review papers that have discussed the effective moment method (Jones, 2003; Pethig, 2010). In the following, we present a summary of the EMM and review the key developments that have been made to apply this method to more complex problems. We then present the MST method based on the theory derived in Sec. II.C and discuss scenarios where using the MST method is essential.

B. Effective moment method and its limitations in complex problems

DEP and the electrorotation response of biological materials have a strong dependence on the frequency of the

nonuniform electric field, and the conductivity of both the ambient medium and the biological material. In the effective moment method, the biological material is replaced by a multipole. For example, a sphere that is exposed to a nonuniform external electric field $\mathbf{e}^e$ that varies over a length scale much larger than the radius of the sphere may be approximated with a single "point" dipole with moment $\mathbf{p}^{\text{tot}}$ (Jones, 2003). Thus, all shape information is lumped into the three-component dipole vector $\mathbf{p}^{\text{tot}}$ in this approximation. The induced electrostatic potential of the sphere is then compared to that of a physical dipole to derive the effective moment. The corresponding force and torque exerted on the sphere are then calculated by substituting this effective moment into the following equations (Lorrain and Corson, 1970; Jones, 2003):

$$\mathbf{F} \approx (\mathbf{p}^{\text{tot}} \cdot \nabla)\mathbf{e}^e \tag{62}$$

and

$$\mathbf{T} \approx \mathbf{p}^{\text{tot}} \times \mathbf{e}^e, \tag{63}$$

respectively.[19] In this approximation, we have kept only the leading-order term in the multipole expansions of the fields.

For a sphere with complex permittivity $\epsilon^{(c)}$ and radius R inside an ambient liquid with permittivity $\epsilon^{(l)}$, we can solve the associated electrostatic problem [see Eqs. (3) and (4)]

$$\begin{aligned} \nabla \cdot (-\epsilon(\mathbf{x})\nabla\xi) &= 0 \quad \text{in } \mathbb{R}^3, \\ -\nabla\xi(\mathbf{x}) &\to \mathbf{e}^e \qquad \text{as } |\mathbf{x}| \to +\infty, \end{aligned} \tag{64}$$

where $\epsilon(\mathbf{x}) = \epsilon^{(c)}$ inside the sphere and is equal to $\epsilon^{(l)}$ elsewhere. Upon solving the previously mentioned boundary value problem for a uniform external electric field $\mathbf{e}^e$, we find that the polarization on the sphere is uniform and given by

---

[19]Using index notation, $F_i = p_j^{\text{tot}}\partial_j e_i^e$ and $T_k = \varepsilon_{ijk} p_i^{\text{tot}} e_j^e$.

$\mathbf{p} = 3\epsilon^{(l)} K \mathbf{e}^e$; hence, using Eq. (62), the dielectrophoretic force is derived as (Pohl, 1958; Jones, 1995)

$$\mathbf{F} = 2\pi R^3 \epsilon^{(l)} K \nabla |\mathbf{e}^e|^2, \qquad (65)$$

where

$$K = \frac{\epsilon^{(c)} - \epsilon^{(l)}}{\epsilon^{(c)} + 2\epsilon^{(l)}} \qquad (66)$$

is the Clausius-Mossotti factor. For $K > 0$, the electric permittivity of the body is higher than the surrounding medium and the body moves toward the region with a strong electric field [positive DEP (pDEP)]. For $K < 0$, the opposite effect takes place when the surrounding medium has a higher electric permittivity and the body moves toward the region with the weaker electric field [negative DEP (nDEP)]; see Fig. 5. In practical biological applications, nDEP is preferred since the cell is not exposed to potentially harmful strong electric fields. Equation (65) can be used to derive other properties in the DEP process such as the length of the chain of particles formed. Under the right circumstances (dictated by how closely the approximations inherent in the equations are realized), these equations have been found to agree well with experiments (Pohl, 1958, 1978).

Biological cells are heterogeneous structures that are made of several organelles across different layers with differing permittivities. Accordingly, replacing a cell with a sphere of uniform permittivity is an oversimplification and, depending on the context, more complex models may be needed to simulate the electrical response of a cell. Within the EMM, a biological cell can be modeled using a spherical shell instead of just a solid sphere. The permittivity of the shell and cell interior is then replaced by an "effective" permittivity using the same approach that was used to derive the effective moment (Jones, 1995; Sukhorukov et al., 2001). For a body with multiple layers, the effective permittivity is calculated by repeating this procedure for each layer (Hu, Joshi, and Beskok, 2009). This effective permittivity can be used in Eq. (65) to calculate the force exerted on the cell.

Experimental observations indicate the strong effect of the frequency of the electric field and the conductivity of the cell and its neighboring medium on their dielectrophoretic response. Therefore, a theory based on static dielectric constants can be inadequate. In a more realistic theory, the effect of both conductivity and frequency should be considered. The DEP force exerted on the body is a function of the effective dielectric constant (ϵ) of the body and the medium. Further, in some applications of DEP, the dipole approximation of the body does not provide accurate results. For instance, the megahertz range frequency of an electric field allows generation of a negative DEP force in the solution that can be used to trap cells singly or as aggregates (Voldman et al., 2001; Gray et al., 2004). In this application, it is necessary to have a high gradient electric field for the DEP force to be significant. As a result of the high gradient, a dipolar approximation of the body is too inaccurate (Schnelle et al., 1999), and higher-order multipolar approximations are needed.
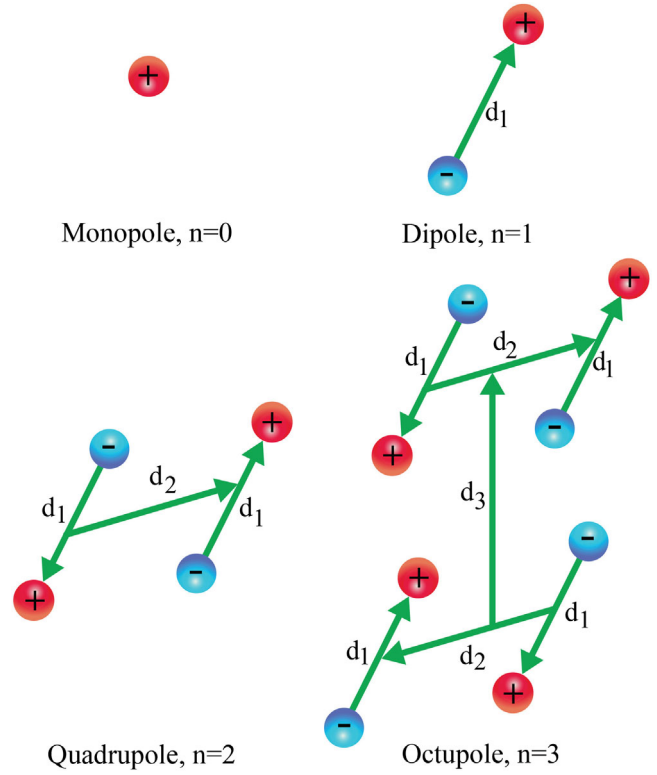

FIG. 6. Stratton scheme (Stratton, 1941) for generation of the moment of a general multipole of order $n + 1$ using two particles of opposite polarity of order n displaced by the vector d_{n+1}. From Jones and Washizu, 1996.

To overcome the limitation of the dipolar approximation, the effective multipole method (Jones and Washizu, 1996) employs higher-order multipoles of ascending order (Stratton, 1941); see Fig. 6. Using these multipoles, the general expression for DEP force and torque can be derived to any desired degree of accuracy. Consider a spherical dielectric body with a complex permittivity ϵ^c of radius R, placed in a medium with a complex permittivity constant $\epsilon^{(l)}$ under the external time-dependent electric field of the form

$$\mathbf{e}^e(\mathbf{r}, t) = \mathrm{Re}[\underline{\mathbf{e}}(\mathbf{r}) \exp(i\omega t)], \qquad (67)$$

where the complex quantity $\underline{\mathbf{e}}(\mathbf{r})$ is the phasor electric field vector. The DEP force on the body can be derived using the usual multipole expansion, as described earlier. The general expression of the time averaged DEP force and electrorotation torque are found as follows (Jones and Washizu, 1996):

$$\langle \mathbf{F}^{(n)} \rangle = \frac{1}{2} \mathrm{Re} \left[\frac{\mathbf{p}^{(n)}[\cdot]^{(n)}(\nabla)^{(n)} \underline{\mathbf{e}}^*}{n!} \right] \qquad (68)$$

and

$$\langle \mathbf{T}^{(n)} \rangle = \frac{1}{2} \mathrm{Re} \left[\frac{1}{(n-1)!} [\mathbf{p}^{(n)}[\cdot]^{(n-1)}(\nabla)^{(n-1)}] \times \underline{\mathbf{e}}^* \right], \qquad (69)$$

respectively. In Eq. (68) the symbol $[\cdot]^{(n)}$ is the n dot product on the tensors, $(\nabla)^{(n)}$ is the n vector ∇ operation, and the

asterisk indicates the complex conjugate of the quantity. Moreover, the quantity $\mathbf{p}^{(n)}$ is the effective multipolar moment and may be calculated as

$$\mathbf{p}^{(n)} = \frac{4\pi\underline{\varepsilon}^l R^{2n+1} n}{(2n-1)!!} \underline{K}^{(n)} (\nabla)^{n-1} \underline{\mathbf{e}}, \tag{70}$$

where $\underline{\varepsilon}^l = \mathrm{Re}(\varepsilon^{(l)})$ and

$$\underline{K}^{(n)} = \frac{\varepsilon^c - \varepsilon^l}{n\varepsilon^c + (n+1)\varepsilon^l}. \tag{71}$$

The importance of higher-order moments for approximating the body was first investigated in a dielectrophoretic field cage where the experiments showed a significant contribution of the quadrupole forces for particles larger than a quarter of the electrode spacing (Schnelle *et al.*, 1999). The evolution of biomedical technology toward microelectrodes and nano-electrodes (Hughes, 2000; Freer *et al.*, 2010) (see Fig. 7) has resulted in an increase in the number of cases where a higher-order approximation is inevitable. Moreover, under the effect of an external uniform field, the only nonzero moment of a spherical body is a dipole, but for nonspherical bodies higher-order moments can become nonzero (Nili and Green,

2014). This fundamental difference is important because, despite the fact that shape approximation by a sphere is an attractive model widely used for force calculation in DEP (due to its simplicity), most biological cells are not spherical. Higher-order moment terms are shown to constitute more than 40% of the DEP force on nonspherical bodies such as ellipsoidal and cylindrical particles (Nili and Green, 2014).

C. Maxwell stress tensor approach

As previously indicated, an alternative approach to calculating the DEP force is to determine the variations of the total electrical energy of the body (Pohl and Crane, 1972) with respect to changes in the geometric configurations. From the discussions in Sec. II.C, using Eq. (32) the DEP force and electrorotation torque on a body can be written as

$$\mathbf{F}^{\mathrm{DEP}} = \int_{\partial\Omega^+} \boldsymbol{\sigma}_{\mathrm{MW}} \mathbf{n} \, dA \tag{72}$$

and

$$\mathbf{T}^{\mathrm{ROT}} = \int_{\partial\Omega^+} \mathbf{x} \times (\boldsymbol{\sigma}_{\mathrm{MW}} \mathbf{n}) \, dA, \tag{73}$$

respectively.[20] Upon solving Eq. (64) for local electric fields, we can calculate the exact DEP force and electrorotation torque on the particle using the previously mentioned integrals; see Rosales and Lim (2005) and Al-Jarro *et al.* (2007). In addition, using a calculation similar to that in Sec. III.B, we can elucidate the precise approximation behind the EMM formulas (62) and (63).

Unlike the EMM formulas (68) and (69), the MST method based on Eqs. (72) and (73) is not restricted to spherical homogeneous particles as long as the electrical field is obtained by solving the boundary value problem in Eq. (64). The MST method is essential for an accurate estimate of the DEP force and electrorotation torque if the cell dimension is comparable to that of the electrode (Khoshmanesh *et al.*, 2011) or if the cell moves to the proximity of the electrode and the cell itself can affect the electric field. Note that the MST approach has also been combined with models that account for cell membrane
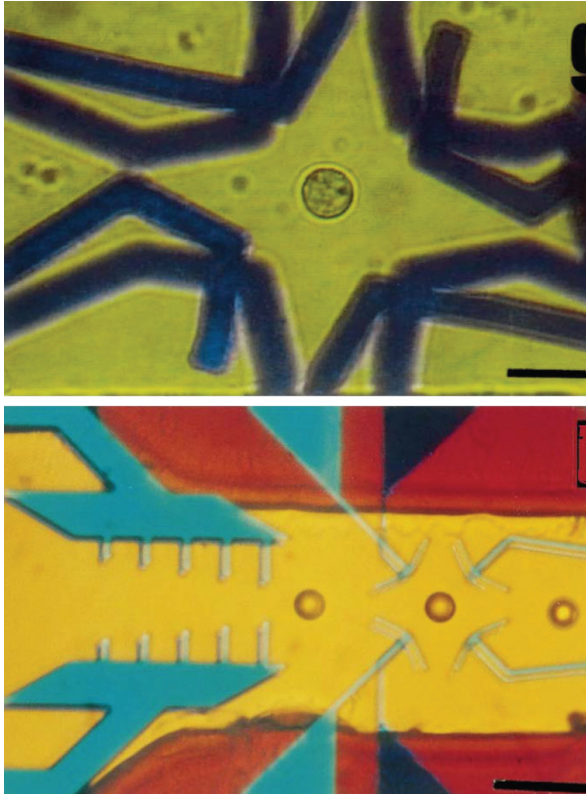

FIG. 7. Thin microelectrodes of 200 nm thickness used for imposing DEP force on biological cells. Top panel: electric field of 8 V with a frequency of 5 MHz is used to trap Jurkat cells within the microsystem. The bar represents 20 μm. Bottom panel: electric field of 5 V with a frequency of 10 MHz is used to position latex particles in different field minima of the microsystem. The bar represents 50 μm. From Müller *et al.*, 1999.

---

[20]Consider an electric field harmonically varying in time with the form

$$\mathbf{e}(\mathbf{r}, t) = \mathrm{Re}[\mathbf{e}(\mathbf{r}) \exp(i\omega t)] = \tfrac{1}{2}[\mathbf{e}(\mathbf{r}, t) + \mathbf{e}^*(\mathbf{r}, t)] \tag{74}$$

in the conductive medium and body. Substituting this electric field into the Maxwell stress tensor (32), we can divide the stress into two parts (Wang, Wang, and Gascoyne, 1997): the time averaged term

$$\boldsymbol{\sigma}'_{\mathrm{MW}^{(1)}} = \tfrac{1}{4}\mathrm{Re}(\xi)[(\mathbf{e} \otimes \mathbf{e}^* + \mathbf{e}^* \otimes \mathbf{e}) - |\mathbf{e}|^2 \mathbf{I}] \tag{75}$$

and the instantaneous term

$$\boldsymbol{\sigma}'_{\mathrm{MW}^{(2)}} = \tfrac{1}{4}\mathrm{Re}(\xi)[\mathbf{e} \otimes \mathbf{e} + \mathbf{e}^* \otimes \mathbf{e}^* - \tfrac{1}{2}(\mathbf{e} \cdot \mathbf{e} + \mathbf{e}^* \cdot \mathbf{e}^*)\mathbf{I}], \tag{76}$$

which vanishes under time averaging.

viscoelasticity, which then has been used to calculate the viscosity and shear elastic modulus of red blood cells (Engelhardt, Gaub, and Sackmann, 1984; Engelhardt and Sackmann, 1988). Moreover, the MST method can be applied to the DEP-induced electrodeformation of biological cells (Qiang *et al.*, 2018).

We can obtain either positive or negative DEP depending on whether the particle is more or less polarizable than the medium at a given applied frequency. There is a critical frequency at which we switch between nDEP and pDEP (Fig. 5). In such a case, in Eq. (66) the factor K will become a function of frequency-dependent dielectric constants. We may then define the so-called crossover frequency for a DEP device at which the DEP force is zero. The crossover frequency can be evaluated both experimentally (Green and Morgan, 1999; Wei, Junio, and Daniel Ou-Yang, 2009; Honegger *et al.*, 2011) and theoretically. The theoretical evaluation of the crossover frequency is usually based on the effective dipole moment method due to its simplicity. However, for the case of spherical particles, when compared to numerical analysis using the MST approach, the dipole moment method was shown to be inaccurate and to significantly overestimate the crossover frequency for particles with a diameter larger than 4.6 μm (Weng *et al.*, 2016). This critical diameter is important given that most biological cells have larger diameters.

Another instance where an application of the MST approach has proven to be necessary is in the analysis of DEP and electrorotation of particle-particle and particle-wall interactions. The particle-particle interaction is important when suspended particles that are randomly distributed in a medium are subjected to a uniform electric field and form an oriented chain structure along the direction of the electric field (Takashima and Schwan, 1985; Velev, Gangwal, and Petsev, 2009). The so-called pearl chain that forms in this process brings the particles into proximity with each other. Thus, the symmetry of the nonuniform electric field around the center of the particle breaks, which induces a mutual DEP force on each particle. It has been suggested that the resulting interaction-induced DEP force depends on the size of particles, the interparticle distance, and a characteristic length scale that quantifies the nonuniformity of the electric field (Kadaksham, Singh, and Aubry, 2005); see Fig. 8. The particle-wall interaction is important since most of the applications of DEP occur in channel-bounded devices. The magnitude of the DEP forces due to this interaction depends on the separation gap between the particle and the wall.

An application of the EMM method for analyzing a particle-particle interaction is valid when the distance between the particles is larger than the particle diameter (Aubry and Singh, 2006; Kang and Li, 2006). In the general case, the use of the MST method is necessary. In the literature, the MST model has been applied to particle-particle interactive motion (Ai and Qian, 2010) and particle-wall interaction (Kang, 2015) using different numerical schemes (Kang and Li, 2006; House, Luo, and Chang, 2012; Hossan *et al.*, 2013).

In the MST approach to particle-particle and particle-wall interactions, the effect of hydrodynamic forces can be accounted for by assuming a viscous fluid with a small Reynolds number. The mass and momentum conservation of the fluid is given by the following Stokes equations:
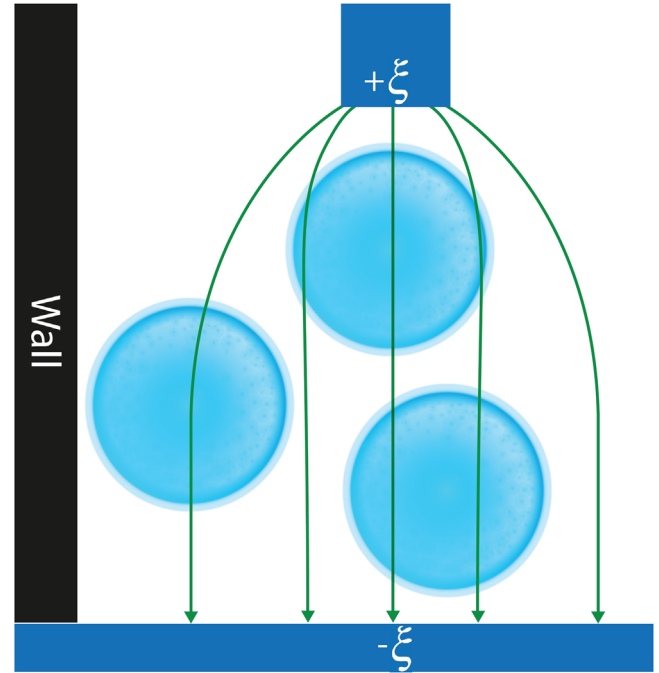

FIG. 8. In a system of multiple particles in proximity to a wall, the interaction of particles with each other and the surrounding wall can break the symmetry of the electric field around the center of each particle and induce a mutual DEP force between them. The resulting force is a function of the particle size, the interparticle (wall-particle) distance, and a characteristic length scale that quantifies the nonuniformity of the electric field.

$$\text{Re}\frac{\partial \mathbf{v}}{\partial t} - \nabla^2 \mathbf{v} - \nabla p = 0, \quad \nabla \cdot \mathbf{v} = 0, \tag{77}$$

where Re is the Reynolds number and $\mathbf{v}$ and p are the fluid velocity and pressure, respectively. The fluid velocity on the jth particle surface is

$$\mathbf{v}^j = \mathbf{V}^{pj} + \boldsymbol{\omega}^{pj} \times (\mathbf{x}^{sj} - \mathbf{x}^{pj}), \tag{78}$$

where $\mathbf{V}^{pj}$ and $\boldsymbol{\omega}^{pj}$ are the translational and rotational velocities of the jth particle and $\mathbf{x}^{sj}$ and $\mathbf{x}^{pj}$ are the position vector of the surface and the center of the particle, respectively. The hydrodynamic force exerted on each particle is then

$$\mathbf{F}^{\text{hydro}:j} = \int \boldsymbol{\sigma}_H \mathbf{n} dA^j, \tag{79}$$

where

$$\boldsymbol{\sigma}_H = -p\mathbf{I} + [\nabla \mathbf{v} + (\nabla \mathbf{v})^{\text{T}}] \tag{80}$$

is the Cauchy stress tensor. Consequently, using Eqs. (72), (73), and (79) the translation and rotation of the jth particle is described by

$$m^{pj}\frac{d\mathbf{V}^{pj}}{dt} = \mathbf{F}^{\text{DEP}} + \mathbf{F}^{\text{hydro}} \tag{81}$$

and

$$I^{pj}\frac{d\boldsymbol{\omega}^{pj}}{dt} = \int (\mathbf{x}^{sj} - \mathbf{x}^{pj}) \times [(\boldsymbol{\sigma}_{\mathrm{MW}} + \boldsymbol{\sigma}_H)\mathbf{n}]dA^j, \quad (82)$$

where m^{pj} and I^{pj} are the mass and moment of inertia of the jth particle.

Simulation results based on the previous equations have shown that nDEP particle-particle interactions tend to align particles parallel to the dc field while pDEP tends to chain the particles perpendicular to the field. Further, the particle-particle interaction has also been investigated for an ac electric field using a transient numerical method (Ai, Zeng, and Qian, 2014). This model accounts for the coupling in particle–fluid–electric field interactions and showed that the nDEP always tends to align the particles parallel to the applied ac field.

Finally, we highlight that most of the aforementioned studies consider the dielectric bodies to be rigid. However, biological cells often undergo large deformations under the effect of the electric field. Few works have attempted to combine DEP and electrodeformation of the cell. Exceptions include works that studied the combined effect for droplets (Kim *et al.*, 2007; Singh and Aubry, 2007; Zagnoni and Cooper, 2009). In an experimental study (Guido, Jaeger, and Duschl, 2009), the mechanical properties of the cell were measured using the deformation of the cell under the effect of the DEP force. Deformation of a cell under hydrodynamic and electrical forces in a cell trap was studied numerically (Le Duc *et al.*, 2008) for a single cell, but the bending energy of the membrane was neglected. In another study, the dynamic behavior of two cells under a nonuniform electric field involving stretching and bending of the membrane as well as intercellular aggregation was investigated using the MST method (Ye, Li, and Lam, 2011).

IV. TOPOLOGICAL AND MORPHOLOGICAL CHANGE IN LIPID MEMBRANES UNDER AN EXTERNAL ELECTRIC FIELD

A biological cell will deform under the action of an external electrical field even if the net force on the cellular body is zero and there is no motion. The deformation can be due to flexoelectricity or (more commonly) the Maxwell stress mechanism. Cell membranes play a central role in the mediation of the interaction between the mechanical deformation of the cell and the electrical field. The lipid bilayer is impermeable to ions and water molecules and ion channels regulate what passes in and out of the cell. Electrically speaking, the membrane can be thought of as a dielectric capacitor embedded in an ambient conductive fluid; see Fig. 9. The surrounding fluid maintains a potential difference across the membrane and the *in vivo* transmembrane potential of the biological cells is governed by the ion concentration of the fluid inside and outside the cell. Typical values of this transmembrane potential range from -40 to -70 mV (Phillips *et al.*, 2012). However, this preexisting transmembrane potential can be altered by the application of an external electric field.

Under moderated electric fields, a vesicle merely deforms and changes shape; e.g., an initially spherical vesicle can
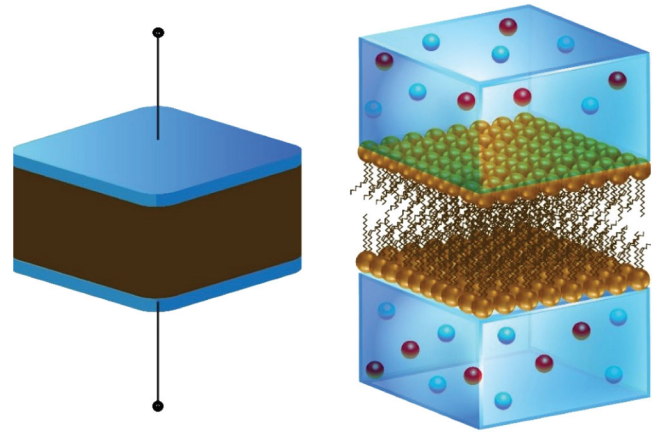

FIG. 9.   The lipid bilayer as a capacitor. The ionic solution acts as the electrode and the impermeable lipid bilayer is the dielectric material of the capacitor.

transform into prolate, oblate, or spherocylindrical shapes. High intensity electrical fields can create topological changes such as the formation of pores in the lipid membrane, and thus can increase permeability to drugs and charged molecules (Weaver and Chizmadzhev, 1996). The pore formation process can also trigger a fusion of vesicles provided that the vesicles are brought into contact (Chernomordik and Kozlov, 2008). These processes have important applications in biological science ranging from materials characterization to drug delivery (Vlahovska *et al.*, 2009; Kim and Lee, 2017; Kar *et al.*, 2018; Kotnik *et al.*, 2019).

Compared to lipid vesicles, the response of biological cells to electric fields is somewhat more complicated due to the presence of the cell cytoskeleton. The electric field can cause conformational changes in cytoskeleton elements such as actin filaments (Perrier *et al.*, 2019) and microtubules (Kirson *et al.*, 2004) and/or can modify the chemical compounds in the cytosol, which eventually may disrupt the elements of the cytoskeleton (O'Brien, Salmon, and Erickson, 1997). Evidence suggests that the disruption of cytoskeleton elements can affect membrane permeability when exposed to electric fields (Muralidharan *et al.*, 2021). Further, it has been shown that electroporation of mammalian cells is directly related to the thickness and integrity of the actin structure (MacQueen *et al.*, 2012). Aside from these general observations, we avoid discussion of the role of the cytoskeleton in an electric field–cell interaction and refer the interested reader to a recent review of the growing research in this subfield (Graybill and Davalos, 2020). In this section, we summarize the physical modeling of the topological and morphological change in lipid membranes under the action of the electrical fields.

A. Electrodeformation

1. Experimental observations

The change of shape of a biological cell or a vesicle (electrodeformation) has been used to characterize the mechanical properties of cells (Chen *et al.*, 2011). Experimental observations (Riske and Dimova, 2005, 2006;
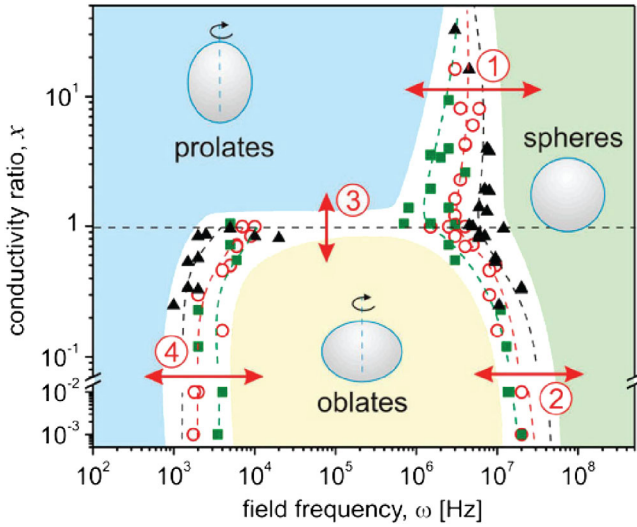
FIG. 10. Change in the lipid vesicle morphology in an ac field for different frequencies and conductivity ratios. The conductivity inside the vesicles in μS/cm is 15 (squares), 65 (open circles), and 130 (triangles). Four types of transition can be distinguished. At higher frequency and irrespective of the conductivity ratio, the vesicle exhibits a spherical shape. The two arrows show the transitions from (1) prolate and (2) oblate shapes to the spherical shape. The third type of transition occurs at intermediate frequency level and by changing the conductivity ratio. The fourth type of transition is observed only for $\chi < 1$ and by increasing the frequency level. From Aranda et al., 2008.

Dimova et al., 2007; Aranda et al., 2008) show that the change in the morphology of the vesicle under an electric field depends not only on the type of the applied electric field (ac or dc) but also upon the frequency of the field and the conductivity of the interior and exterior solutions (σ_{int} and σ_{ext}, respectively); see Fig. 10. It is useful here to define the "capacitor" charging time as relevant for a biological cell or a vesicle. In the case of the membrane of a spherical vesicle, this timescale is defined as (Grosse and Schwan, 1992)

$$\tau^C = RC^m \left(\frac{1}{\sigma_{int}} + \frac{1}{2\sigma_{ext}} \right), \qquad (83)$$

where R is the vesicle radius, C^m is the membrane capacitance, and σ_{int} and σ_{ext} are the interior and exterior fluid conductivities, respectively. This characteristic timescale becomes important when one contends with exposure to ac electric fields or dc fields with different pulse durations. Since in a high frequency ac field the field direction changes faster than the time required for the ions to change, the vesicle remains spherical. However, as shown in Fig. 10, at low frequencies the vesicle can adopt a prolate shape (if $\chi = \sigma_{int}/\sigma_{ext} > 1$) or undergo a prolate-oblate transition (if $\chi = \sigma_{int}/\sigma_{ext} < 1$) at $\omega = 10^3$ Hz (Aranda et al., 2008). In a dc field, the change in morphology of the vesicle depends on the ratio of the conductivity of the inner and outer fluids, as well as the duration of the exposure to the electric field (Riske and Dimova, 2005). For instance, vesicles are found to deform to a spherocylindrical shape in the presence of salts (Riske and Dimova, 2006). The spherocylindrical vesicles can adopt

prolate ($\chi > 1$) or oblate ($\chi < 1$) shapes. Riske and Dimova also implied that the exposure of a vesicle to an electric field for a prolonged period of time, even if the intensity is relatively weak, can result in the rupture of the vesicle, while exposure to a short pulsed high intensity field may not cause such a drastic effect. This claim needs further investigation, and Joule heating or electrochemical effects remain as relevant features to explore.

2. Theory of vesicle morphology in a uniform ac and dc field

The early theoretical studies aimed at understanding electrodeformation were based on the minimization of the total free energy of the lipid membrane in an ac field (Helfrich, 1974; Winterhalter and Helfrich, 1988a; Kummrow and Helfrich, 1991). The total free energy in these models involved Helfrich elastic bending energy of the membrane and the electrical energy defined over an initially spherical vesicle. The electrical energy W^{elect} of the system emerges from work done by the force due to the Maxwell stress tensor on the interfaces defined for three mediums: the interior fluid, the membrane, and the exterior fluid. As a simplifying assumption, earlier works would typically consider the conductance of the exterior and the interior fluids to be the same ($\sigma_{int} = \sigma_{ext} = \sigma_{water}$) (Winterhalter and Helfrich, 1988a). However, an extension of the model (Peterlin, 2010; Yamamoto et al., 2010) allowed for the asymmetric conductivity condition $\sigma_{ext} \neq \sigma_{int}$.

As we indicated in Sec. II.C, the mechanical effects of electrical fields can be directly accounted for by the Maxwell stress tensor. For an external ac field of constant amplitude, the stationary shape of the vesicle can be determined using the Euler-Lagrange equations (51). If the elastic behavior of the membrane is specified as the Helfrich-Canham membrane with the free-energy density function given by Eq. (53), the stationary shape is dictated by Eq. (57), which, under the assumption of small deflection in the sense that $(H - H_*)/H_* \sim \varepsilon \ll 1$, implies the following simplified equations on $\mathbb{S} = \partial\Omega$:

$$\kappa_b(H - H_*)H_*^2 + (\kappa_b/2)\Delta_s H - 2H\lambda - (\mathbf{t}_e + \mathbf{t}_b) \cdot \mathbf{n} = p, \qquad (84)$$
$$\nabla_s \lambda + \mathcal{P}_{\mathbf{n}}(\mathbf{t}_e + \mathbf{t}_b) = 0,$$

where the traction $\mathbf{t}_e$ due to the Maxwell stress is given by Eq. (46) and $\mathbf{t}_b \equiv 0$ if hydrodynamic effects are neglected.

The morphology of the vesicle under the application of an electrical field is largely dictated by the electric traction $\mathbf{t}_e$. Explicit solutions can be found for spherical vesicles by solving Eq. (40) if the external far field is uniform. In that case, the electric potential for the three media ($i = int, m,$ and ext) is given by (Jackson, 1962)

$$\xi^{(i)}(r, \theta) = -e_c^{(i)} r \cos\theta + \frac{\mu^{(i)} \cos\theta}{r^2}, \qquad (85)$$

where θ is the angle of the external electric field $\mathbf{e}^e$ with the position vector at each point and, assuming $e^{(int)} = e^{(ext)}$,

$$e_c^{(\text{int})} = \frac{9|\mathbf{e}^e|\beta}{(2+\beta)(1+2\beta) - 2\gamma^3(1-\beta)^2},$$

$$e_c^{(\text{m})} = \frac{3|\mathbf{e}^e|(1+2\beta)}{(2+\beta)(1+2\beta) - 2\gamma^3(1-\beta)^2},$$

$$e_c^{(\text{ext})} = |\mathbf{e}^e|,$$

$$\mu^{(\text{int})} = 0,$$

$$\mu^{(\text{m})} = \frac{3|\mathbf{e}^e|r_{\text{int}}^3(1-\beta)}{(2+\beta)(1+2\beta) - 2\gamma^3(1-\beta)^2},$$

$$\mu^{(\text{ext})} = \frac{|\mathbf{e}^e|(\gamma^3-1)(1-\beta)(1+2\beta)}{(2+\beta)(1+2\beta) - 2\gamma^3(1-\beta)^2}. \tag{86}$$

In Eq. (86) $\beta = \epsilon^{(\text{m})}/\epsilon^{(\text{int})}$, $\gamma = r_{\text{int}}/r_{\text{ext}}$, and r_{int} and r_{ext} are the interior and external radii of the vesicle, respectively.

The resulting vesicle shape at low frequencies of the electric field in this model is always prolate for the symmetric conductivity condition. The asymmetric conductivity condition can result in both prolate and oblate shapes. However, the quantitative results are not consistent with experimental observations (Yamamoto *et al.*, 2010). The underlying mechanism responsible for the observed shape transition is suggested to be the electric pressure of the Maxwell stress, as well as the force density resulting from the interaction of the electric field with the accumulated charges by the so-called Maxwell-Wagner mechanism; see Fig. 11 (bottom panel).

The basic developments described thus far have been extended in several ways. For example, Gao, Feng, and Gao (2009) considered additional contributions of surface tension and flexoelectricity. They found that flexoelectricity can significantly impact the morphology of vesicles in an electrical field and induce asymmetry in its evolution. They also noted that flexoelectricity may cause a change in the equilibrium position of a vesicle in an electric field (compared to if flexoelectricity is ignored), thus opening up the prospects for using vesicle flexoelectric coupling as a route to manipulating cells and vesicles.

A more comprehensive theory that enjoys good quantitative agreement with experimental observations takes into account the variation of membrane tension resulting from the conserved number of lipid molecules in each monolayer, as well as the hydrodynamics of the interior and exterior media (Vlahovska *et al.*, 2009; McConnell, Vlahovska, and Miksis, 2015; Liu *et al.*, 2017). Such a framework can be developed based on the balance of all the forces exerted on the membrane. Denote by $\mathbf{y} = \mathbf{x}(\cdot, t)$ a time-dependent parametrization of the current configuration $\partial\Omega_t$ of the membrane and by $\mathbf{v}^{(i)}(\cdot, t)$ ($i = \text{ext}, \text{int}$) the velocity field. The flows then necessarily satisfy the following Stokes equations:

$$\mu^{(i)}\nabla^2\mathbf{v}^{(i)} - \nabla p^{(i)} = 0, \quad \nabla \cdot \mathbf{v}^{(i)} = 0, \tag{87}$$

where $\mu^{(i)}$ denotes the viscosity of the interior and exterior fluids. On the interface $\partial\Omega_t$, we assume that there is no slippage between the membrane and flow, implying that

$$\mathbf{v}^{(\text{ext})} = \mathbf{v}^{(\text{int})} = \mathbf{v}^{(\text{m})} := \frac{d\mathbf{x}}{dt} \quad \text{on } \partial\Omega_t. \tag{88}$$
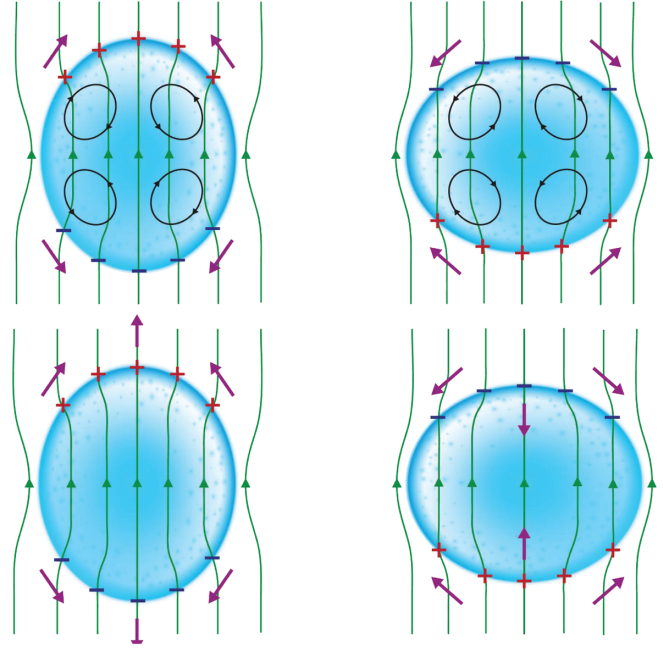

FIG. 11. The suggested underlying mechanism of electrodeformation based on electrohydrodynamic forces and the surface charge accumulation. Top panel: a vesicle in an electric field experiencing the streamlines of the electrohydrodynamics (EHD) flow and the surface charge distributions. For the vesicle to the left (right) the interior fluid is more (less) conductive than the exterior one and the resulting shape is prolate (oblate) because the EHD flow pushes fluid toward the poles (equator). From Vlahovska *et al.*, 2009. Bottom panel: electric charge distribution using the Maxwell-Wagner mechanism on a vesicle in the electric field. The interaction of the accumulated charge with the electric field results in force densities that for the left (right) vesicle, where $\sigma_{\text{int}} > \sigma_{\text{ext}}$ ($\sigma_{\text{int}} < \sigma_{\text{ext}}$) creates prolate (oblate) shapes. Adapted from Yamamoto *et al.*, 2010.

The boundary value problems in Eqs. (87) and (88) completely determine the interior and exterior flows for any given motion of the membrane $\mathbf{v}^{(m)}$, and hence determine the hydrodynamic traction on the membrane in terms of $\mathbf{v}^{(m)}$:

$$\mathbf{f}^{\text{hydro}} = \mathbf{f}^{\text{hydro}}[\mathbf{v}^{(m)}] = (\mathbf{T}^{\text{hydro:ext}} - \mathbf{T}^{\text{hydro:int}})\mathbf{n}, \tag{89}$$

where

$$T_{jk}^{\text{hydro}} = -\delta_{jk}p + \mu\left(\frac{\partial v_j}{\partial x_k} + \frac{\partial v_k}{\partial x_j}\right). \tag{90}$$

Setting $\mathbf{t}_b = \mathbf{f}^{\text{hydro}}[\mathbf{v}^{(m)}]$ and $p = p^{(\text{int})} - p^{(\text{ext})}$ in Eq. (84), we obtain an evolution equation for the parametrization $\mathbf{y} = \mathbf{x}(\cdot, t)$. Explicit solutions were obtained for quasispherical membranes by Liu *et al.* (2017).

According to the results of this model, at low frequencies prolate deformation occurs due to the electric pressure resulting from polarization charges pulling the vesicle at the poles. On the other hand, the oblate shape occurs due to the negative pressure and transient electrohydrodynamic flow resulting from the induced free surface charges; see Fig. 11 (top panel).
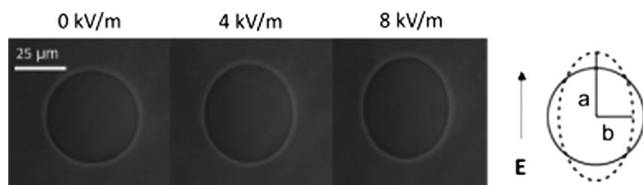
FIG. 12. An initially spherical vesicle deforms into an ellipsoid under a uniform ac electric field. This electrodeformation may be used to determine the electromechanical properties of the membrane. From Faizi, Dimova, and Vlahovska, 2021.

In practical applications pertaining to the electrodeformation of vesicles, a well-calibrated theory can be used to extract electromechanical properties of membranes, such as bending rigidity, tension, and capacitance, through a stepwise increase of the ac field strength and recording the shape deformation of the vesicle (Harbich and Helfrich, 1979; Niggemann, Kummrow, and Helfrich, 1995; Gracia et al., 2010; Faizi, Dimova, and Vlahovska, 2021), as shown in Fig. 12.

Unlike the stationary shapes of the vesicle under an ac field, vesicle deformation under a short pulsed dc field is transient and dynamic (Dimova et al., 2009). The electric field used in these experiments often has a high strength and result in poration of the membrane. Owing to the transient nature of the response, for vesicles that are hundreds of nanometers in size, direct optical observation is difficult and alternative techniques are used to extract data about poration, and deformation of the vesicle (Kakorin, Liese, and Neumann, 2003). In contrast, when giant vesicles of tens of micrometers in size are used in the experiments, the direct optical observation can provide significant useful information about the dynamic response of the vesicle. A high-speed imaging system is used to study the deformation and relaxation of the vesicle, and the observed results are explained using the effect of the Maxwell stress tensor (Riske and Dimova, 2005) that results in the following lateral tension in the membrane (also called electric tension) λ_e (Needham and Hochmuth, 1989):

$$\lambda_e = \epsilon \left(\frac{t}{2t_e^2} \right) \xi_{\text{trans}}^2, \tag{91}$$

where t is the total thickness and t_e is the dielectric thickness of the lipid membrane. As with the ac field, the deformation depends on the ratio of the conductivity of the solution inside and outside the vesicle. However, at a critical value of the transmembrane potential the poration process begins (see Sec. IV.B) and the bilayer becomes conductive and permeable. Thus, below the electroporation limit the vesicle keeps its integrity and behaves like a dielectric insulator, while above the threshold due to the poration and leakage of the volume no area or volume conservation is in place and the deformation can depend on the change in area or volume (Riske and Dimova, 2005). Thus, to create a prolate-oblate transition using a dc field, the single pulse should remain below the poration threshold. However, such pulse intensity might not be strong enough to allow observation of the transition. A proposed solution to this problem involves the application of a two-step pulse where the first pulse has a high intensity but its duration is less than the characteristic timescale of the
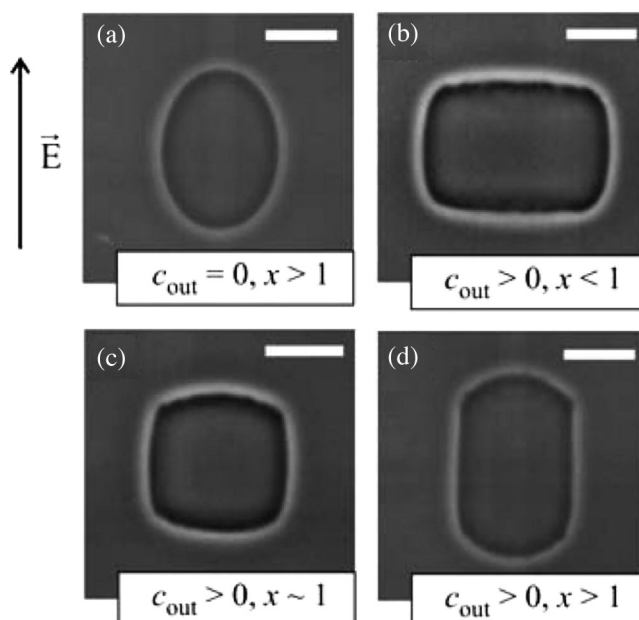

FIG. 13. Electrodeformation of vesicles under a dc field. (a) If there is no salt in the exterior solution, the vesicle will deform into a prolate shape. If salt is added to the exterior solution, depending on the conductivity ratio of the exterior to the interior solution, the vesicle can deform into (b) a disk, (c) a square, or (d) a tube. From Riske and Dimova, 2006.

membrane τ^C and the second pulse has an intensity lower than the poration threshold. If $\sigma_{\text{int}} < \sigma_{\text{ext}}$, under this two-step pulse the vesicle first adopts an oblate shape and then transitions to a prolate spheroid shape (Salipante and Vlahovska, 2014).

The conductivity ratio is not the only factor that regulates the shape of the vesicle deformation under a strong dc field. In the presence of salt outside the vesicle, irrespective of its content, a somewhat irregular deformation of the vesicle may be observed (Riske and Dimova, 2006). The presence of salt adds a compressive force perpendicular to the electric field that results in alignment of the vesicle wall with the electric field lines (Riske and Dimova, 2006). When $\sigma_{\text{int}} < \sigma_{\text{ext}}$ the vesicle deforms into a disk shape, when $\sigma_{\text{int}} \sim \sigma_{\text{ext}}$ the vesicle adopts a squarelike cross section, and when $\sigma_{\text{int}} > \sigma_{\text{ext}}$ the vesicle deforms into a short-lived prolate shape (Riske and Dimova, 2006); see Fig. 13.

B. Electroporation

1. Experimental observations

A high intensity external electric field can form transient and conductive electropores in cell membranes (Fig. 14). This well-studied phenomenon of electroporation has been widely used to transport drugs, DNA, nucleic acids, and other types of molecules into the cell (Sukharev et al., 1992; Gehl and Mir, 1999; Xie et al., 2013; Frandsen, Vissing, and Gehl, 2020).

Early studies of cell membranes (during the 1950s and 1960s) under high intensity electric fields showed that at a critical membrane potential a sudden increase in transmembrane current occurs (Stampfli, 1958; Crowley, 1973; Zimmermann, Pilwat, and Riemann, 1974; Hibino et al.,
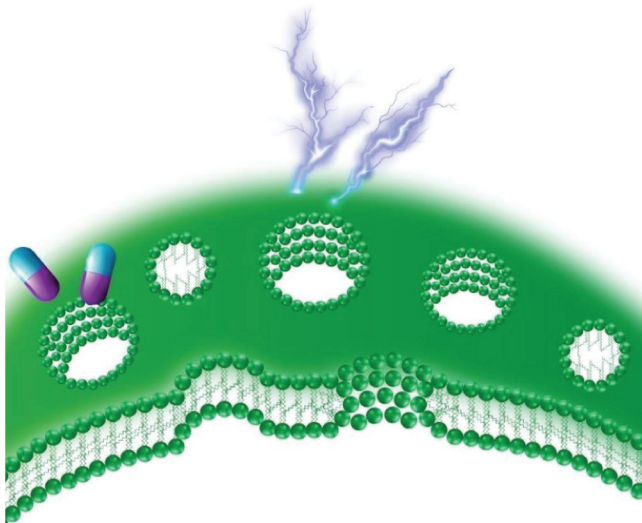
FIG. 14. Illustration of electroporation in lipid bilayers. The pores can be unstable hydrophobic pores or metastable hydrophilic pores. The mechanism can be used to deliver different materials from drugs to DNA molecules into the cell.

1991). The dielectric breakdown of the membrane and formation of pores was suggested as the reason behind the increase in current. No direct evidence of electroporation was initially found, and this phenomenon was primarily studied using indirect indicators[21] such as the change in transmembrane potential and the change in fluorescence of membrane in the presence of fluorescence dye (Kinosita et al., 1988; Bartoletti, Harrison, and Weaver, 1989; Tekle, Dean Astumian, and Boon Chock, 1991; Djuzenova et al., 1996; Sun et al., 2006; Pakhomov et al., 2007). Some of these characterization approaches revealed that pores could also be resealed without permanent damage to the cell membrane (reversible electroporation), provided that the electric field is applied in short pulses and the ensuing transmembrane potential difference does not exceed a threshold that is governed by the type of cell and the electrical field pulse parameters (Baker and Knight, 1978; Benz, Beckers, and Zimmermann, 1979; Gauger and Bentrup, 1979; Lopez, Rols, and Teissie, 1988; Weaver and Chizmadzhev, 1996). The formation of these reversible pores then forms a facile route for introducing small molecules (such as drugs and DNA) into the cell (Zimmermann, Vienken, and Pilwat, 1980; Wong and Neumann, 1982; Fromm, Taylor, and Walbot, 1986). However, a transmembrane potential larger than the threshold or with a sufficiently long pulse duration can result in the expansion of the pores and rupture of the lipid membrane (irreversible electroporation) (Abidor et al., 1979).

One important feature of this phenomenon is that the membrane lifetime, defined as the time span after the application of a high intensity electric field and prior to formation of the pores, does not show a deterministic

---

[21]Experimental methods are rapidly being developed (Nguyen et al., 2012; Sengel and Wallace, 2016) that may provide direct information on cellular deformation and phenomenon such as electroporation.

behavior. In fact, repeating the same experiment on lipid membranes shows that, while the transmembrane current after the breakdown is qualitatively similar, the lipid membrane lifetime behaves stochastically. Higher intensity electric fields increase the probability of rupture of the lipid membrane and decrease the membrane lifetime (Abidor et al., 1979; Benz, Beckers, and Zimmermann, 1979).

2. Simplified theoretical models

Many of the simpler models do not explicitly model the pore itself. We first describe a minimal theoretical model of electroporation before discussing the state-of-the-art models. This model is based on the notion that once a "critical" electric field is reached in the membrane a pore will be formed. Prior to the sudden increase in the conductivity of the membrane (upon the pore formation), Maxwell's equations (3) and (4) are used to calculate the resulting transmembrane potential under the action of an imposed external electric field. For instance, exerting a field $\mathbf{e}_0$ on a spherical cell induces transmembrane potential that can be calculated to be (Plonsey and Altman, 1988; Vernier et al., 2004)

$$\xi_{\text{trans}} = 1.5R|\mathbf{e}_0|\cos\theta[1 - \exp(-t/\tau^C)], \tag{92}$$

where θ is the angle between tangents at the site on the spherical cell, τ^C is the membrane charging time constant as described by Eq. (83), t is the time after initiation of the external field, and R is the cell radius. The transmembrane potential can be related to the membrane lateral tension using Eq. (91). If the critical lateral tension required for membrane rupture is known, then the model can predict the critical membrane potential at which electroporation will occur. This model has been applied to problems involving small external electric fields where the transmembrane potential $\xi_{\text{trans}} <$ 500 mV (Needham and Hochmuth, 1989; Vernier et al., 2004). However, this simplified model is unable to describe many features of the electroporation phenomenon, such as the mechanistic underpinnings of why pores are formed and the stochasticity of the membrane lifetime.

The initial efforts to describe the pore formation relied on deterministic theories suggesting that electromechanical collapse of the lipid membrane results in rupture (Crowley, 1973). The lipid membrane in this approach is replaced by a uniform isotropic elastic material sandwiched between two semi-infinite electrically conducting liquids. The liquids maintain a fixed transmembrane potential, and hence an electrical pressure $P_e = (1/2)\varepsilon_d(\xi/t)^2$ is exerted on the membrane. Assuming a constant Young's modulus E, the total compression of the elastic membrane can be derived by integrating Hooke's law over the thickness of the membrane and equating it with the electrical pressure as follows:

$$E\int_{t_0}^t \frac{dt'}{t'} = E\ln\left(\frac{t}{t_0}\right) = -\frac{1}{2}\varepsilon_d\left(\frac{\xi}{t}\right)^2, \tag{93}$$

where t_0 is the original thickness of the membrane. It can be shown that the compression of the elastic membrane derived from this equation diverges at $\varepsilon_d\xi^2/2Et_0^2 \simeq 0.18$, which indicates an electromechanical instability. This model overestimates
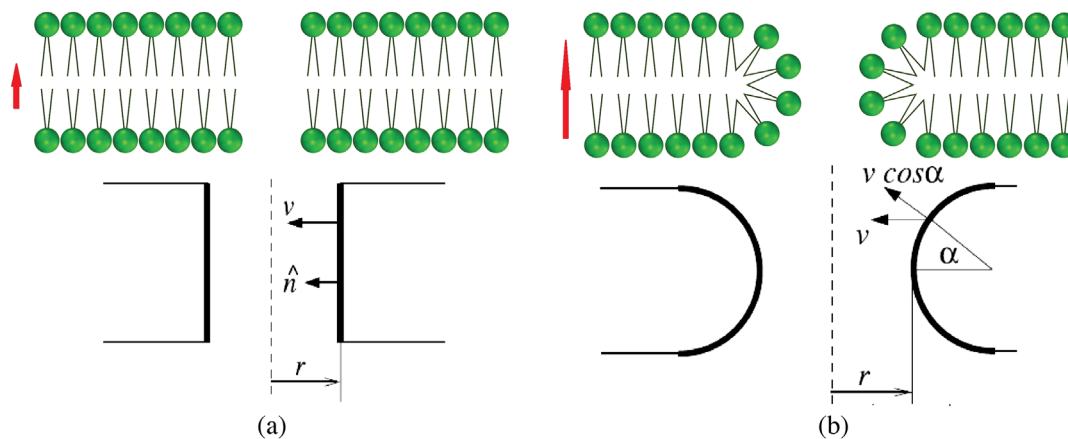
FIG. 15. Geometrical parametrization of the two types of pores: (a) hydrophobic and (b) hydrophilic. From Neu, Smith, and Krassowska, 2003.

the transmembrane potential required for the rupture of the membrane by an order of magnitude. Alternative approaches were developed to overcome this drawback. These include electrohydrodynamic stability models (Michael and O'Neill, 1970; Taylor and Michael, 1973), a wave instability model of the membrane that accounts for viscoelastic properties (Maldarelli *et al.*, 1980; Steinchen, Gallez, and Sanfeld, 1982), and a model that takes into account the effect of the electric field on the orientation of the lipid headgroup dipoles and its coupling with the membrane shape (Bingham, Olmsted, and Smye, 2010). While these alternative approaches were able to more accurately predict the critical transmembrane potential, they all failed to account for the stochastic behavior of electroporation as well as the strong dependence of the membrane lifetime on the transmembrane potential.

3. Theoretical models explicitly taking into account pore formation

The most comprehensive models consistent with experimental observation are stochastic in nature. They employ an energetic balance and the mechanics associated with the process of pore formation as a starting point. The initial step of electroporation is the formation of short-living hydrophobic pores; see Fig. 15(a). Next, owing to the inversion of lipids molecules on the edge of the pore, the hydrophilic pores will form; see Fig. 15(b).

In an initial model that accounts only for mechanical effects, formation of a pore can be considered a balance between the gain in the edge energy γ of the pore and the loss of surface tension energy Γ in the circular region of the pore (Litster, 1975; Taupin, Dvolaitzky, and Sauterey, 1975):

$$W^{\text{pore}}(r_p) = 2\pi\gamma r_p - \Gamma\pi r_p^2. \tag{94}$$

The energy contribution of the electrical effects was later included by Abidor *et al.* (1979) predicated on the notion that the lipid membrane behaves like a capacitor. The capacitance of the membrane changes once a pore is formed and the "lost" lipid membrane material is replaced by water. For a circular pore of radius r_p, the electrical energy contribution may be written as

$$W^{\text{elect}}(r_p) = \tfrac{1}{2}\pi C_{LW}\xi_{\text{trans}}^2 r_p^2,$$

where $C_{LW} = (\varepsilon_d^{(w)}/\varepsilon_d^{(m)} - 1)C_0$ is the change in the specific capacitance of the membrane with the pores, $\varepsilon_d^{(w)}$ and $\varepsilon_d^{(m)}$ are the permittivities of the pure water and lipid membrane, respectively, and C_0 is the capacitance of the pore free membrane. Upon minimizing $W^{\text{pore}} + W^{\text{elect}}$ against pore size r_p, with transmembrane potential ξ_{trans} as a parameter, we can predict whether the formation of pores is energetically favorable and, if so, the consequent equilibrium pore size.

The previously mentioned electrical energy assumes that both the membrane and water filling the pore are purely dielectric and the system is always kept at a fixed transmembrane potential ξ_{trans}. Such assumptions are valid only for small pores with negligible conductance. Even an extension of this model that accounts for the flow of current through the pores (Pastushenko and Chizmadzhev, 1982) is applicable only to instances that result in small pores ($r_p < 1$ nm) and does not provide accurate results for larger pores. Formation of small pores is often observed in experiments with high intensity electric field and short pulses (Kakorin and Neumann, 2002). However, experiments that are performed with the goal of delivering materials such as DNA into the cell require a larger pore size with diameters in the range of tens of nanometers.[22] Such larger pores can be created by using low intensity and long duration pulses[23] (Gehl and Mir, 1999; Vanbever *et al.*, 1999).

---

[22]The underlying mechanism of gene transfer is not well understood. For some DNA molecules, an endocytosislike mechanism follows electroporation (Chernomordik, Sokolov, and Budker, 1990). It has also been suggested that genes of all different sizes can get direct access to the cytosol, although it is not clear whether these genes translocate the membrane using large enough pores (Sachdev *et al.*, 2020). For a comprehensive review of these underlying mechanisms, see Rosazza *et al.* (2016).

[23]For decades, millimicrosecond pulses have been used in electroporation to facilitate DNA transfer. However, recently it was shown that gene transfer can also be achieved using nanosecond pulses by regulating pulse repetition frequency (Ruzgys *et al.*, 2018).

A more rigorous approach is necessary to account for the general behavior of the pores at all sizes and over the entire timescale of the poration process. Such a model includes electromechanical effects via the Maxwell stress and stochastic processes pertaining to the evolution of pores. To that end, we consider the geometry of the pore in Fig. 15. Both the membrane and the ambient fluid are assumed to be dielectric with complex dielectric constants. From a fundamental viewpoint, the electrical force that drives the formation and growth of pores has to be conservative and hence can be written as the derivative of the energy $W^{\text{elect}}(r)$. Accordingly, the rate of work done by the electrical forces on the membrane is given by (Neu, Smith, and Krassowska, 2003)

$$\frac{d}{dt} W^{\text{elect}}(r) = v \frac{d}{dr} W^{\text{elect}}(r) = \int_S v \cos \alpha (\mathbf{n} \cdot \boldsymbol{\sigma}_{\text{MW}} \mathbf{n}) da,$$

where $v = dr/dt$ is the rate of change of the pore radius, the Maxwell stress $\boldsymbol{\sigma}_{\text{MW}}$ is given by Eq. (32) and evaluated at the exterior boundary of the membrane, S is the surface of the pore (in Fig. 15), and $\mathbf{n}$ is the outward normal on the membrane. At any given pore radius, we can solve the electrostatics equation and find the Maxwell stress. For the cylindrical and toroidal geometry of the pore [which represents hydrophobic and hydrophilic pores, respectively, as shown in Fig. 15 (Smith, 2011)], the relevant quantities must be computed numerically, but the following analytical (and approximate) expression for a toroidal pore can be derived (Neu, Smith, and Krassowska, 2003; Son et al., 2016):

$$W^{\text{elect}}(r_p) = -F_{\max} \left[r_p + r_h \ln \left(\frac{r_t + r_h}{r_p + r_t + r_h} \right) \right] \xi_{\text{trans}}^2, \quad (95)$$

where r_t and r_h are constants and $F_{\max}$ is the maximum pore expanding force.[24] A similar expression may also be obtained for a cylindrical pore (Neu, Smith, and Krassowska, 2003).

Finally, we note that the formation of pores requires a packing of lipids along the wall side of the pore. This effect, especially for narrow pores ($r_p \ll t$), leads to a substantial deformation of the molecular order. This requires one to account for an additional energy contribution arising from the strong hydration interaction that causes repulsive force between the hydrophilic compounds of the pore wall (Glaser et al., 1988). The contribution due to this steric repulsion of the lipid headgroups may be defined as (Smith, 2011)

$$W^{\text{steric}}(r_p) = B \left(\frac{r_*}{r_p} \right)^b + C, \quad (96)$$

in which B, C, and b are phenomenological constants and r_* is the radius of the pore at the peak of the energy barrier before the rupture (Abidor et al., 1979; Smith, 2011).

To summarize, the total free energy of the pore formation can be written as

---

[24]Strictly speaking, it is a forcelike term but not an actual force since its dimensions are those of force per volt².

$$W^{\text{pore}}(r_p) = 2\pi\gamma r_p - \Gamma \pi r_p^2 + W^{\text{steric}}(r_p) + W^{\text{elect}}(r_p). \quad (97)$$

By examining the variation of the total free energy of the pore as a function of the pore radius r_p for different transmembrane potentials (Smith, 2011), we can observe a minimum after an initial energy barrier for $\xi_{\text{trans}} < 300$ mV. This is indicative of the presence of stable pores at low transmembrane potential. Once the transmembrane potential is amplified, this minimum vanishes and a high intensity electric field will result in the rupture of the membrane (Kotnik et al., 2019), provided that the pulse duration is long enough.

In addition to the prediction of the critical transmembrane potential, a stochastic theory of electroporation is considered (Weaver and Mintzer, 1981; Weaver and Chizmadzhev, 1996; Neu and Krassowska, 1999) to predict the membrane lifetime prior to rupture as well as the probability distribution of the pore sizes. The stochastic models are predicated on the energetic considerations that were just discussed. In one of the approaches, a probability distribution function (PDF) of pore size $n = n(r_p, t)$ (Pastushenko, Chizmadzhev, and Arakelyan, 1979) was introduced. In other words, $n(r_p, t)$ is the normalized number density of pores with a size between r_p and $r_p + dr_p$ at t. Treating pores as classical noninteracting entities, we may postulate the probability flux of the pores in pore radius space to be given by

$$J_{\text{pore}} = -D_{\text{pore}} \left(\frac{\partial n}{\partial r_p} + \frac{n}{k_B T} \frac{\partial W^{\text{pore}}}{\partial r_p} \right), \quad (98)$$

where D_{pore} is the pore diffusion constant and $k_B T$ is the thermal energy. That is, the rate of change of the probability satisfies the condition that, for any $r_2 > r_1 > 0$,

$$\int_{r_1}^{r_2} \frac{\partial n(r_p, t)}{\partial t} dr_p = -J_{\text{pore}}(r_2, t) + J_{\text{pore}}(r_1, t). \quad (99)$$

Inserting Eq. (98) into Eq. (99) and sending $r_2 \to r_1$, we obtain the evolution of the PDF $n = n(r_p, t)$ of the electropore size as

$$\frac{\partial n(r_p, t)}{\partial t} = D_{\text{pore}} \frac{\partial}{\partial r_p} \left(\frac{\partial n}{\partial r_p} + \frac{n}{k_B T} \frac{\partial W^{\text{pore}}}{\partial r_p} \right), \quad (100)$$

which can be recognized as the Smoluchowski or the Fokker-Planck equation (Freeman, Wang, and Weaver, 1994). Like the Liouville equation for a Hamiltonian system of interacting particles, the Smoluchowski equation contains complete information on the dynamics of the pores (Chavanis, 2019). In fact, in a system of Brownian particles we can derive the Smoluchowski dynamics of the particles using a Liouvillian evolution of the full classical model (Prigogine, 2017; Fantoni, 2019).

Equation (100) can be solved to derive a transmembrane potential–dependent average membrane lifetime (Weaver and Chizmadzhev, 1996). The population of pores has a strong dependence on the electric pulse parameters (Barnett and Weaver, 1991). However, a numerical solution of Eq. (100) predicts that for reversible electroporation long pulse durations result in the creation of a small number of pores with

large diameters (on the order of tens of nanometers) while short pulse durations create a larger number of small-sized pores (∼1 nm).

The theoretical models presented for electroporation have been further improved by accounting for other parameters like membrane curvature and surface tension (Neu and Krassowska, 1999; Smith, Neu, and Krassowska, 2004), the effects of conductivity of the membrane due to pore creation (Freeman, Wang, and Weaver, 1994; Krassowska and Filev, 2007), and the combined effect of electroporation and electrodeformation of the lipid membrane (Shamoon et al., 2019). When these models use appropriate values for the model parameters, they appear to be in good agreement with experimental observations and lead to reasonable predictions.

C. Electrofusion

The fusion of cells and vesicles in living organisms is a vital process for life that allows cells to take cellular and subcellular material and components. The in-plane fluidity and flexibility of the lipid membranes of the vesicles and cells in proximity allow them to destabilize their structure and deform substantially to fuse together. The destabilization of the structure of the lipid bilayer that often accompanies the creation of pores corresponds with the crossing of a large energy barrier. For the *in vivo* examples of fusion, such as synaptic vesicle fusion (Rizo and Rosenmund, 2008) and exocytosis (Zhou et al., 2017), crossing this energy barrier requires a docking of proteins for triggering the process; see Fig. 16(b). The *in vitro* examples of fusion of vesicles, which lack docking proteins, need a different kind of driving force for a crossing of the energy barrier of the lipid bilayer (Chernomordik and Kozlov, 2008). This driving force can be membrane stress
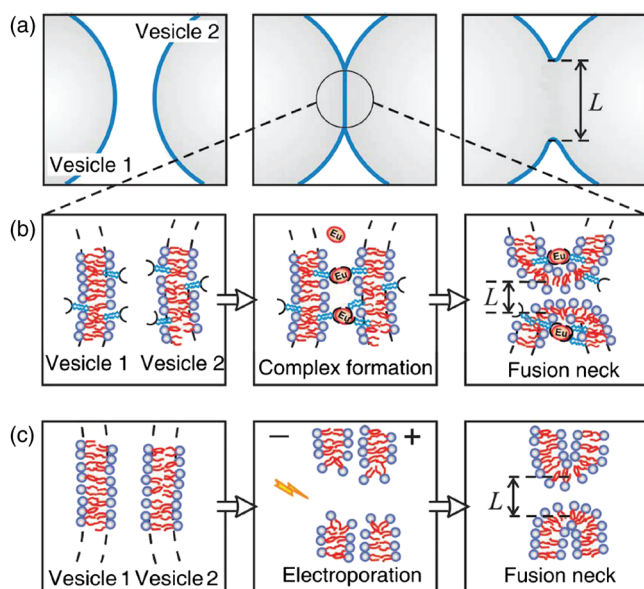

FIG. 16. Lipid membrane fusion. (a) Vesicles are brought into contact, and the necking of the vesicles then begins. (b) Docking proteins cross the energy barrier of destabilization of the lipid membrane. (c) The structure of the lipid membrane is broken using electroporation, which serves as a precursor to fusion. From Haluska et al., 2006.

(Cohen, Akabas, and Finkelstein, 1982; Shillcock and Lipowsky, 2005), a photosensitive surfactant (Suzuki et al., 2017), or an electric field (Strömberg et al., 2000).

The fusion of cells and vesicles using an electric field is called electrofusion. This process can be precisely controlled and used for applications including gene transfer, drug delivery (Schoeman et al., 2018; Geboers et al., 2020), antibody production, and the preparation of cell vaccines for cancer therapies (Kandušer and Ušaj, 2014). Early efforts at electrofusion were reported at around the same time that advances were made in the application of electroporation (Sencia et al., 1979; Zimmermann and Scheurich, 1981). This is due to the fact that the initial step for triggering the mechanism of electrofusion is similar to electroporation, in which the membrane of the vesicles that are brought into contact experience electrically mediated destabilization of their structure; see Fig. 16(c).

The electrofusion mechanism often begins with a dielectrophoresis mechanism where an ac electric field aligns the vesicles. Next a dc field is applied that amplifies the transmembrane potential of the membrane beyond a critical value, thereby causing poration. Necking of the membranes occurs at the contact area. This was first observed using fast video microscopy (Haluska et al., 2006; Riske et al., 2006). Vesicles in the absence of salt were found to fuse at multiple necks, while the presence of salt resulted in a single or smaller number of fusion necks. The opening of the fusion neck with radius 2 μm was fast (100 μs) due to the dissipation of high membrane tension (Dimova, Riske, and Damijan, 2016). However, once the tension is released, the opening slows down at larger radii until the completion of fusion and the formation of a single vesicle.

From a practical viewpoint a process like cell-cell electrofusion can be used for the preparation of hybrid cells for several biomedical applications (Scott-Taylor et al., 2000). Moreover, electrofusion of vesicles can be used to mix their contents (Yang, Lipowsky, and Dimova, 2009) [see Fig. 17 (top panel)] or their membrane (Bezlyepkina et al., 2013) [see Fig. 17 (bottom panel)].

To our knowledge, models of vesicle electrofusion that include the pore formation and the large deformation of the necking process have not been developed. However, there is an extensive literature on the mechanism of vesicle fusion in the absence of electric fields (Shillcock and Lipowsky, 2006; Kasson, Lindahl, and Pande, 2010). It will be interesting to see whether future investigation of the effect of electric field on the mechanism of vesicle fusion can provide more insight into the process.

D. Electrostatics and membrane rigidity

Thus far we have provided some examples of morphological changes to the cell membrane under the effect of the electric field. Analyzing the shape of the membrane during these morphological changes requires knowledge of the membrane elastic properties, namely, the bending rigidity κ_b and the Gaussian rigidity κ_g. Lipid membranes are complex structures made of two monolayers of amphiphile lipid molecules surrounded by water. The elastic resistance emerges primarily from the energy required to displace the
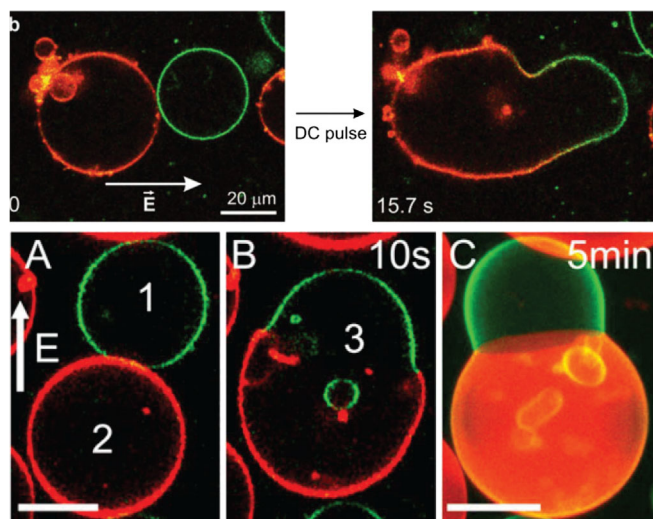
FIG. 17. Electrofusion as a microreactor. Top panel: for mixing large vesicles loaded with Na_2S in red (left) and $CdCl_2$ in green (right). The final product is quantum-dot-like CdS nanoparticles visualized under laser excitation. From Yang, Lipowsky, and Dimova, 2009. Bottom panel: for mixing lipid components. Vesicle 1 is composed of eSM/cholesterol (Chol) (0/70/30), and vesicle 2 is composed of DOPC/Chol (80/0/20). A high intensity electric field (400 kV/m) with a short duration (150 μs) was exerted on the vesicles. From Bezlyepkina et al., 2013.

lipid molecules from their equilibrium configuration in this structure. The bending of the membrane involves compression in one monolayer and tension in the other. Thus, the bending rigidity depends on the bilayer thickness t and the area compression modulus K_a; for further details, see Sec. V.4 of Boal (2001).

In addition to short-range lipid-lipid interactions, the elastic properties of the lipid membranes may also be affected by long-range interactions between molecules such as van der Waals, electrostatic interactions (Dean and Horgan, 2006) and electromechanical coupling such as flexoelectricity (Liu and Sharma, 2013). The effect of electrostatic interactions was originally studied by investigating the interactions of membrane surface charges predicated on the Poisson-Boltzmann mean-field theory (Winterhalter and Helfrich, 1988b; Lekkerkerker, 1990; Kumaran, 2001). In this approach, a net curvature is imposed on the membrane and the change in electrostatic energy is calculated. The correction to the bending and Gaussian rigidity is determined from the additional contribution to the curvature energy. The results of these studies showed that, for fixed symmetric surface charges, the renormalization of the bending rigidity κ_b is positive due to the repulsive forces between the charges. However, for the Gaussian rigidity κ_g, the renormalization is negative.

Experimental evaluations of the rigidity of the charged membrane have been in good agreement with theoretical results (Bivas and Ermakov, 2006; Loubet, Hansen, and Lomholt, 2013). A common tool for systematic measurement of these quantities are giant unilamellar vesicles (GUVs). Use of GUVs allow good control of composition; in addition, the measurements are not affected by high membrane curvature,

as may be the case in submicron-sized liposomes (Faizi et al., 2019). Various GUVs have been used to measure the bending rigidity of lipid membranes with different mole fractions of ionic surfactants, and the results show an increase in rigidity by up to $10 k_B T$ (Rowat, Hansen, and Ipsen, 2004; Vitkova et al., 2004; Mitkova et al., 2014).

V. ION CHANNELS: ION TRANSPORT, GATING MECHANISM, AND IMPLICATIONS FOR THE SENSORY SYSTEM

As previously mentioned, the lipid membrane is impermeable to ions. Consequently, biological cells rely primarily on membrane proteins like ion channels and pumps for the transport of ions into and out of the cell.[25] Ion channels are essentially gated transmembrane proteins that selectively allow only particular ions to pass through while filtering others. The various functions of ion channels are crucial for the regular operation of biological cells in all animals and range from maintaining the membrane potential to regulating the volume of the cell (Hille, 2001). In particular, in excitable cells like neurons and muscle cells, the transmission of electrical signals containing information relies on positively charged ions like potassium, sodium, and calcium moving in and out of the cell through ion channels (Zheng and Trudeau, 2015).

The large family of ion channels can be classified based on their gating mechanism and the type of ion that they transport (Hille, 2001). Classification based on the gating mechanism relies on the stimulus that triggers the opening and closing of the channel. This stimulus can be the change in membrane potential, the exerted mechanical force, the binding of specific ligand molecules, or other stimuli (Alberts, 2018). In particular, voltage-gated ion channels open and close in response to the change in membrane potential as a result of the interaction of the electric field with the channels' protein structure. Thus, these channels provide a fine example of the coupling of mechanical deformation and electrostatic fields. The voltage-gated ion channels are highly selective and are classified based on the type of ion that they can transport. The five main groups of voltage-gated ion channels are represented in Fig. 20.

Voltage-gated ion channels are found mostly in excitable cells such as nerve and muscle cells and facilitate the propagation of an electric signal. This electrical signal occurs as a fast spike called the action potential and is the basis of intercellular communication. It is of fundamental importance to most biological processes, from the transmission of nerve impulses for controlling our actions to the underlying mechanisms responsible for our perception of reality through our senses (Phillips et al., 2012). To provide more insight into the function of ion channels, we first present the basic mechanism of action potential propagation and the crucial role of voltage-gated ion channels in this mechanism.

---

[25]The transport of ions in ion channels is a passive mechanism where the gradient of ion concentration and the electric potential regulate the direction of transport. However, in ion pumps the release of energy from ATP molecules provides an active mechanism that pushes the ions against the gradient of ion concentration and the electric potential (Gadsby, 2009).
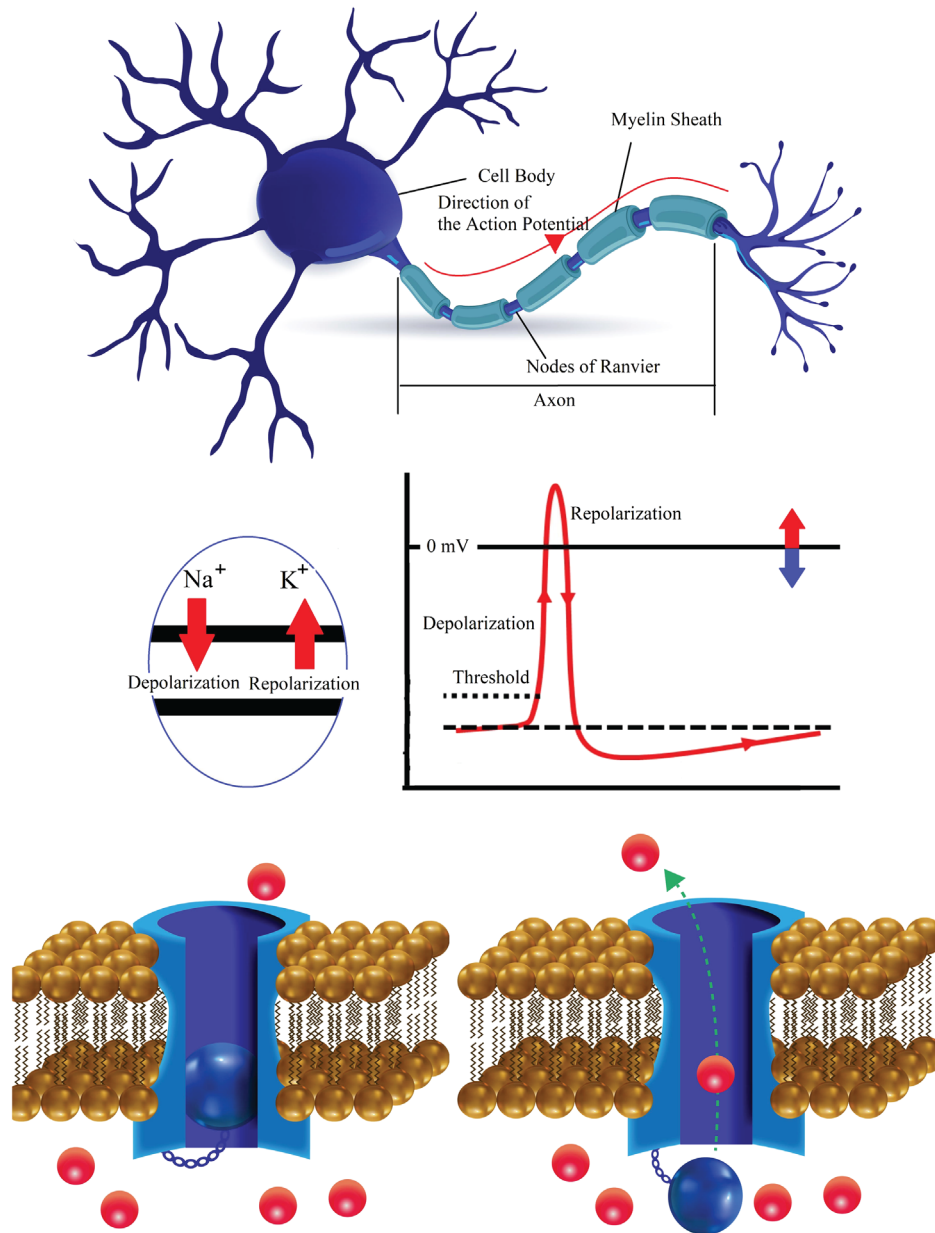
FIG. 18.   Top panel: illustration of a typical nerve cell. The action potential travels down the axon. The nodes of Ranvier are enriched in ion channels that allow the exchange of ions and the regeneration of the action potential at these nodes. Middle panel: the ion exchange includes the flow of Na^+ ions into and K^+ ions out of the nerve cell. Bottom panel: voltage-gated ion channels open and close in response to a change in transmembrane potential and allow the transport of ions.

Figure 18 (top panel) shows a typical nerve cell and its axon, where the signal can propagate down to the nerve terminal. The main compartments of the axon are the myelin sheath and the nodes of Ranvier. The myelin sheath is an extended plasma membrane that acts as an insulator and allows the signal to transmit quickly and effectively. The voltage-gated sodium and potassium channels are preferentially accumulated at the nodes of Ranvier. After the signal is generated in the cell body, it travels down the myelin sheath and arrives at the nodes of Ranvier. The ion channels, originally in the closed state at the nominal membrane resting potential, sense the arrival of the signal due to slight depolarization of their medium. Once this slight depolarization (or graded potential) reaches a critical value, the probability of the channels being in the open state increases. First, voltage-gated sodium channels that are exposed to the graded potential open and allow the passage of Na^+ ions into the cell, resulting in further depolarization of the cell membrane. Next, as the Na_v channels begin to close, the voltage-gated potassium channels open and allow K^+ ions to flow out of the cell, resulting in repolarization of the membrane; see Fig. 18 (middle panel). In a similar mechanism, the neighboring ion channels at the location of the action potential sense the slightly depolarized membrane and the process repeats, allowing the spike to travel down the nerve and to the next myelin sheath (Ashcroft, 1999; Bean, 2007). The process also involves the flow of Ca^{2+} and Cl^- ions, which affect the shape of the spike. Once the spike has traveled down the axon,

the action of the ion pumps helps the nerve cell return to its resting state.

Extensive experimental and theoretical research on the mechanisms underpinning their selectivity, gating, and ion transport has been motivated by the crucial role of ion channels in biological processes. Arguably the first mathematical description of the permeability of the membranes to K^+ and Na^+ ions and propagation of the action potential were developed by, in a now classic work, Hodgkin and Huxley (1952) without the explicit knowledge of the existence of ion channels. It was not until the end of the 20th century that, using x-ray crystallography, the protein structure of ion channels was discovered for potassium channels (Doyle *et al.*, 1998), and later for several other types of channels (Jiang *et al.*, 2002; Jiang, Lee *et al.*, 2003; Miyazawa, Fujiyoshi, and Unwin, 2003; Payandeh *et al.*, 2011; Hou *et al.*, 2012). This breakthrough discovery provided the impetus toward understanding the molecular basis of various aspects of ion-channel functions.

Using the atomic structure of the channels, computational methods such as molecular dynamics were developed that attempted to provide atomic-level resolution to the functioning of ion channels (Tieleman *et al.*, 2001; Beckstein *et al.*, 2003; Flood *et al.*, 2019) and (as long as the force fields are chosen appropriately) can describe several aspects of the phenomenology with high fidelity. In particular, all-atom molecular dynamics simulations have proved to be effective in capturing the properties of ion channels. While these methods have been around for decades, early simulations were limited to short timescale problems (< 1 ns) and small size scales. Later advancements in computer technology and computational tools, as well as the discovery of the crystal structure of many other ion channels, allowed for simulation of the ion conductivity in the channel and conformational change of the molecules on the timescale of several nanoseconds (Allen *et al.*, 2000; Guidoni, Torre, and Carloni, 2000; Shrivastava and Sansom, 2000; Åqvist and Luzhkov, 2000; Berneche and Roux, 2001; de Groot and Grubmüller, 2001). In recent years, development of the computational technologies has reached a point where molecular dynamics simulations, with some approximations such as coarse-grained atoms, can be used to study the entire ion channel, including the lipid membrane and solvent, with a time span of up to milliseconds (Dror *et al.*, 2012; Perilla *et al.*, 2015). These methods can be applied to problems involving permeation and selectivity of ion channels, conformation of the protein associated with a gating mechanism, and exploration of drug binding to ion channels. A comprehensive review of the methods and application of molecular dynamics simulation was given by Flood *et al.* (2019).

Despite the large number of studies on ion channels using molecular dynamics simulations, there are several limitations. First, if the atomic-resolution structure of the ion channel is not accessible, the molecular dynamics simulation cannot be performed. Second, the force fields that are designed to describe the interatomic interaction of the proteins are not perfect, and the accuracy of the model is limited to the accuracy of the force field. Third, even if the atomic structure of the channel is available and the defined force field is

reasonably accurate, execution of molecular dynamics simulations is computationally expensive and several aspects of the ion-channel modeling remain beyond reach (especially those that pertain to including larger size scales and realistic timescales).

Given the success of the Helfrich model for the mechanical response of membranes and continuum electrostatics in describing their electrical behavior, the notion of using a continuum approach to model the ion channel and its surrounding environment has attracted attention (Maffeo *et al.*, 2012). The complex protein structure of the channel and its interaction with surrounding lipid molecules can influence the selectivity, gating, and transport of ions, and continuum models necessarily involve simplifications. For instance, in the context of ion transport, the lipid membrane and the water are often assumed to be rigid, and only their dielectric properties are considered to play a role (Nogueira and Corry, 2019). As a result, the ion channel is treated as a biomolecule in an ionic solution. Theoretical models such as Poisson-Boltzmann theory or Poisson-Nernst-Planck theory (described in Sec. V.A) can be used to study the ion transport in the channel. Regarding the gating mechanism, in a limited number of studies the deformation of the lipid bilayer and the protein structure and their coupling effects were simulated using a continuum approach (Reeves *et al.*, 2008; Argudo *et al.*, 2016), which we describe Sec. V.C. The problem of selectivity is often treated using molecular dynamics simulations since the consideration of chemistry is paramount and a mean-field approach may be inappropriate for handling a small number of ions in a confined space (Miller, 1999).

A. Theory of ion transport through ion channels

We first examine the considerations pertaining to the transport of ions through membrane proteins. This ion transport forms the basis for signal transmission in excitable cells such as neurons. One approach to studying this system is to model both the protein structure and its neighboring ionic solution as continuum media.

We denote by Ω_m the domain occupied by the macromolecules with a bare charge distribution of $\rho_m : \Omega_m \to \mathbb{R}$, and $\Omega_s = \mathbb{R}^3 \backslash \Omega_m$ is the ambient ionic solution. Assuming that there are N_s species of ions with concentration C_j and charges q_j, the charge distribution in $\mathbb{R}^3$ is given by

$$\rho(\mathbf{x}) = \begin{cases} \rho_m(\mathbf{x}) & \text{if } \mathbf{x} \in \Omega_m, \\ \sum_j^{N_s} q_j C_j(\mathbf{x}) & \text{if } \mathbf{x} \in \Omega_s. \end{cases} \quad (101)$$

For simplicity, we model both the molecules in the protein structure and the solution as linear dielectric media with permittivity given by ϵ_m and ϵ_s, respectively. Considering the charge density in the Maxwell equation (1), we note that the electric potential $\xi : \mathbb{R}^3 \to \mathbb{R}$ necessarily satisfies

$$\nabla \cdot [-\epsilon(\mathbf{x})\nabla\xi(\mathbf{x})] = \rho(\mathbf{x}), \quad (102)$$

where $\epsilon(\mathbf{x})$ takes the value of ϵ_m (ϵ_s) in Ω_m (Ω_s). The Poisson equation (102) relates the charge density distribution $\rho(\mathbf{x})$ to

the spatial variation of the potential $\xi(\mathbf{x})$. However, unlike previous electrostatics problems, such as those in Sec. IV.A.2, this equation cannot yet be used to determine the electric field, since the concentrations C_j are unknowns. For the ionic solution in Ω_s, it is possible to assume that the regions in the material respond in a mean-field description. In this approach, the ion species in the ionic solution are represented by continuum ion concentration instead of discrete ions (Levitt, 1986; Tieleman *et al.*, 2001; Roux *et al.*, 2004). To have a closed system, we recall that for noninteracting ions in the solution the electrochemical potential of the jth ion species in the mean-field approach is assumed to be uniform throughout the solution and is represented at any point $\mathbf{x}$ using its entropic contribution and electrostatic contribution as (Kittel and Kroemer, 1970; Sharp and Honig, 1990)

$$\mu_j(\mathbf{x}) = k_B T \ln C_j(\mathbf{x}) + q_j \xi(\mathbf{x}). \tag{103}$$

Physically, the quantity $-\nabla \mu_j$ can be interpreted as the driving force on the jth ion. Therefore, for stationary equilibrium states we have $-\nabla \mu_j \equiv 0$ on Ω_s for all $j = 1, \ldots, N_s$. In other words,

$$C_j(\mathbf{x}) \propto \exp[-q_j \xi(\mathbf{x})/k_B T] \quad \forall \ \mathbf{x} \in \Omega_s. \tag{104}$$

Inserting Eq. (104) into Eq. (102), we obtain the following general form of the Poisson-Boltzmann (PB) equation:

$$\begin{aligned} \nabla \cdot (-\epsilon_m \nabla \xi) &= \rho_m && \text{on } \Omega_m, \\ \nabla \cdot (-\epsilon_s \nabla \xi) &= \sum_j C_j^0 q_j \exp\left(\frac{-q_j \xi}{k_B T}\right) && \text{on } \Omega_s, \end{aligned} \tag{105}$$

where C_j^0 is the normalization constant such that the total number of jth ions is equal to what is in the solution, or the concentration at infinity if the electric potential at infinity is chosen to be the ground potential. Across the interface $\partial \Omega_m$, we have the following interfacial conditions:

$$[\![\xi]\!] = 0, \quad [\![-\epsilon(\mathbf{x})\nabla \xi]\!] \cdot \mathbf{n} = 0. \tag{106}$$

Equations (105) and (106) form a closed system to determine the electric field and ion distribution. In particular, for the special case of a 1:1 electrolyte shown in Fig. 19, the ionic concentrations in region Ω_s can be written as

$$C_\pm = C^0 \exp[\mp e_c \xi(\mathbf{r})/k_B T],$$

and hence in Ω_s Eq. (105) takes the form of the following nonlinear Poisson-Boltzman equation (Sharp and Honig, 1990; Gilson *et al.*, 1993; Holst, 1994):

$$\Delta \xi - \kappa^2(\mathbf{r}) \sinh(\xi) = 0, \tag{107}$$

which implies a critical length scale, i.e., the Debye-Hückel length $l_D = 1/\kappa$, given by

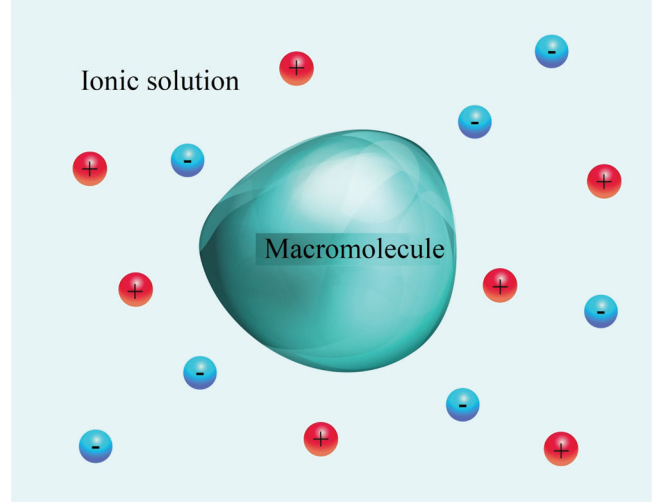$$l_D = \left(\frac{\epsilon_s k_B T}{2 e^2 \bar{C}}\right)^{1/2}, \tag{108}$$

FIG. 19. Different domains in a three-dimensional Debye-Hückel model for a macromolecule in a 1:1 electrolyte.

where $\bar{C}$ is the number density of the positive or negative ions. For a system of charged particles in a solution, the screening of electrostatic interactions is characterized by the Debye-Hückel length l_D. In addition to describing the decayed potential due to external charges, l_D also describes the decay of charge-charge correlation resulting from thermal fluctuation in the ionic solution (Adar *et al.*, 2019; Buyukdagli and Podgornik, 2019).

The Poisson-Boltzmann problem (105) is derived for sharp macromolecule-solvent interfaces. However, the electrostatic potential is long range and its limitation to discrete domains does not provide an accurate representation of the real system. Moreover, it is more convenient for numerical simulation if the governing equation is regularized with smooth coefficients, domains, and solutions. An example of such regularization can be achieved by introducing a characteristic function for domain Ω_m as follows:

$$S(\mathbf{x}) = \int_{\Omega_m} K_\delta(\mathbf{x} - \mathbf{y}) d\mathbf{y}, \qquad K_\delta(\mathbf{x}) = K_0 \exp\left[\frac{-|\mathbf{x}|^2}{\delta^2}\right],$$

where the normalization constant K_0 is such that $\int_{\mathbb{R}^3} K_\delta(\mathbf{x}) = 1$, and the original problem (105) can be replaced by

$$\nabla \cdot (-\epsilon_S \nabla \xi) = S\rho_m + (1 - S) \sum_j q_j C_j \exp\left[-\frac{q_j \xi}{k_B T}\right], \tag{109}$$

where

$$\epsilon_S = S\epsilon_m + (1 - S)\epsilon_s. \tag{110}$$

Equation (109) can be obtained as the Euler-Lagrange equation of the variational principle (Wei, 2010) as follows:

$$\min\{G[\xi]: \text{all admissible potential } \xi\},$$

where the energy functional $G[\xi]$ is given by

$$G[\xi] = \int_{\mathbb{R}^3} \left[\tfrac{1}{2}[S\varepsilon_m + (1-S)\varepsilon_s]|\nabla\xi|^2 - S\rho_m\xi \right.$$
$$\left. + (1-S)k_BT\sum_j C_j \exp\left(-\frac{q_j\xi}{k_BT}\right) \right].$$

The mean-field approximation resulting in the PB equation (105) neglects ion correlations and charge fluctuations. The model is limited mostly to dilute solutions. Since in modeling ion channels the dilute solution assumption is reasonable, several studies have used the PB equation to investigate various aspects related to the physics of ion-channel transport, such as the change in free energy to bring a charge from infinity to the channel interior (Moy *et al.*, 2000; Jogini and Roux, 2005). The mean-field theories developed for the transport of monovalent charges can be refined to describe multivalent charge-driven exotic transport by including the effect of ion-ion correlations using correlation corrected theories (Buyukdagli, 2020). Such an augmented method can be applied to various processes, including drift-driven polymer translocation through biological and synthetic nanopores (Buyukdagli and Ala-Nissila, 2017). In addition, the PB model can be generalized to account for nonelectrostatic effects through an addition of pertinent terms to the free energy of the system (Ben-Yaakov *et al.*, 2009). For instance, an extralinear coupling term between the concentration of ions and the deformation can account for van 't Hoff stress (osmotic pressure). The relevant article and textbook that derived the chemomechanical coupling terms in a thermodynamically consistent manner were given by Anand and Govindjee (2020) and Mozaffari, Liu, and Sharma (2022), respectively. The article in which the osmotic pressure were derived using the mean-field approach directly was given by Buyukdagli and Podgornik (2021).

Moreover, the model can be immediately generalized to address ion transport when the system deviates from its equilibrium state. Assuming linear responses of ions (i.e., the velocity of the ions is given by $\mathbf{v}_j \propto -\nabla\mu_j$), the ion flux $\mathbf{J}_j$ of the jth species can be written as

$$\mathbf{J}_j = -D_j n_j \nabla \frac{\mu_j}{k_BT}, \qquad (111)$$

where D_j is the diffusivity of the jth ion type. Inserting μ_j from Eq. (103) into Eq. (111) and using the conservation of ions $\partial C_j/\partial t + \nabla \cdot \mathbf{J}_j = 0$, we obtain the following Nernst-Planck equation:

$$\frac{\partial C_j}{\partial t} - \nabla \cdot \left[D_j \left(\nabla C_j + \frac{q_j C_j}{k_BT} \nabla\xi \right) \right] = 0, \qquad (112)$$

which together with Eq. (105) form the Poisson-Nernst-Planck (PNP) model framework for analyzing the ion transport in ion channels. In comparison to the PB model, which describes the equilibrium energetics of the ion channel, the PNP model is a nonequilibrium approach. Given that the timescale of the permeation is often of the order of tens of nanoseconds to milliseconds, the PNP model has an advantage over molecular dynamics simulations as well (Maffeo *et al.*, 2012). However, the mean-field assumption used in this method has some disadvantages since it neglects the change in the dielectric response of ionic solutions and ion-ion correlations (Maffeo *et al.*, 2012; Levy, Andelman, and Orland, 2013; Buyukdagli, 2020). For these reasons, the application of the PNP method to ion channels and the extent of its validity has been the subject of much debate. Comprehensive reviews of these methods and their limitations were given by Roux *et al.* (2004) and Coalson and Kurnikova (2005).

To our knowledge, the combined effect of deformation and ion transport (and the consequent implications for selectivity and gating) has not yet been addressed. We just outlined the central equations of transport in a manner that would make it simple to incorporate deformation and investigate the ramifications of electrodiffusion-mechanical coupling. Limited experimental evidence was provided by Petrov *et al.* (1993), who proposed that flexoelectricity may provide the driving force for ion transport in certain potassium ion channels. A detailed model that links these two phenomena together is absent, however, and would be an interesting future endeavor. In Sec. V.D, where we discuss the hearing mechanism, we describe a model that couples the gating probability (albeit not the transport itself) to flexoelectricity.

B. Intermolecular interactions between biomolecules

Although it is not directly germane to the topic of the review, for contextual reasons we discuss the interaction of the biomolecules. This includes interactions of two or more proteins and proteins with DNA. Interactions between proteins and lipid membranes are discussed in Sec. V.C. The dominant factor involved in the interaction of two proteins with nonzero net charge is the Coulomb forces between the charged amino acid residues. The Coulombic interactions depend on the solution pH and electrolyte concentration. The solution pH controls the total charge of the proteins, while the concentration of the electrolyte governs the effective length of the Coulombic interactions through the Debye screening length λ_D.

Most of the models describing the protein interactions assume a fixed set of charges on the protein (Carlsson, Malmsten, and Linse, 2001; Allahyarov *et al.*, 2002), which is a valid approach if the net charge of the protein is significant. However, if a protein is neutral (with its isoelectric point equal to pH), its interaction with another highly charged protein will lead to an alteration in the charge distribution due to the distortion of the electrostatic field and a change in the local ionic environment (Lund and Jönsson, 2005). Thus, the magnitude of the surface charge and the potential of the protein can be altered to help the protein adapt to a change in the chemical environment. The process that originates in migration of protons between titratable sites is typically referred to as charge regulation (Pujar and Zydney, 1997; Lund and Jönsson, 2005; Adžić and Podgornik, 2016). The charge response resulting from the aforementioned perturbation can be described by the charge capacitance of the biomolecule, which is the variance of the mean charge. When a biomolecule is exposed to an external electric field, the capacitance is in fact a measure of how much charge can be induced (Lund and Jönsson, 2005).

For decades, researchers have used the energy minimization of intermolecular potentials as a tool to analyze biomolecule interactions. In these models, the total free energy has contributions from the interaction of the two charge distributions that are affected by both electrolyte concentration and pH. Since the focus of this review is not MD or MC simulations, we encourage the interested reader to consult other reviews that focus on such simulation methods (Schlick *et al.*, 2011). For the theoretical formulation of this concept, see Adžić and Podgornik (2016).

C. Lipid-protein interactions and implications for the gating mechanism

Since the discovery of the structure of voltage-gated ion channels, several studies have elucidated the principles of voltage-dependent gating (Aggarwal and MacKinnon, 1996; Bezanilla, 2000; Lu, Klem, and Ramu, 2002; Long, Campbell, and MacKinnon, 2005; Batulan, Haddad, and Blunck, 2010; Kalstrup and Blunck, 2018). The protein structure of a voltage-gated ion channel involves two distinct domains: a central pore and the surrounding voltage sensing elements. For instance, the voltage-gated potassium (K_v) channel contains four subunits of six transmembrane segments; see Fig. 20. Four of the segments (S1–S4) are the voltage sensors (VSDs), and two of them (S5 and S6) form the centrally located pore structure of the channel (Sigworth, 1994; Bezanilla, 2000). Similar structures exist for other types of voltage-gated ion channels; see Fig. 20 for an overview of the protein structure of the superfamily of voltage-gated ion channels. The pore region is responsible for selectivity and transport of the ions across the membrane. The gating of the pore region is facilitated by the motion of the domains of the voltage sensor. For instance, in K_v channels the amino acid structure of S4 contains four to eight positive charges (arginine residue), which are called gating charges (Aggarwal and MacKinnon, 1996). For the central pore (S5 and S6) to open or close, the S4 segment needs to move perpendicularly to the membrane by 15–20 Å positive charges while deforming the S4-S5 linker. The motion that S4 undergoes while carrying its charge in the electric field couples the conformational change of the channel to the transmembrane potential (Jiang, Ruta *et al.*, 2003). The motif of the four-domain structure of the voltage sensor is common across different voltage-gated ion channels (Yellen, 2002). Thus, the voltage-dependent motion of the VSD is the regulator of the ion-channel gating.

While the membrane potential is the main stimulus for gating, other elements can also affect the function of the channel. These include the amino acid sequence of the voltage sensor (Li *et al.*, 2014), protein phosphorylation (Vacher and Trimmer, 2011), intracellular Ca^{2+} (Gamper, Li, and Shapiro, 2005), and the surrounding lipid molecules (Heginbotham, Kolmakova-Partensky, and Miller, 1998; Hilgemann, Feng, and Nasuhoglu, 2001; Hite, Butterwick, and MacKinnon, 2014). In particular, significant work exists on the role of lipid membranes in a gating mechanism (Gu, Juranka, and Morris, 2001; Schmidt, Jiang, and MacKinnon, 2006; Hite, Butterwick, and MacKinnon, 2014; Ahuja *et al.*, 2015). Experimental observations indicate that in some channels
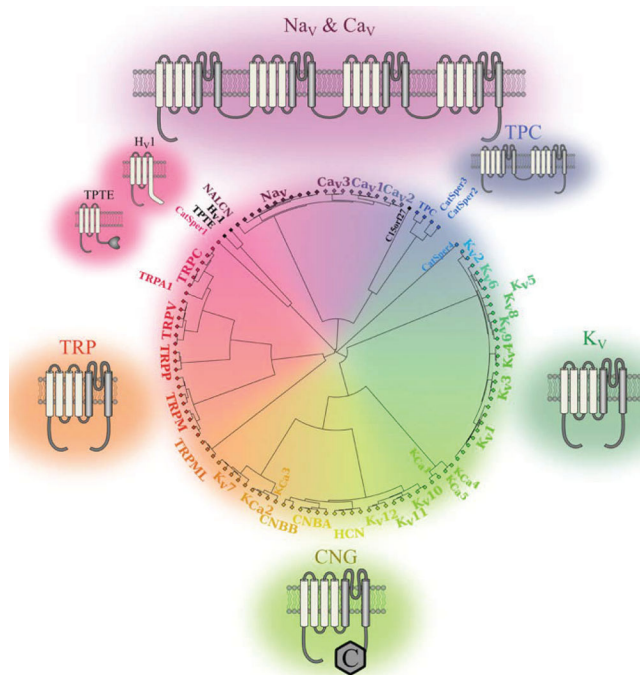

FIG. 20. Protein sequence of the voltage sensor and the pore domain for various members of the superfamily of voltage-gated ion channels. For instance, Na_v and Ca_v (also shaded in purple) have a VSD in each of their four domains. Two-pore channels (TPCs) (also shaded in blue) have a VSD motif in their two homologous domains. Transient receptor potential (TRP), K_v, and cyclic nucleotide-gated (CNG) channels also assemble as homotetramers. Putative tyrosine-protein phosphatase (TPTE) and H_v1 (also shaded in black) show the members of the pore domain–lacking group of proteins. The voltage-sensor segments are shown in light gray and the pore domains are in dark gray throughout. From Moreau, Gosselin-Badaroudine, and Chahine, 2014.

the role of lipid membrane is so significant that for some cases (such as the K_vAP channel) it becomes completely inactive in nonphospholipid membranes (Schmidt, Jiang, and MacKinnon, 2006). Moreover, the lipid composition of the membrane affects the activation voltage of the channel by shifting the midactivation voltage to lower or higher values, depending on the lipid type. For instance, one study showed that in K_v channels the intracellular phosphatidic acid can shift the midpoint of the activation curve by 50 mV in a direction that represents the stable closed conformation of the voltage sensor (Hite, Butterwick, and MacKinnon, 2014), as shown in Fig. 21.

The underlying molecular driving forces that regulate the motion of the voltage sensor and its interaction with the pore domain as well as the mechanism that lipid molecules contribute to the gating are not fully understood. Some models have been suggested to describe the electromechanical coupling that opens the pore as a result of the motion of the S4 domain (Vargas, Bezanilla, and Roux, 2011; Chowdhury and Chanda, 2012; Hite, Butterwick, and MacKinnon, 2014). According to these models, first and upon membrane depolarization, in each of the domains of the ion channel the S4 charge moves upward within the membrane independently and applies a force onto the S4-S5 linker. Next, during a
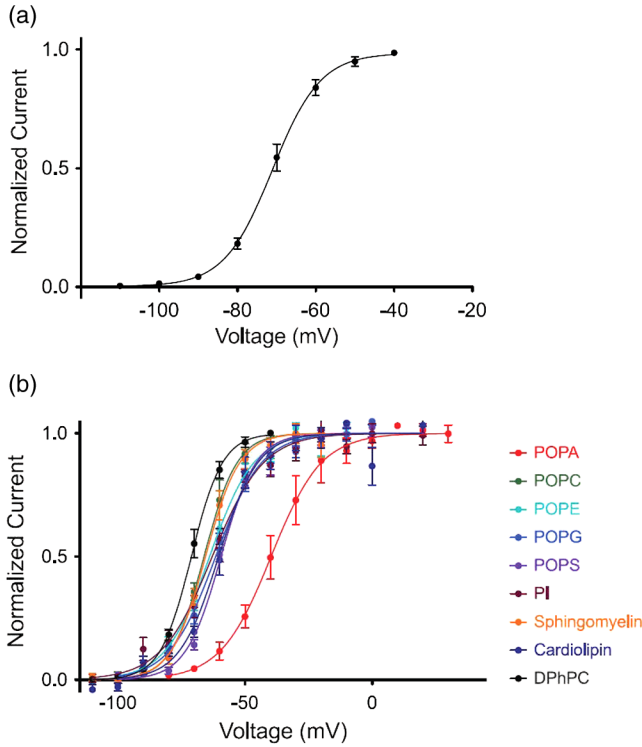
(a)

(b)

FIG. 21. Different lipid mixtures modifying the channel gating. (a) Boltzmann function representing the normalized tail currents in the K_v channel in diphytanoylphosphatidylcholine (DPhPC) lipid shows a midactivation voltage of $V_{mid} = -71 \pm 1$ mV. (b) Variation of the lipid composition shifts the midactivation voltage. For DPhPC:1-palmitoyl 2-oleoyl phosphatidic acid (POPA) $(3:1)$, the midactivation voltage is $V_{mid} = -41 \pm 2$ mV. From Hite, Butterwick, and MacKinnon, 2014.

cooperative conformational change of the S4 charge of the domains, the energy is released to the pore domain, which results in a widening of the bundle crossing at the intracellular S6 gates (Pathak *et al.*, 2005; Kalstrup and Blunck, 2018). Recently, for several K_v channels, it was shown that VSD can exert force on the pore domain in an assembly that makes the S4-S5 linker dispensable. For instance, a molecular dynamics simulation of HCN channels suggested that the S4 domain breaks into two subhelix during the downward movement of the VSD. The lower subhelix of S4 then replaces the S4-S5 linker (Kasimova *et al.*, 2019). Unlike the S4 segment, the movement of the S4-S5 linker is not associated with any charge, and limited dynamic information is available for the mechanism of its motion (Faure *et al.*, 2012). On the other hand, the underlying mechanism of the coupling between anionic lipid molecules and voltage-sensor segments is suggested to be either through their negative charges or through interaction of the end of the negatively charged molecule with the positively charged amino acid in the voltage sensor of the channel (Hite, Butterwick, and MacKinnon, 2014). The mechanism in which other lipid types such as cholesterol affect gating is not well understood.

A limited number of continuum studies have tried to provide insight on the gating mechanism by accounting for all energy contributions from various elements in the complex

system (Reeves *et al.*, 2008). This free energy comprises the mechanical energy of the lipid membrane deformation and the protein conformation and the electrostatic energy associated with the interaction of the voltage sensor with the ionic solution and dielectric material of the membrane. The total free energy of the system is first calculated for various positions of the voltage sensor. Next the total free-energy difference ΔG_{oc} between the position of the voltage sensor that is associated with the open and closed states of the pore is estimated. Using this free energy, one can describe the probability of the channel being in the open state using (Reeves *et al.*, 2008)

$$P_{open} = \frac{1}{1 + \exp(\Delta G_{oc}/k_B T)}. \tag{113}$$

Evidently, an estimate of the total free-energy difference between the open and closed states is a reasonable starting point for the gating mechanism. We first discuss the mechanical energy associated with the deformation of the lipid membrane. The membrane forces and its intrinsic elastic properties are shown to affect the gating mechanism (Calabrese *et al.*, 2002; Lundbæk *et al.*, 2004, 2005; Morris and Juranka, 2007). It has been suggested that the coupling of the more flexible lipid membrane with ion-channel rigid proteins occurs through the deformation of the lipid membrane in its entirety and can be explained using the concept of hydrophobic mismatch between the lipid tail and the hydrophobic domain of the protein (Jensen and Mouritsen, 2004). The physical underpinning of this deformation can be traced back to the idea of self-assembly of lipid molecules. In the macroscopic theory, the lipid membrane is studied as a two-dimensional surface using Helfrich theory (Helfrich, 1973b). However, when the membrane deformation in the vicinity of its guest protein is of the same order as the membrane thickness, a theory based on the elastic energy of two leaflets is required. Lipid membranes adapt their structure to the conformational change of the protein through the stretching, pinching, and variation of their thickness close to the interface (Goulian *et al.*, 1998). There are several different models that have provided energetic refinements of the lipid-protein interaction by including additional factors such as a higher-order term in the form of the elastic energy (Argudo *et al.*, 2016). A fairly general form of the free energy associated with deformation of the two leaflets of the membrane in contact with a reservoir of lipids with chemical potential μ may be proposed as (Bitbol, Constantin, and Fournier, 2012)

$$\begin{aligned} \Delta G_{mem}^{\pm} = {}&\pm f_H H^{\pm} \pm f'_H (a^{\pm} - a_0) H^{\pm} + f''_H (H^{\pm})^2 + f_K K^{\pm} \\ &+ \tfrac{1}{2} f_a (a^{\pm} - a_0)^2 + \alpha (\nabla a^{\pm})^2 + \beta \nabla^2 a^{\pm} \\ &+ \gamma (\nabla^2 a^{\pm})^2 - \mu, \end{aligned} \tag{114}$$

where variables associated with the upper and lower leaflets are denoted by $+$ and $-$, $H^{\pm}$ and $K^{\pm}$ are the local mean and Gaussian curvature of the leaflets, $a^{\pm}$ is the area per lipid of each leaflet, and f_H, f'_H, f''_H, f_K, f_a, α, β, and γ are related to constitutive constants of the monolayer. Using the Monge representation and for the case of small deformation of an
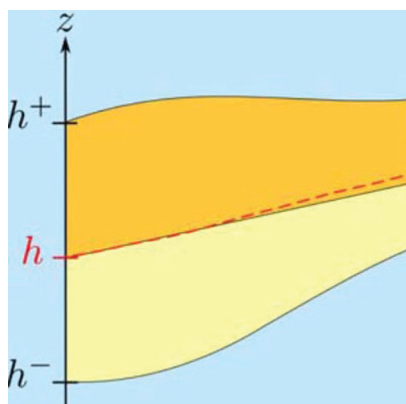
FIG. 22. Parametrization of small deformation of an infinite flat membrane. The midplane deformation h is the average of the deformation of the two leaflets h^+ and h^-. From Bitbol, Constantin, and Fournier, 2012.

infinite flat membrane, we have $H^\pm \simeq \nabla^2 h^\pm/2$ and $K^\pm \simeq \det(\partial_i \partial_j h^\pm)$; see Fig. 22.

We now assess the contribution of the electrostatic energy associated with the motion of the voltage sensor in the dielectric medium. This may be obtained via the Poisson-Boltzmann equation (105). Once the potential field is evaluated over the domain, the total electrostatic energy can be calculated using

$$\Delta G_{\text{elect}} = \int_\Omega \xi(\mathbf{r})\rho_m(\mathbf{r})d\Omega. \tag{115}$$

Additional contributions may be added to the energy for an improved calculation of the gating probability. For instance, the nonpolar energy associated with isolating large molecules from water and the corresponding solvent reorganization can be estimated using a continuum approach (Sitkoff, Ben-Tal, and Honig, 1996). This approach assumes that the energy required to stabilize the molecule in the hydrophobic domain of the membrane is proportional to the solvent accessible surface area (SASA). Thus, the nonpolar energy can be written as (Choe, Hecht, and Grabe, 2008)

$$\Delta G_{\text{np}} = a(A_{\text{mem}} - A_{\text{sol}}) + b, \tag{116}$$

where A_{mem} and A_{sol} are SASA proteins in the membrane and solution, respectively.

The equilibrium state of the membrane can be determined by minimization of the total free energy

$$\Delta G_{\text{tot}} = \Delta G_{\text{mem}} + \Delta G_{\text{elect}} + \Delta G_{\text{np}}. \tag{117}$$

This leads to a free-energy plot with a double minima indicating the position of the S4 domain in the closed and open states. The free-energy difference between the two states is then used in Eq. (113) to calculate the probability of the channel being in the open state. To our knowledge, no theoretical model has included electromechanical coupling effects such as the Maxwell stress and flexoelectricity of the membrane in the gating mechanism (with the exception of a model discussed in Sec. V.D). It would be interesting to see

how these coupling effects affect lipid-protein interactions and, consequently, the gating mechanism.

D. Flexoelectricity and a case study in the implications for sensory systems: The hearing mechanism

In one manner or the other, electromechanics plays an important role in adjudicating the response of our sensory systems (Brownell et al., 2001). In what follows, adhering closely to a summary given by Deng et al. (2019), we primarily highlight its relevance for the hearing mechanism.

Like some of the other sensory systems in animals, such as tactile sensing and vision, the auditory mechanism also offers an interesting study due to numerous extraordinary features. In the context of human hearing, the ears are capable of resolving a frequency difference as small as 1/30th of the span between two successive piano keys (one semitone). Our discernible auditory range runs across 3 orders of magnitude (20 Hz–20 kHz), and we are able to accommodate amplitudes across 6 orders of magnitude (Martin, Hudspeth, and Jülicher, 2001; Hudspeth, 2014). Arguably one of the most interesting features pertaining to our hearing mechanism is that the auditory apparatus is not a passive sensor. To appreciate this, we remain cognizant of the fact that significant dissipation of the energy of sound waves occurs as they travel into the fluid-filled cochlea. Stemming from the groundbreaking work of Gold (1948) and various more recent works (Choe, Magnasco, and Hudspeth, 1998; Camalet et al., 2000; Hudspeth, 2005; Hudspeth, Jülicher, and Martin, 2010; Ó Maoiléidigh and Hudspeth, 2013), it is now widely accepted that our hearing apparatus actively supplies energy to mitigate the dissipation and amplify sound (Nadrowski, Martin, and Jülicher, 2004; Hudspeth, Jülicher, and Martin, 2010). Specifically, the active nature of the auditory process is encapsulated by three extensively discussed attributes and a viable physical model must (at a minimum) be able explain them: amplification, compressive nonlinearity, and frequency tuning. The amplification feature refers to the ability of the ear to amplify the acoustic signals that it intercepts by several times in magnitude (Martin and Hudspeth, 1999, 2001). The compressive nonlinearity permits exquisite sensitivity to even the faintest sound while simultaneously possessing the capability of enduring extremely loud noises (such as those produced during rock and roll concerts). Although the ear can handle sound wave amplitudes that span a millionfold, the actual physical response within the cochlea is compressed into only a hundredfold (several nanometers to hundreds of nanometers) (Eguíluz et al., 2000; Martin and Hudspeth, 2001; Kern and Stoop, 2003; Hudspeth, Jülicher, and Martin, 2010). Thus, for weak input signals, the cochlea amplifies the sound, while if the input is too loud, to protect our auditory apparatus the amplitude is diminished by the active process. Last, the tuning feature endows the mammalian ears with a sharp frequency selectivity (Spiegel and Watson, 1984). Figure 23 schematically outlines some of the key features related to the active processes of the auditory mechanism for a generic non-mammalian vertebrate.

The active processes and the various features of the hearing mechanisms discussed thus far are related to the hair cells in the cochlea. There are several important differences between
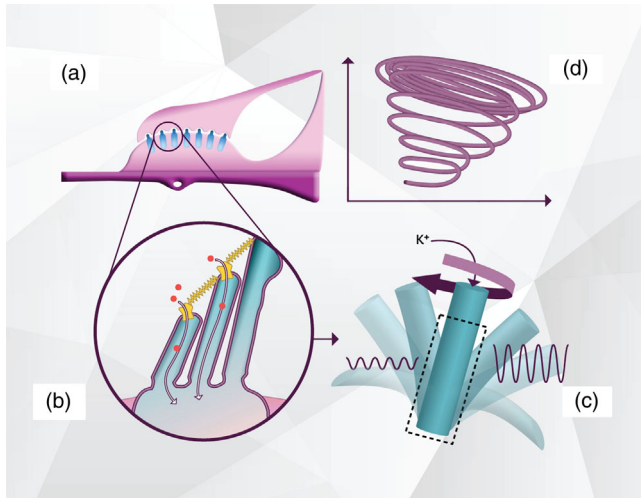
FIG. 23. (a)–(d) Key ideas pertaining to the active process and its importance to the amplification function of the hearing system. Shown is a cross section of the receptor organ in the hearing organ of a generic nonmammalian vertebrate. Located on top of the basement membrane are hair cells whose hair bundles penetrate into the upper tectorial membrane. The acoustic wave propagating in the basilar membrane causes the vibration of the hair cells and the hair bundles. The hair bundle itself consists of "hairlike" objects called stereocilia. As shown in (b), each stereocilium is connected to its tallest neighbor by a fine molecular strand called a tip link. It is believed that on each hair bundle and around the connection to the tip link are several mechanosensitive ion channels. When the hair bundle is deflected, the increase in tip-link tension causes the opening of the ion-channel gates, which allows the influx of ions (both K^+ and Ca^{2+} ones). The charge flow triggers the active motion of the hair bundle through a somewhat debated electromechanical coupling mechanism. As shown in (c), since the charge flow changes the voltage of the hair bundle, it affects the shape and, consequently, the motion of each stereocilium. (d) Evidently, nature has evolved to tune parameters like ion concentration, the membrane's bending stiffness, and even the length and spring constant of the tip links in subtle ways such that the system runs on the verge of the so-called Hopf bifurcation. Being on the verge of instability is speculated to be the key mechanism that allows the amplification of weak sounds in a specific way and results in several other critical and idiosyncratic features. From Deng *et al.*, 2019.

mammalian and nonmammalian hearing mechanisms, but those distinctions are beyond the scope of our review. We are concerned primarily with the role of electromechanics for the hair cells that leads to the attributes that were just mentioned. We simply remark that a hair bundle's motility is believed to play an important role in the active process of the cochlea for both mammals with outer hair cells (Chan and Hudspeth, 2005; Kennedy, Crawford, and Fettiplace, 2005; Ó Maoiléidigh and Jülicher, 2010) and nonmammals without them (Hudspeth, 1997; Choe, Magnasco, and Hudspeth, 1998; Tinevez, Jülicher, and Martin, 2007; Fettiplace and Kim, 2014). In general, the role of hair bundle motility versus somatic motility has been intensely debated in the literature (Lagarde *et al.*, 2008; Ashmore *et al.*, 2010; Peng and Ricci, 2011). Our discussion is largely independent of this debate and is centered primarily around the electromechanical

coupling that leads to hair bundle electromotility and its role in promoting active processes.

Figures 23(a)–23(d) present the key ingredients highlighting, in some sense, a minimal and widely accepted physical model for the active processes in the hearing mechanism. While hair bundle motility is considered important for the hearing of both mammals and nonmammals, the figure depicts the cellular structure germane to nonmammals. Figure 23(a) is the cross section of the receptor organ in the hearing organ of a generic nonmammalian vertebrate. The organ comprises hair cells on the basement membrane (BM). The hair bundle forms the tip of the hair cells and is formed of (to the order of 100) individual "strands" called stereocilia. Incoming acoustic signals vibrate the BM, and thus the attached hair cells and hair bundles. The hair bundle is shown in Fig. 23(b). Each strain has a different height and in the figure, for simplicity, three stereocilia of the bundle are shown. Neighboring stereocilia are linked with a threadlike tip link and mechanosensitive ion-channels are speculated to be populated around the tip link (Hudspeth, 1989, 2005; Camalet *et al.*, 2000). Hair bundle deflection leads to a change in the tip-link tension and thus the opening of the ion-channel gates and a consequent influx of ions (both K^+ and Ca^{2+} ones). Figure 23(c) shows that the vibration of a stereocilium is actively coupled to the charge flow through its channel gates (Choe, Magnasco, and Hudspeth, 1998; Ó Maoiléidigh and Hudspeth, 2013). This active motion of the stereocilium is able to amplify a vibration with small amplitude onto another with much larger amplitude. Thus, the nonlinear electromechanical behavior of the stereocilium is thought to be the reason for the active motion and the amplification. The charge flow alters the transmembrane electric field and, due to the electromechanical coupling, the shape and thus the motion of the stereocilium is also impacted. The pioneering work of Choe, Magnasco, and Hudspeth (1998), Martin and Hudspeth (1999, 2001), Chan and Hudspeth (2005), and Hudspeth (2005) appears to indicate that parameters such as ion concentration, membrane bending stiffness (which impacts deflection), and geometry of the stereocilia are such that dynamical oscillations occur on the verge of Hopf bifurcation; this is schematically shown in Fig. 23(d). The trajectory of the stereocilia motion is shown in phase space. Any disturbance will displace the system from its stationary point. In a characteristically short time, the radius of oscillation will always eventually enter a limit cycle. Hudspeth and coworkers were probably the first to link the active process in cochlea to Hopf bifurcation (Choe, Magnasco, and Hudspeth, 1998; Martin and Hudspeth, 1999, 2001; Chan and Hudspeth, 2005; Hudspeth, 2005).

As one may appreciate following this description, electromechanical coupling plays a central role in the entire process. The precise underpinnings of the electromechanical coupling in stereocilia are still under debate. Some assume that a mechanism such as piezoelectricity is present (Choe, Magnasco, and Hudspeth, 1998; Ó Maoiléidigh and Jülicher, 2010; Ó Maoiléidigh and Hudspeth, 2013). It is evident, however, that stereocilia are not piezoelectric, as they lack the atomistic structure to act that way: this phenomenon is

typically restricted to crystalline structures that lack centrosymmetry (Nowick, 2005).

Flexoelectricity, like electrostriction, is a universal electromechanical coupling mechanism that is present in all dielectrics, including biological membranes (Petrov, 2002). There are strong indications in the work of Brownell, his colleagues, and others that flexoelectricity is a key element of the hair bundle's electromotility (Raphael, Popel, and Brownell, 2000; Brownell *et al.*, 2001; Breneman, Brownell, and Rabbitt, 2009; Krichen and Sharma, 2016). Brownell and collaborators advocated for the viewpoint that membrane flexoelectricity is the source for the electromechanical coupling in hair bundles (Raphael, Popel, and Brownell, 2000; Brownell *et al.*, 2001; Breneman, Brownell, and Rabbitt, 2009). Using a theoretical model, they showed that flexoelectricity is a possible source for the hair bundle's fast adaptation (Breneman, Brownell, and Rabbitt, 2009). Petrov and Sokolov (1986) and Petrov (2002, 2006) argued that flexoelectricity of the nanometer thick biomembranes is the basic mechanoelectric effect for living matter. Within a lipid bilayer membrane, lipids are organized to form a liquid crystal membrane. This membrane exhibits a strong flexoelectric response due to its limited thickness (∼4 to 5 nm) and low bending stiffness (∼10–19 J). In a lipid bilayer membrane, the polarization caused by the direct flexoelectric effect is proportional to its mean curvature (Petrov and Sokolov, 1986; Petrov, 2002, 2006). A phenomenological expression for this relationship is given by $p_s = \mu H$, where p_s (in C/m) is the electric polarization per unit area, H (in 1/m) denotes the membrane's mean curvature (defined as the sum of the membrane's two principal curvatures), and μ (in coulombs) is the area flexoelectric coefficient. Note that p_s relates to the polarization volume density P given by Deng, Liu, and Sharma (2014b) and Ahmadpoor *et al.* (2013), and that $p_s = Ph$, where h is the thickness of the membrane. The direction of p_s is assumed to remain normal to the middle plane during the deformation. Since the coupling between p_s and H is two way, a change in p_s or the transmembrane potential also results in a change of the membrane's mean curvature (Petrov, 2002) due to the converse flexoelectric effect. Experimentally, this converse flexoelectric effect has been observed using an AFM to measure the deformation of a biomembrane (Mosbacher *et al.*, 1998; Zhang, Keleshian, and Sachs, 2001) and optical tweezers to pull membrane tethers and measure their force production (Brownell, Qian, and Anvari, 2010) in response to an applied voltage. The membrane tethers had a geometry similar to that of stereocilia, lacking only their actin cores. In particular, it was experimentally observed that the length of stereocilia changes during current flow (Hakizimana *et al.*, 2012).

Various models in the literature have combined the notion of ion-channel operation with electromotility to explain the hearing mechanism. Notable work came from Ó Maoiléidigh and Jülicher (2010) and Ó Maoiléidigh and Hudspeth (2013), who created a nonlinear dynamical system model that combines the somatic motility of outer hair cells and the hair bundle's motility to illustrate that Hopf bifurcation is responsible for the active process in the cochlea. They proposed an adaptation spring model that ascribes electromechanical coupling to hair bundles and that the adaptation spring located

right at the ions' channel gate is sensitive to Ca^{2+} cations. The flow of cations in the channel and its binding to the adaptation spring is conceived to lead to a decrease in the spring constant. From a mathematical viewpoint, this is an interesting premise, although it is unclear what the physical basis of this adaptation spring is. In particular, they combined the motions of outer hairs and hair bundles and considered the outer hair cells piezoelectric. The notion of piezoelectricity of outer hair cells is somewhat troubling since symmetry requirements for that phenomenon would appear to prohibit it in outer hair cells.

Breneman, Brownell, and Rabbitt (2009) focused on the flexoelectricity of stereocilia as the critical electromechanical coupling mechanism. Flexoelectricity is certainly a plausible eletromechanical coupling mechanism; however, the model of Breneman, Brownell, and Rabbitt is linear in terms of hair bundle dynamics and, as a result, Hopf bifurcation cannot occur (and thus some of the nonlinear aspects of the hearing mechanism remain unexplained, although it is capable of capturing frequency selectivity of the hair bundles).

In a recent work, Deng *et al.* (2019) constructed a physical model based on three facts: (1) the rotation of the hair bundle changes the tension of the tip links; (2) the ion-channel gates are mechanosensitive, and the change of tip-link force therefore impacts the opening state of the gates; and (3) the ions flowing through the channel gate can significantly change the voltage of the hair bundle and then alter the shape of the stereocilia due to the flexoelectric effect. These three ideas when combined with the Hamilton principle and the equations of mechanics, thermodynamics, and electrodynamics appear to yield a nonlinear system of equations that combines several of the key elements present in the models of Hudspeth, 1989, 1997, 2005, 2014; Choe, Magnasco, and Hudspeth, 1998; Martin and Hudspeth, 1999, 2001; Eguíluz *et al.*, 2000; Raphael, Popel, and Brownell, 2000; Brownell *et al.*, 2001; Chan and Hudspeth, 2005; Breneman, Brownell, and Rabbitt, 2009; Hudspeth, Jülicher, and Martin, 2010; Ó Maoiléidigh and Hudspeth, 2013). A key attribute of these models is that, without fitting any artificial parameters (and using only the thermodynamically defined properties of biomembranes determined by experiments), the current model shows that the hair bundle indeed runs at the edge of a Hopf bifurcation for typical values of the intracellular charge density and the membrane bending stiffness. The model also indicates that, as the two previously mentioned parameters deviate from their normal value, Hopf bifurcation and the active motion of the system are severely suppressed. In particular, their models find that flexoelectricity can be a possible cause for the fast adaptation of the hair bundle's motility and serve as an essential ingredient for the occurrence of Hopf bifurcation. The models quantitatively relate the intracellular cations' concentration and the membrane's mechanical properties to the nonlinear dynamic behavior of the hair bundle.

VI. THE RESPONSE OF CELLS TO MAGNETIC FIELDS

A. Overview

Two considerations primarily prompted the initial interest in the interaction of living matter and magnetic fields: (i) The noteworthy ability of nearly 50 species of animals, including

sharks, the European robin, sea lobsters, and certain insects, to detect the terrestrial magnetic field (Maeda *et al.*, 2008; Lohmann, 2010). (ii) The potential adverse health impact of magnetic fields on humans (Wertheimer and Leeper, 1979; Adair, 2000; Matthes *et al.*, 2003). Subsequently, the use of magnetic fields in therapeutic and biomedical contexts has also received significant attention: transcranial magnetic stimulations of brain cells for the treatment of diseases like epilepsy (time-varying magnetic field), and the targeted delivery of drugs and stem cells (Huang *et al.*, 2010; Vaněček *et al.*, 2012; Tukmachev *et al.*, 2015), among others (Corchero and Villaverde, 2009; Krishnan, 2010; Tran and Webster, 2010; Huang *et al.*, 2012). One of the recurrent and mystifying themes of magnetobiology has been the absence of any evidence of so-called magnetoreceptors (unlike electro-receptors). This has led to many works purporting to under-stand the precise mechanism by which magnetic fields interact with biological cells (and arguably the most intensely researched topic within this category is the ability of magneto-reception in certain animals). Several reviews exist on the general aspects of the interaction of magnetic fields and biology; see Zhadin (2001), Binhi (2002), Binhi and Savin (2003), Rosen (2003), Engstrom (2004), Dini and Abbro (2005), Miyakoshi (2005), Saunders (2005), Funk, Monsees, and Özkucur (2009), Zablotskii *et al.* (2016), Zhang, Yarema, and Xu (2017), and Zablotskii, Polyakova, and Dejneka (2018). As is evident from the aforementioned reviews as well as the general literature, there are several complex and controversial issues (Makinistian *et al.*, 2018) pertaining to magnetic fields in biology. A detailed discussion of all such aspects is beyond the scope of this review and we limit our discussion to certain items, as elaborated in the following. An example of research that we do not dwell on is how low magnetic fields may impact chemical kinetics; e.g., low static magnetic fields (to the level of 120 mT) were found to lead to small but discernible eduction in the peak calcium current amplitude in cultured GH3 cells (Rosen, 1996). We do not mention quantum effects at all. Our primary focus is on how deformation and magnetic fields govern the interaction at the cellular scale. This is consistent with our thesis that (while arguably speculative) deformation mediated interaction is one of the primary mechanisms governing the impact of magnetic fields on cellular function. In fact, the thesis by authors such as Rosen (1996) is that it is the deformation-magnetic coupling that also impacts the chemical kinetics. We reiterate and caution the reader that our statements on overemphasizing magnetic-deformation coupling should be viewed as specu-lative, although we contend that it is well grounded based on the existing experimental and theoretical literature; see Bryant and Wolfe (1987), Vlahovska *et al.* (2009), and Sadik *et al.* (2011) as well as our own original research (Krichen, Liu, and Sharma, 2017). The notion is that magnetic fields are first translated into mechanical deformation in the cell and cell membrane, which in turn may trigger an electrical response via (as one example) tension-activated ion channels. In general, once magnetic fields are transduced into a mechani-cal signal, there is a vast literature supporting the latter's effect in the context of cellular behavior including phenomena such as cell proliferation, endocytosis, and many others (Corchero and Villaverde, 2009; Bhushan, 2017).

As we alluded to in Sec. I, the treatment of magnetic fields is mathematically analogous to that of electrical fields. However, this similarity is deceptive when it pertains to the physical underpinnings of the interaction of biological cells and magnetic fields. The first point to be noted is that magnetic fields can be imposed wirelessly, i.e., without contact. In fact, we are all pervasively subjected to a near-uniform (but weak) magnetic field of Earth. Our second observation is that most living matter is transparent to magnetic fields and there is no attenuation of the field, as it penetrates biological matter. Unlike electrostatics, there are no free magnetic "charges" to screen the externally imposed magnetic field. Finally, and this a rather critical point, magnetic forces in living matter tend to be weak, in contrast to the electrical counterparts.

Unlike electric fields, the primary source of magnetic fields is exogenous. While moving electric charges in our cellular machinery in a magnetic field would be subjected to a Lorentz force, this is weak compared to the thermal noise. Zablotskii *et al.* (2016) declared that magnetic forces would become comparable to Coulombic forces only in the vicinity of magnetic neutron stars that are capable of fields as large as 1 MT. Accordingly, discussions usually center around the weak magnetic fields due to Earth or those due to electronic devices, power lines, or any of the sundry sources of electromagnetic fields that pervade modern technology. Stronger magnetic fields (such as those greater than 1 T) are always intentionally imposed in the context of medicine (e.g., magnetic resonance imaging.

There appear to be five key (broadly interpreted) mecha-nisms that are operative in the aforementioned interaction (Fig. 24).[26] First, analogous to the electrical Maxwell stress that has played such a central role in electrical effects, the Maxwell magnetic stress may play a role. As we show in Sec. VI.B, the magnetic Maxwell stress is proportional to the difference between the magnetic susceptibility of the cell and the ambient environment, i.e., $\chi_{\text{cell}} - \chi_{\text{ambient}}$. Given that most biological cells are diamagnetic, with susceptibility close to water (and hence only marginally different than vacuum), the magnetic Maxwell stress is ordinarily exceedingly small. An important exception to this may occur if a magnetic material is present in the cell [Fig. 24(a)]. A central theme of research on this topic is based on the fact that iron oxide particles (magnetite) were found in some magnetically sensitive ani-mals. For example, they were located within cells in the olfactory lamellae of trout (Walker *et al.*, 1997; Diebel *et al.*, 2000) and the upper beaks of pigeons (Winklhofer *et al.*, 2001; Fleissner *et al.*, 2003; Solov'yov and Greiner, 2009; Treiber *et al.*, 2012, 2013). Since these materials are capable of being magnetized, the resulting interaction could poten-tially cause an interaction of the cell and the magnetic field. Magnetite may be in the form of a single domain particle (and thus with an intrinsic magnetic moment) or multidomain where there is no intrinsic moment. In both cases however, an

---

[26]There is a distinct parallel between magnetic-deformation coupling in biological cells and advancements being made in the materials science of soft magnetic materials; see Kim *et al.* (2018), Zhao *et al.* (2019), and Ze *et al.* (2020) and references therein.
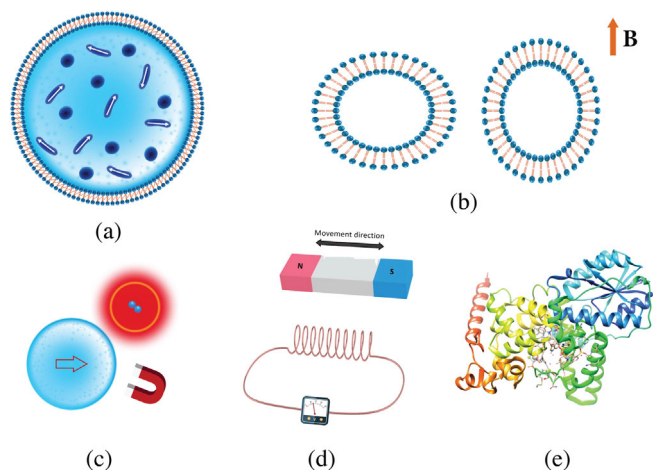
FIG. 24. Major mechanisms governing the interaction for magnetic fields with cellular functions. In (a), the presence of magnetic particles within the cell and their interaction with an applied magnetic field could conceivably activate sensory mechanisms. In addition, on average the cell's magnetic susceptibility may become different than the ambient medium, leading to a noticeable magnetic Maxwell stress. (b) Even in the absence of any magnetic material, another mechanism that may be operative is what is often termed as anisotropic diamagnetism. The key idea here is that the magnetic susceptibility of a biological cell membrane is anisotropic, and its in-plane component differs from its out-of-plane value. It can then be readily shown that the deformation and magnetic field interact with a factor proportional to $\chi_{\mathrm{in}} - \chi_n$. Physically, the deformation proceeds due to the attempt by the lipid molecules to reorient under the action of an applied magnetic field such that the vesicle then stretches parallel to the field. (c) For nonhomogeneous magnetic fields, like dielectrophoresis (discussed in Sec. III.A), a force proportional to the gradient of the magnetic field is developed, i.e., $\mathbf{B} \cdot \nabla \mathbf{B}$. (d) In the phenomenon of magnetic induction, an electric current is generated due to the temporal variation of the magnetic field. Alternatively, this also occurs when a charged object moves in a magnetic field. (e) Magnetic fields can in principle alter chemical reactions and have been proposed to impact free-radical recombination rates. In some migratory birds, it has been proposed that light-induced radical pairs in cryptochrome flavoproteins in the retina lead to an interaction with magnetic fields.

argument can be made that on average the cell acts as a material with magnetic permeability that is not ambient and thus may lead to a noticeable magnetic Maxwell stress. Most works distinguish the mechanism based on whether the material is paramagnetic or ferromagnetic, although the two can be treated with a similar mathematical framework (which we present in Sec. VI.B). That said, how this interaction results in a measurable conversion to an electrical signal is still a subject of controversy. We revisit this topic in Sec. VI.E, where we discuss the phenomenon of magnetoreception. Even in the absence of any magnetic material, another mechanism that may be operative is what is often termed as anisotropic diamagnetism in the literature [Fig. 24(b)]. Although it is usually invoked without reference to the magnetic Maxwell stress, we show that this effect emerges from the same framework. The key idea here is that the magnetic susceptibility of a biological cell membrane is anisotropic and its in-

plane component χ_{in} differs from its out-of-plane value χ_n. It can then be readily shown that the deformation and magnetic field interact with a factor proportional to $\chi_{\mathrm{in}} - \chi_n$. Physically, the deformation proceeds due to the attempt by the lipid molecules to reorient under the action of an applied magnetic field such that the vesicle then stretches parallel to the field. Anisotropic diamagnetism of lipid bilayer membranes and its consequent translation of magnetic fields into deformation has been widely studied. This effect is much weaker (Klara *et al.*, 2016) than the stresses operative in Fig. 24(a), and thus is relevant only for high static magnetic fields. For nonhomogeneous magnetic fields, like dielectrophoresis (discussed in Sec. III.A), a force proportional to the gradient of the magnetic field is developed, i.e., $\mathbf{B} \cdot \nabla \mathbf{B}$ [Fig. 24(c)]. A spectacular example of this effect is the so-called magnetic levitation illustrated on living matter (Beaugnon and Tournier, 1991; Valles *et al.*, 1997), where the developed forces are sufficient to overcome gravity. For this effect to have biological consequences, high gradients are necessary, and these are almost certainly possible only artificially, with no prospects of this occurring under natural conditions that we know of. The textbook phenomenon of magnetic induction, i.e., the production of an electric current due to the temporal variation of the magnetic field, is shown in Fig. 24(d). Alternatively, this also occurs when a charged object moves in a magnetic field. Thus, in principle, this would be an important effect given the widespread reliance of biological systems on electrical signaling. However, it barely crosses the thermal noise threshold, except at large magnetic fields and high frequencies, such as in the therapy related to transcranial magnetic stimulation. The final, and arguably most exotic, interaction mechanism involves the effect of magnetic fields on free-radical recombination rates [Fig. 24(e)]. The interaction energy of molecules involved in such reactions with moderate magnetic fields is low compared to thermal noise, and thus its relevance is somewhat controversial (and still being actively researched). We consider a detailed discussion of this particular mechanism to be beyond the scope of this review, choosing to invoke it only in passing; see Hore (2012), Hore and Mouritsen (2016), and references therein for further information.

The mechanisms in Figs. 24(a) and 24(d) and (to some extent) Fig. 24(e) is discussed primarily in relation to magnetoreception. We examine the mechanisms in Figs. 24(b) and 24(c) separately in Secs. VI.C and VI.D, respectively. We deemphasize the mechanisms in Figs. 24(d) and 24(e) due to their lack of connection to deformation, although some interesting examples exist in connection to them. For example, Kranjc Brezar *et al.* (2020) found that by applying a time-varying magnetic field cell membrane permeability could be dramatically increased through generation of an electrical current and essentially cause an electroporation by proxy.

In what follows, we begin in Sec. VI.B by presenting the mathematical theory that allows one to couple mechanical deformation and magnetic fields. We show that seemingly disparate approaches in the literature can be unified and can emerge from a single framework, and the differences are often the unstated assumptions made. Specifically, we infer the basic scaling relations between the forces and stress in the cells due to the magnetic fields and the physical reasons for the difference between electrical field–induced stresses.

With the theory at hand, we discuss how cells deform under magnetic fields due to the phenomenon of anisotropic diamagnetism in Sec. VI.C and specifically focus on the unique effects of gradients in a magnetic field in Sec. VI.D. We finally present in detail the theories related to cellular mechanisms underpinning the emergent phenomenon magnetoreception in animals (Sec. VI.E).

B. Theory of magnetic-field-deformation interaction in cells

In parallel to the previously outlined electroelastic theory, the magnetoelastic theories can be obtained using a similar construction. In particular, for a deformable and possibly magnetizable body described by deformation $\mathbf{y}:\Omega_R \to \Omega$ and magnetization $\mathbf{m}:\Omega \to \mathbb{R}^3$, the total free energy can be identified as

$$\mathcal{F}[\mathbf{y}, \mathbf{m}] = \mathcal{U}[\mathbf{y}, \mathbf{m}] + \mathcal{E}^{\mathrm{mag}}[\mathbf{y}, \mathbf{m}] + W^{\mathrm{ext}}[\mathbf{y}, \mathbf{m}]. \quad (118)$$

We denote by $\mathbf{h} = \mathbf{h}^e - \nabla\zeta$ the total spatial magnetic field, where $\mathbf{h}^e:\mathbb{R}^3 \to \mathbb{R}^3$ is the external magnetic field, i.e., the magnetic field in space upon removing the body, and the self magnetic field $-\nabla\zeta$ is determined by the magnetization $\mathbf{m}$ via the Maxwell equation ($\chi_\Omega = 1$ on Ω and 0 otherwise):

$$\begin{aligned} \nabla \cdot (-\nabla\zeta + \mathbf{m}\chi_\Omega) &= 0 \quad \text{in } \mathbb{R}^3, \\ -\nabla\zeta &\to 0 \quad \text{as } |\mathbf{x}| \to +\infty. \end{aligned} \quad (119)$$

The terms in Eq. (118) are identified as ($\tilde{\mathbf{M}} = J\mathbf{m}$ is the magnetization per unit volume as seen from the reference configuration)

$$\begin{aligned} \mathcal{U}[\mathbf{y}, \mathbf{m}] &= \int_{\Omega_R} \psi(\nabla_\mathbf{x}\mathbf{y}, \tilde{\mathbf{M}}), \\ \mathcal{E}^{\mathrm{mag}}[\mathbf{y}, \mathbf{m}] &= \frac{\mu_0}{2} \int_V |\nabla\zeta|^2, \\ W^{\mathrm{ext}}[\mathbf{m}] &= -\mu_0 \int_{\Omega_R} \mathbf{h}^e \cdot \tilde{\mathbf{M}}, \end{aligned} \quad (120)$$

where μ_0 is the ambient[27] magnetic permeability and $\psi = \psi(\nabla_\mathbf{x}\mathbf{y}, \tilde{\mathbf{M}})$ is the free-energy density function associated with the deformable and magnetizable body.

The equilibrium state of the system may be determined by the principle of minimum free energy:

$$\min\{\mathcal{F}[\mathbf{y}, \mathbf{m}] : \text{all admissible } \mathbf{y}, \mathbf{m}\}. \quad (121)$$

For ideal paradiamagnetic materials with deformation-independent magnetic susceptibility tensor ($\boldsymbol{\mu} \in \mathbb{R}^{3\times3}_{\mathrm{sym}}$ is the magnetic permeability tensor)

$$\chi = \frac{1}{\mu_0}(\boldsymbol{\mu} - \mu_0\mathbf{I}), \quad (122)$$

where we recall that $\mathbf{I}$ is the identity matrix. The free-energy function can be decomposed into

$$\psi(\nabla_\mathbf{x}\mathbf{y}, \tilde{\mathbf{M}}) = \psi^{\mathrm{elast}}(\nabla_\mathbf{x}\mathbf{y}) + \frac{\mu_0}{2J}\tilde{\mathbf{M}} \cdot \chi^{-1}\tilde{\mathbf{M}}.$$

Using similar calculations to those in Eq. (25), we can show that the Euler-Lagrange equations associated with the variational principle (121) are given by (Liu, 2014b)

$$\begin{aligned} \nabla \cdot (\boldsymbol{\sigma}^{\mathrm{elast}} + \boldsymbol{\sigma}_{\mathrm{MW}}) &= 0 \quad \text{on } \Omega, \\ \chi^{-1}\mathbf{m} - \mathbf{h} &= 0 \quad \text{on } \Omega, \end{aligned} \quad (123)$$

where

$$\boldsymbol{\sigma}^{\mathrm{elast}} = \frac{1}{J}\frac{\partial\psi^{\mathrm{elast}}(\mathbf{F})}{\partial\mathbf{F}}\mathbf{F}^T$$

is the elastic Cauchy stress contributed by the elastic free-energy function $\psi^{\mathrm{elast}}(\mathbf{F})$, $\mathbf{b} = \mu_0(\mathbf{h} + \mathbf{m}) = \boldsymbol{\mu}\mathbf{h}$ is the magnetic flux, and

$$\boldsymbol{\sigma}_{\mathrm{MW}} = \mathbf{h} \otimes \mathbf{b} - \frac{\mathbf{b} \cdot \mathbf{h}}{2}\mathbf{I} \quad (124)$$

is the Maxwell stress due to the magnetic fields.

The mechanical effects of magnetic fields on an ideal paradiamagnetic continuum body is entirely captured by the Maxwell stress (124). Depending on the applications and features of the external magnetic fields, we may focus on one of two separate effects: the deformation due to the Maxwell stress or the overall force and torque on the body (deformable or not). To explicitly demonstrate how to account for these two effects, we consider the configuration of a paradiamagnetic body Ω with magnetic permeability tensor $\boldsymbol{\mu} \in \mathbb{R}^{3\times3}_{\mathrm{sym}}$ embedded in an infinite ambient medium with permeability μ_0 under the application of an external field $\mathbf{h}^e$.

If the externally applied magnetic field $\mathbf{h}^e$ is uniform in space and the body Ω is a thin film perpendicular or parallel to the magnetic field, we find that the magnetic field inside the thin film as determined by Eq. (119) satisfies the following conditions:

(i) If the film is perpendicular to $\mathbf{h}^e$,

$$\mathbf{b} = \boldsymbol{\mu}(\mathbf{h}^e - \nabla\zeta) = \mu_0\mathbf{h}^e.$$

(ii) If the film is parallel to $\mathbf{h}^e$,

$$\mathbf{h} = \mathbf{h}^e - \nabla\zeta = \mathbf{h}^e.$$

Consequently, the Maxwell stress inside the film is determined as follows:

(i) If the film is perpendicular to $\mathbf{h}^e$,

$$\boldsymbol{\sigma}_{\mathrm{MW}}^{\mathrm{int}} = \mu_0^2[(\boldsymbol{\mu}^{-1}\mathbf{h}^e) \otimes \mathbf{h}^e - \tfrac{1}{2}(\mathbf{h}^e \cdot \boldsymbol{\mu}^{-1}\mathbf{h}^e)\mathbf{I}].$$

---

[27]μ_0 is the permeability of the ambient media not the vacuum, although, practically speaking, those are not much different in most biological media. In the case of the biological cell, this would correspond to the permeability of the extracellular fluid.

(ii) If the film is parallel to $\mathbf{h}^e$,

$$\boldsymbol{\sigma}_{\mathrm{MW}}^{\mathrm{int}} = \mathbf{h}^e \otimes (\boldsymbol{\mu}\mathbf{h}^e) - \tfrac{1}{2}(\mathbf{h}^e \cdot \boldsymbol{\mu}\mathbf{h}^e)\mathbf{I}.$$

Further, we notice that the magnetic field in the ambient medium remains just $\mathbf{h}^e$ because of the specific geometry of the body (thin film),[28] and hence the exterior Maxwell stress is given by

$$\boldsymbol{\sigma}_{\mathrm{MW}}^{\mathrm{ext}} = \mu_0 \mathbf{h}^e \otimes \mathbf{h}^e - \tfrac{1}{2}\mu_0 |\mathbf{h}^e|^2 \mathbf{I}.$$

As indicated by the mechanical balance equation (123), the actual traction due to the Maxwell stress that drives the deformation of the film is given by ($\mathbf{n}$ is the outward unit normal on $\partial\Omega$)

$$\mathbf{t}_{\mathrm{MW}} = [\boldsymbol{\sigma}_{\mathrm{MW}}^{\mathrm{ext}} - \boldsymbol{\sigma}_{\mathrm{MW}}^{\mathrm{int}}]\mathbf{n} = \boldsymbol{\sigma}^{\mathrm{elast}}\mathbf{n} \quad \text{on } \partial\Omega. \quad (125)$$

Next we calculate the resultant force and torque on the body Ω of general shape under the application of a generally nonuniform external magnetic field $\mathbf{h}^e$. To this end, we recall the following multipole expansion of the far field concerning the solution to Eq. (119) (Jackson, 1962):

$$4\pi\zeta = \frac{(\mathbf{m}^{\mathrm{tot}} \cdot \hat{\mathbf{x}})}{r^2} + \frac{\hat{\mathbf{x}} \cdot \mathbf{Q}\hat{\mathbf{x}}}{2r^3} + o(1/r^4), \quad (126)$$

where $r = |\mathbf{x}| \gg 1$, $\hat{\mathbf{x}} = \mathbf{x}/r$, $\mathbf{m}^{\mathrm{tot}} = \int_\Omega \mathbf{m}$ is the total magnetic dipole, and $\mathbf{Q}$ is the associated quadrupole. In the current configuration, the Maxwell stress on the exterior boundary of the particle is given by $\boldsymbol{\sigma}_{\mathrm{MW}} = \mathbf{h} \otimes \mathbf{b} - [(\mathbf{h} \cdot \mathbf{b})/2]\mathbf{I}$, satisfies

$$\nabla \cdot \boldsymbol{\sigma}_{\mathrm{MW}} = 0 \quad \text{in } \mathbb{R}^3\backslash\Omega,$$

and can be decomposed into

$$\boldsymbol{\sigma}_{\mathrm{MW}} = \boldsymbol{\sigma}_{\mathrm{MW}}^{\mathrm{ext}} + \boldsymbol{\sigma}_{\mathrm{MW}}^{\mathrm{self}} + \boldsymbol{\sigma}_{\mathrm{MW}}^{\mathrm{inter}},$$

where the external (self, interaction) Maxwell stress is given by

$$\boldsymbol{\sigma}_{\mathrm{MW}}^{\mathrm{ext}} = \mu_0 \mathbf{h}^e \otimes \mathbf{h}^e - \frac{\mu_0}{2}|\mathbf{h}^e|^2\mathbf{I}$$
$$\left(\boldsymbol{\sigma}_{\mathrm{MW}}^{\mathrm{self}} = \mu_0 \nabla\zeta \otimes \nabla\zeta - \frac{\mu_0}{2}|\nabla\zeta|^2\mathbf{I},\right.$$
$$\left.\boldsymbol{\sigma}_{\mathrm{MW}}^{\mathrm{inter}} = \mu_0[-\mathbf{h}^e \otimes \nabla\zeta - \nabla\zeta \otimes \mathbf{h}^e + (\mathbf{h}^e \cdot \nabla\zeta)\mathbf{I}]\right). \quad (127)$$

Therefore, the resultant force and torque on the force are given by

$$\mathbf{F}^{\mathrm{mag}} = \int_{\partial\Omega^+} \boldsymbol{\sigma}_{\mathrm{MW}}\mathbf{n} = \int_{\partial B_R} \boldsymbol{\sigma}_{\mathrm{MW}}^{\mathrm{inter}}\hat{\mathbf{x}},$$

$$\mathbf{T}^{\mathrm{mag}} = \int_{\partial\Omega^+} \mathbf{x} \times (\boldsymbol{\sigma}_{\mathrm{MW}}\mathbf{n}) = \int_{\partial B_R} \mathbf{x} \times (\boldsymbol{\sigma}_{\mathrm{MW}}^{\mathrm{inter}}\hat{\mathbf{x}}), \quad (128)$$

---

[28]This is fortuitous and will not be the case for a general shape.

where $B_R \supset \Omega$ is the ball of radius R. The external magnetic field $\mathbf{h}^e$ around the particle Ω is typically approximated by a Taylor expansion,

$$\mathbf{h}^e(\mathbf{x}) \approx \mathbf{h}_0^e + (\nabla\mathbf{h}^e)_0 \mathbf{x}, \quad (129)$$

where the subscript 0 indicates the evaluation at the center of the body Ω. Inserting Eq. (129) into Eq. (128) and sending $R \to +\infty$, taking Eq. (126) we find that, to the leading order, the resultant force and torque on the particle are given by

$$\mathbf{F}^{\mathrm{mag}} \approx \mu_0 (\nabla\mathbf{h}^e)_0^T \mathbf{m}^{\mathrm{tot}},$$
$$\mathbf{T}^{\mathrm{mag}} \approx \mathbf{m}^{\mathrm{tot}} \times \mu_0 \mathbf{h}_0^e. \quad (130)$$

Although Eq. (130) demonstrates an intuitive and simple picture of the resultant force and torque due to the magnetic Maxwell stress, finding the total magnetization $\mathbf{m}^{\mathrm{tot}}$ on the body Ω requires the solution to the boundary value problem formed by Eqs. (132) and (119), which in general is tedious and depends on the precise shape of Ω. Exceptions include shapes of ellipsoids (Brown, 1966) and periodic e-inclusions (Liu, 2008), whose solutions give rise to the important concept of demagnetization matrix and demagnetization energy in the theory of micromagnetics (Brown, 1966). If the geometric effect of the continuum body Ω is completely neglected from a microscopic atomistic viewpoint, we may account for the total magnetization of the body using the susceptibility tensor:

$$\mathbf{m} \approx \boldsymbol{\chi}\mathbf{h}_0^e = \frac{1}{\mu_0}(\boldsymbol{\mu} - \mu_0\mathbf{I})\mathbf{h}_0^e. \quad (131)$$

Combining Eqs. (129) and (131), we arrive at the formulas for resultant force and torque that have been widely used in the literature.

There are quicker ways to arrive at Eq. (130), such as by assuming that the particle is infinitesimal and directly applying a force formula like Eq. (28) for monopoles and dipoles. The effort here is to show that the approach based on the Maxwell stress is precise for addressing magneto-electromechanical coupling, applicable to deformable bodies, and able to recover the familiar simplified formulas in the literature.

Comparing Eqs. (123) and (124) with the electroelastic counterparts (25) and (26), we may conclude that theories for ideal diaparamagnetic materials (i.e., magnetic permeability is constant and independent of deformation), piezomagnetic materials, flexomagnetic materials, and magnetoelastic membranes can be established in parallel. This is indeed the case; see Liu (2014b) and references therein for details. One caveat is that the boundary conditions for determining the magnetic field [see Eq. (119)] and electric field [see Eq. (3)] are different, resulting in different local fields. Therefore, the mechanical effects from the Maxwell stress are sometimes significantly different, even if the geometric configuration and material properties are similar. For instance, the mechanical effect on a dielectric film due to metallic electrodes is *compressive*, whereas the magnetic Maxwell stress is *tensile* for a paramagnetic film immersed in a uniform external magnetic field; see Eq. (125).
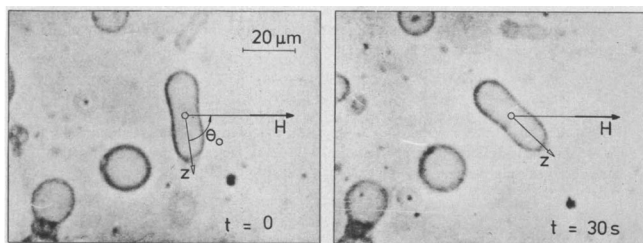
FIG. 25. The time evolution of cylindrical egg lecithin vesicles due to the magnetic anisotropic diamagnetism mechanism. From Boroske and Helfrich, 1978.

C. Deformation of lipid membranes and biological cells under an external magnetic field due to anisotropic diamagnetism

To our knowledge, Helfrich (1973b) was the first to theoretically point out that a spherical biological cell will deform to an ellipsoid under a sufficiently large magnetic field (of the order of 10^4 Oe) due to the fact that the in-plane magnetic susceptibility of the lipid bilayer differs from its out-of-plane value [Fig. 24(b)]. The rotation of the lipid molecules and the consequent stretching of the vesicle are accommodated by the surface tension and bending. In a later work, Boroske and Helfrich (1978) demonstrated the effect experimentally on cylindrical egg lecithin membranes; see Fig. 25. Our previously derived equations are precise and incorporate the case in which the lipid bilayer of a cell displays anisotropic susceptibility and thus subsumes the model first proposed by Helfrich and subsequently modified or improved by many others. The Helfrich model of magnetically deformed cells is approximate, and we outline the underlying assumptions in what follows.

Consider a spherical vesicle whose lipid membrane is endowed with an anisotropic susceptibility tensor (122) subjected to a homogeneous magnetic field. Rather than computing the developed magnetization by solving the boundary value problem caused by Eqs. (123) and (119), we may adapt the approximation (131) from a microscopic atomistic viewpoint. Substituting this approximation into the Zeeman energy (W^{ext}) in Eq. (120), neglecting the energetic contribution of the self-field ($\mathcal{E}^{\text{mag}}$) in Eq. (120), and choosing ψ to be the sum of the bending energy of the Helfrich-Canham membrane (53) and the Zeeman magnetic energy, we obtain the following free energy for the membrane $\mathbb{S}$:

$$\mathcal{F}[\mathbb{S}] = \int_{\mathbb{S}} \frac{1}{2} \kappa_b (H - H_*)^2 - \frac{t\Delta\mu}{2} \int_{\mathbb{S}} (\mathbf{h}_0^e \cdot \mathbf{n})^2, \qquad (132)$$

where t is the thickness of the membrane, $\Delta\mu = \mu_n - \mu_{\text{in}} = \mu_0(\chi_n - \chi_{\text{in}})$ embodies the anisotropy of the magnetic susceptibility, and μ_n (μ_{in}) represents the molecular magnetic permeability in the normal direction of membrane or along the lipid molecules (in the in-plane direction of the membrane or the transverse lipid molecules).[29] Parametrizing the shape of

the membrane using a spherical coordinate system, the deformed shape may be described (to the lowest permitted order) by (Helfrich, 1973b; Iwamoto and Ou-Yang, 2013) $r = r_o + a_{20} Y_{20}(\theta, \phi)$, where $Y_{lm}(\theta, \phi)$ is part of the spherical harmonic series. Minimization of Eq. (132) with respect to the coefficients of the spherical harmonic series, as well as further assumptions that the deformation is small, i.e., $|a_{20}|/r_o \ll 1$, and that the surface area remains constant, provides the solution originally derived as (Helfrich, 1973b)

$$a_{20} = -\frac{r_o^3 \Delta\mu t (\mathbf{h}_0^e)^2}{3\kappa_b(6 - r_o H_*)}. \qquad (133)$$

The equations that we derived in Sec. VI.B [Eqs. (120)] are more precise and may be used to directly obtain a more accurate version of Helfrich's expression in Eq. (133) or (more practically) an improved approximation. That said, the assumptions inherent in Eq. (133) are likely to be physically reasonable except at large fields or magnetic anisotropy.

Equation (133) provides some interesting physical insights. First, the spontaneous curvature is an important parameter (in addition to the applied magnetic field) in terms of controlling the shape evolution of the vesicle. Specifically, the spherical shape may be considered to be in neutral equilibrium for $H_* = 6/r_o$. A rich phase diagram is expected (especially when combined with other external parameters such as pressure) for larger values of the spontaneous curvature. For the situation in which $H_* < 6/r_o$, the deformed shape is an oblate ellipsoid for $\Delta\mu > 0$ and is prolate for $\Delta\mu < 0$. Notably, it was proposed by Helfrich (1973a) that the magnetic field–induced deformation ought to be discernible with a measurement of the change in birefringence of the suspended vesicles.

After the experiments of Boroske and Helfrich (1978), other works (Shklyarevskiy et al., 2005; Manyuhina et al., 2007) verified the key predictions of the previously mentioned model. In particular, Manyuhina et al. (2007) observed that, while the model worked well for low values of the magnetic field (< 1 T), there was a measurable discrepancy at high fields. They proposed adding a fourth-order curvature energy term to the bending energy to explain this observation (Manyuhina et al., 2010). Iwamoto and Ou-Yang (2013) offered an alternative explanation and proposed augmenting the model by considering the constraint of constant vesicle volume and a more careful consideration of the constant area constraint. With these considerations, their model is also able to explain the discrepancy between Eq. (133) and experimental observations at higher fields. Besides the attempts by Manyuhina et al. (2007) and Iwamoto and Ou-Yang (2013), Helfrich's basic model was modified by two other works. Ye and Curcuru (2015) extended the model for a time-varying magnetic field. Salac (2016) considered the effect of hydrodynamics on the vesicle motion and deformation under magnetic fields.

An interesting consequence of diamagnetism anisotropy–induced deformation was explored by Liburdy, Tenforde, and Magin (1986), who found that, at temperatures higher than the phase transition temperatures, permeability of the membrane to solute ingress increased due to an applied magnetic field.

---

[29]At times in the biophysical literature the magnetic susceptibility is not dimensionless, since the anisotropic difference of the permeability is not normalized with the ambient medium. Our expression may therefore appear to be slightly different.

They explained their results by suggesting that bilayer forms local ripple structures that lead to instabilities in its elastic response under the action of the magnetic field. The instability facilitates permeation of solutes. Their combination of the domain or ripple structure instability with anisotropic diamagnetism–induced mechanism is critical since increased permeability to solutes was observed at low magnetic fields of 30 mT, while fields as large as 4 T are needed for the magnetic and thermal energies to be comparable (for the anisotropic diamagnetism mechanism). The same mechanism was used by Liburdy, Tenforde, and Magin (1986) to engineer drug release by liposome vesicles under the action of a magnetic field.

The notion of the formation of clusters of lipids in prephase transition temperatures and diamagnetic anisotropy has been invoked to explain other phenomenology as well. In particular, Rosen (1993) argued that the anisotropic diamagnetism–induced deformation caused by magnetic fields is responsible for a temperature-dependent impact on the operation of ion channels. The idea of lipid clusters or domains is essential in this mechanism for explaining the effect of otherwise modest magnetic fields (of the the order of a few hundred millitesla). Specifically, experiments showed that modest magnetic fields (123 mT) could impact both the central nervous system and neuromuscular junctions (Rosen and Lubowsky, 1987; Rosen, 1992). As a comparison, fields as high as 24 T are needed if the Lorentz force mechanism is used to affect axonal conduction (Rosen, 1993). In particular, Rosen (2003) detailed several arguments supporting the thesis that Ca^+ ion channels are impacted by the distortion of clusters and lipids in their vicinity and that levels of a few hundred millitesla suffice for such a result. We note that this mechanism impacting ion channels is a competing explanation for the so-called free-radical-pair mechanism (Tenforde, 1985; Steiner and Ulrich, 1989). Some limited (but not conclusive) support for this mechanism was found in the experiments of Hughes et al. (2005), who tested recombinant mechanosensitive ion channels in artificial liposomes.

An interesting extension of the work on this topic would pertain to the direct solution of Eqs. (120) for a vesicle or a cell without one's resorting to the approximations. Another notable possibility is a detailed exploration of the instabilities of a vesicle under a magnetic field. Dutta and Ray (2007) did consider the formation of patterns in membranes under an applied magnetic field.

D. The effect of gradients of magnetic fields

The phenomenon of magnetophoresis, in analogy with dielectrophoresis, which was described in Sec. III.A, can potentially interact with biological cells by imposing forces and torques proportional to the gradient of the applied magnetic field. In general, gradients of magnetic fields could potentially cause deformation mechanisms not possible in a homogeneous field. This topic has received relatively less attention due to the central preoccupation of the research into magnetoreception by some animals of Earth's magnetic field. Given that Earth's field is relatively homogeneous (and weak), gradient effects are unlikely to play a role in magnetoreception.

Zablotskii et al. (2016) and Zablotskii, Polyakova, and Dejneka (2018) completed reviews on this topic. One of their contentions is that some of the contradictory experimental results may be explained by the fact that the vast literature is concerned with the absolute value of the applied magnitude and that the gradients of the field may play a larger role than what is typically assumed. Specifically, while some claim strong effects of magnetic fields on cell biology (Dini and Abbro, 2005; Miyakoshi, 2005; Saunders, 2005; Funk, Monsees, and Özkucur, 2009; Zhang, Yarema, and Xu, 2017), others claim little to no effect (Binhi and Savin, 2003; Miyakoshi, 2005; Romeo et al., 2016). This apparent contradiction motivated Zablotskii et al. (2016) and Zablotskii, Polyakova, and Dejneka (2018) to urge a re-examination of the importance of gradient effects.

Our formulation in Sec. VI.B may be used to obtain the often-used expressions for magnetophoresis. The external magnetic field $\mathbf{h}^e$ around a particle may be approximated by the following Taylor expansion:

$$\mathbf{h}^e(\mathbf{x}) \approx \mathbf{h}_0^e + (\nabla \mathbf{h}^e)_0 \mathbf{x}, \tag{134}$$

where the subscript 0 indicates the evaluation at the center of the particle. Inserting Eq. (129) into Eq. (128) and sending $R \to +\infty$, using Eq. (126) we find that, to the leading order, the result force and torque on the particle are given by Eqs. (130). Further, combining Eqs. (134) and (131), we arrive at the formulas for the resultant force and torque that were used by Zablotskii et al. (2016),

$$\mathbf{F}^{\mathrm{mag}} \approx \mu_0 (\nabla \mathbf{h}^e)_0^T (\boldsymbol{\chi} \mathbf{h}_0^e) \sim \boldsymbol{\mu} - \mu_0,$$
$$\mathbf{T}^{\mathrm{mag}} \approx \mu_0 \mathbf{h}_0^e \times (\boldsymbol{\chi} \mathbf{h}_0^e) \sim \boldsymbol{\mu} - \mu_0, \tag{135}$$

where, in this context, the scaling $\sim(\boldsymbol{\mu} - \mu_0)$ is simply the contrast between the permeability of the cell membrane and the ambient medium (and not the diamagnetic anisotropy). There are quicker ways to arrive at Eq. (135), such as by directly applying a force formula like Eq. (28) for monopoles and dipoles. The effort here is to show that the approach based on the Maxwell stress is precise for addressing magneto-electromechanical coupling, which is applicable to deformable bodies, and recovering the familiar simplified formulas in the literature. Again it is clear that current models that attempt to take into account magnetophoresis make the previously noted simplifying assumptions.

A magnetic field must vary across the size scale of a cell for the gradient effect to be of any impact, and furthermore the magnetic susceptibility contrast must not be too low. In the former case, fields of gradients sufficient to have an impact on cellular function can be produced only artificially. In particular, it was found (Zablotskii, Polyakova, and Dejneka, 2018) for some known values of susceptibility contrast that a gradient of roughly 1 kT/m is necessary to compete with gravitational force. Notably, through modern technology that includes micromagnets and nanomagnetic particles, among others, field gradients as high as 10^7 T/m may be easily achievable.

With reference to Eq. (135), we note that, for a positive magnetic susceptibility contrast, a cell or vesicle will tend to migrate toward regions of high field gradient and vice versa for a negative contrast. This principle was used for forming a stem cell network by Zablotskii *et al.* (2013). Biomedical applications of cell motion in a magnetic field gradient were reviewed by Binhi and Savin (2003). In general, speculation is that high magnetic field gradients may impact phenomena ranging from cytoskeleton remodeling to genetic damage. Many such studies remain theoretical at this point, although limited experimental evidence supports some of the claims.

E. The emergent phenomenon of magnetoreception in some animals

Although often associated with migratory birds, the presence of magnetoreception is rampant across the animal kingdom.[30] Examples include (Fig. 26) sea turtles, sharks, bats, lobsters, and many others. Recent work also appears to indicate the ability of the human brain to sense the terrestrial magnetic field (Wang *et al.*, 2019). There is ample evidence suggesting that magnetoreceptive animals use Earth's magnetic field to ascertain both directional and (for a subset of animals) positional information (Wiltschko and Wiltschko, 1972, 1995; 2003, 2005; Johnsen and Lohmann, 2005a; Lohmann and Lohmann, 2006). We quote Lohmann, Lohmann, and Putman (2007) and Lohmann (2010) in saying that some of the animals essentially have a low-resolution biological equivalent of the geophysical positioning system. It is in the emergent ability of magnetoreception in animals where the collective mechanisms of magnetic interaction with biological cells (discussed earlier) come together in the form of a high-functioning biological ability that extends beyond medical applications. That said, despite significant attention to research on this topic, a definitive consensus regarding the mechanisms underpinning magnetoreception is still absent. Multiple articles have provided a review of this field (Mouritsen and Ritz, 2005; Wiltschko and Wiltschko, 2005; Begall *et al.*, 2013; Mouritsen, 2018; Lohmann and Lohmann, 2019). In particular, we cite the article by Lohmann (2010), who provided an incisive perspective on the open questions pertaining to this subject.

Unlike electrical field detection by cells, no analogous magnetoreceptors have been discovered to date. Biological tissue is practically transparent to magnetic fields and we do not have much of an option to remove the pervasive geomagnetic field, thus compounding the difficulty in locating magnetoreceptors (Skiles, 1985).

Three competing theories appear to exist that purport to explain the mechanism of magnetoreception. These are broadly consistent with the general cell–magnetic field interaction mechanism that we already outlined in Sec. VI.A. The three proposed mechanisms are electromagnetic induction, the presence of magnetite particles, and "chemical" magnetoreception (Ritz, Dommer, and Phillips, 2002; Johnsen and Lohmann, 2005a, 2008; Mouritsen and Ritz, 2005; Lohmann,

FIG. 26. Magnetosensitive animal. Top photo: European robins have an avian magnetic compass that has been extensively researched. Bottom photo: sharks are among numerous marine animals that can perceive Earth's magnetic field. From Krichen, Liu, and Sharma, 2017.

2010; Solov'yov, Domratcheva, and Schulten, 2014; Hore and Mouritsen, 2016).

Lorenzini ampullae cells are highly sensitive electroreceptors typically found in aquatic saltwater fish such as sharks, skates, and rays (Murray, 1974). They work as highly sensitive electroreceptors. This germinated the notion of electromagnetic induction as the underlying mechanism of magnetoreception. The fish is electrically conductive and, when it swims in a conductive medium (saltwater) in the presence of a stationary terrestrial magnetic field, induction will ensue, leading to an electrical current that could in principle be detected by the electroreceptors. This requires both the animal body and the ambient medium to be electrically conductive. While this is indeed the case for seawater fish, induction cannot explain magnetosensitive animals such as birds that navigate in nonconductive air (Kalmijn, 1974; Lohmann and Johnsen, 2000). In other words, the induction mechanism might be operative for aquatic fish but is hardly a universal mechanism that can explain magnetoreception in general.[31]

---

[30]This section closely follows the outline given by Krichen, Liu, and Sharma (2017).

[31]On this note, perhaps there is no *general* and *universal* mechanism that can explain magnetoreception in all animals, and each magnetosensitive animal has its own idiosyncratic mechanism.
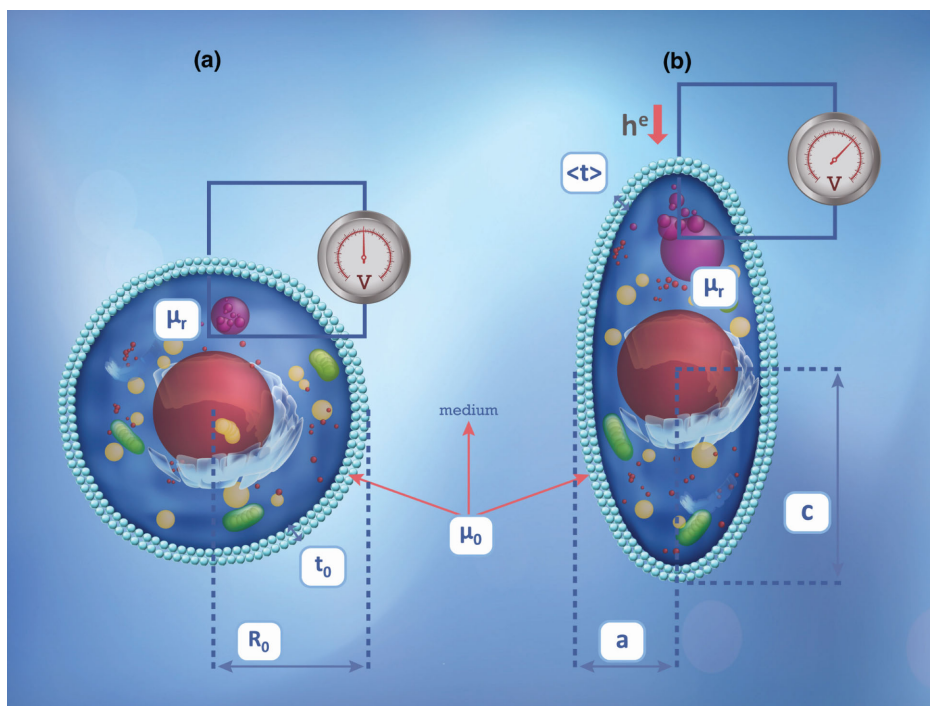
FIG. 27. The cell is enclosed by a soft homogeneous dielectric thin membrane of dielectric permittivity ε_r, and we assume that the permeability of the membrane and its surroundings are about the same as vacuum ($\mu_r = 1$). However, the interior of the cell may have a different magnetic permeability ($\mu_r > 1$). (a) The state where the cell is perfectly spherical is hypothetical but useful as a reference to explain the mechanism outlined in the text. (b) As is well known, we consider the cell membrane to possess a preexisting (or resting) voltage across its thickness. The electrical field due to the resting voltage leads to the so-called electrical Maxwell stress and polarizes the membrane. We assume that our starting configuration is a nearly spherical ellipsoid, as discussed in the text. The magnetic field is now "switched on." The magnetic Maxwell stress causes further deformation and, consequently, alters the preexisting electric field across the membrane. From Krichen, Liu, and Sharma, 2017.

As we mentioned earlier, magnetite [i.e., iron oxide (Fe$_3$O$_4$)] particles have been discovered in some animals sensitive to geomagnetism, such as within cells in the olfactory lamellae of trout (Walker *et al.*, 1997; Diebel *et al.*, 2000) or in the upper beaks of pigeons (Winklhofer *et al.*, 2001; Fleissner *et al.*, 2003; Solov'yov and Greiner, 2009; Treiber *et al.*, 2012, 2013). The premise is that magnetites align themselves with field triggering sensory structures (Kirschvink and Gould, 1981; Edmonds, 1996; Shcherbakov and Winklhofer, 1999; Winklhofer and Kirschvink, 2010). While neither the presence of ferrous particles nor their importance can be disputed, it is entirely unclear how the cells might convert the detected change in magnetic field into detectable electrical signals.

Finally, the chemical origin of magnetoreception, which is predicated on how magnetic fields may alter chemical reactions at the cellular level, has received much attention (Ritz, Adem, and Schulten, 2000; Johnsen and Lohmann, 2005a, 2008; Wang, Mattern, and Ritz, 2006; Ritz *et al.*, 2009, 2010; Rodgers and Hore, 2009; Solov'yov, Mouritsen, and Schulten, 2010; Solov'yov, Domratcheva, and Schulten, 2014; Solov'yov *et al.*, 2014; Hore and Mouritsen, 2016). Indeed, experimental evidence supports the basic principle of magnetic field chemical reactions; see Maeda *et al.* (2008). However, the effect has been confirmed only for magnetic field intensities that far exceed the weak field of Earth (Johnsen and Lohmann, 2005a). Hore (2012) and

Hore and Mouritsen (2016) provided interesting discussions on this topic.

We now outline a model that *prima facie* appears to have broad applicability, and thus merits consideration.[32] The premise is as follows. If a biological cell were to be a magnetoelectric material, then magnetoreception could be explained. Such a material has the property of being able to convert magnetic fields into electrical signals and vice versa: this is thus an analogous phenomenon as piezoelectricity. That said, the known natural single phase magnetoelectric materials are not common and are usually exotic hard crystalline materials. Biological cells lack the symmetry requirements to be magnetoelectric. Krichen, Liu, and Sharma (2017) suggested that a biological cell can indeed behave like a magnetoelectric material under the right conditions. This concept is described in Fig. 27. The intracellular medium, in the absence of a magnetic field, is considered to be of ellipsoidal shape and enclosed by a soft homogeneous dielectric thin lipid membrane. Consistent with what we know about biological cells, we assume that there is no intrinsic magnetoelectric coupling in the cell. Nevertheless, as discussed in Sec. V, it is well known that cell membranes possess a cross-membrane resting potential difference due to actively regulated ion transportation, and there is thus a

---

[32]We acknowledge being biased in this regard.

preexisting electric field in the membrane. We assume the initial configuration of the cell to be ellipsoidal (but nearly spherical). This preexisting electric field will polarize the membrane and deform the overall cell via the electrical Maxwell stress. In other words, owing to the preexisting resting potential across the membrane, the biological cell is deformed and exhibits a residual electric field. Now imagine the action of an external magnetic field on this biological cell. If the magnetic susceptibility of the interior differs from the ambient, then there is also a nontrivial magnetic Maxwell stress (derived in Sec. VI.B), and thus there is further deformation on top of what the resting potential has already caused (i.e., the thickness of the membrane will change). The thinning of the membrane will, due to the constant resting potential across the membrane, induce changes to the electric field and polarization of the membrane, and an overall electrical current (or transportation of ions) in the extracellular medium. In other words, there will be a change in the preexisting electric field upon the action of the magnetic field, which is precisely the magnetoelectric effect. The strength of this effect depends upon how large the susceptibility or permeability contrast is. Thus, we can imagine some animals with weak contrast and hence unmeasurable magnetoelectric response, and some animals with higher contrast. This may also explain higher magnetosensitivity in animals located where magnetite is found.

We now outline the mathematical model itself and what it predicts. Consider a dielectric elastic cell membrane separating conducting intracellular and extracellular fluids. To that end, we introduce an *elastic membrane* of relative dielectric permittivity ε_r and magnetic permeability $\mu_r = 1$ separating the cell interior from the outside (electrolytic) media. We assume that the exterior medium is conductive with relative magnetic permeability that of vacuum $\mu_r = 1$. Likewise, the interior medium of the cell is also assumed to be conductive, although we leave its magnetic permeability unspecified and denote it by μ_r. Let $\mathcal{M} \subset \mathbb{R}^3$ be the 3D membrane body with midsurface being $\partial\Omega$. In a reference configuration when there is no magnetic field or potential difference, the membrane body $\mathcal{M}_0$ is a shell of thickness t_0 and inner radius R_0 ($t_0 \ll R_0$). Let $\mathbf{y}: \mathcal{M}_0 \to \mathcal{M}$ be the deformation of the membrane with a reference midsurface $\partial\Omega_0$ and a deformed midsurface $\partial\Omega$. We denote by $\mathbf{p}: \mathcal{M} \to \mathbb{R}^3$ and $\mathbf{m}: \Omega \to \mathbb{R}^3$, respectively, the polarization in the membrane and the magnetization in the intracellular medium in the deformed configuration that describes the thermodynamic state of the system. Since the central idea is related to the nonlinear deformation state, the distinction between the reference and the deformed configuration must be carefully maintained. Constitutively, we assume linear dielectric behavior in the membrane (of relative permittivity ε_r) and magnetic behavior in the intracellular fluid (of relative permeability μ_r)[33]:

$$\mathbf{e} = \frac{\mathbf{p}}{\varepsilon_0(\varepsilon_r - 1)} \quad \text{in } \mathcal{M}, \qquad \mathbf{h} = \frac{\mathbf{m}}{\mu_r - 1} \quad \text{in } \Omega, \quad (136)$$

---

[33]The key nonlinearities that must be accounted for are geometric in nature and not constitutive.

where $\mathbf{e}$ ($\mathbf{h}$) denotes the spatial electric field (magnetic field) and ε_0 (μ_0) denotes the vacuum electric permittivity (magnetic permeability). We are interested in how the external magnetic field $\mathbf{h}^e$ influences the equilibrium state of the system, and, particularly the electric field across the cell membrane.

Under the application of a cross-membrane resting potential V_0 and an external magnetic field $\mathbf{h}^e$, the total free energy of the system can be identified as

$$\mathcal{F}[\mathbf{y}, \mathbf{p}, \mathbf{m}; V_0, \mathbf{h}^e] = \mathcal{U}[\mathbf{y}, \mathbf{p}, \mathbf{m}] + \mathcal{E}^{\text{elect}}[\mathbf{y}, \mathbf{p}]$$
$$+ \mathcal{E}^{\text{mag}}[\mathbf{y}, \mathbf{m}] + W^{\text{ext}}[\mathbf{y}, \mathbf{p}, \mathbf{m}; \mathbf{h}^e], \quad (137)$$

where $\mathcal{U}$ is the energy associated with a polarizable and magnetizable body,

$$\mathcal{U}[\mathbf{y}, \mathbf{p}, \mathbf{m}] = U^{\text{elast}}[\mathbf{y}] + \int_{\mathcal{M}} \frac{|\mathbf{p}|^2}{2\varepsilon_0(\varepsilon_r - 1)} + \int_{\Omega} \frac{\mu_0}{2(\mu_r - 1)} |\mathbf{m}|^2,$$
$$(138)$$

and W^{ext} is the external work done to the system by boundary devices to maintain the imposed boundary conditions:

$$W^{\text{ext}}[\mathbf{y}, \mathbf{p}, \mathbf{m}; \mathbf{h}^e] = \int_{\partial\mathcal{M}} \boldsymbol{\varphi}(-\boldsymbol{\varepsilon}_0\nabla\varphi + \mathbf{p}) \cdot \mathbf{n} - \int_{\mathbb{R}^3} \mu_0\mathbf{h}^e \cdot \mathbf{m}.$$
$$(139)$$

In Eq. (138) U^{elast} is the elastic energy arising from the deformation of the elastic membrane and $\mathcal{E}^{\text{elect}}$ ($\mathcal{E}^{\text{mag}}$) is the energy associated with the electric (magnetic) field. For simplicity, we make the assumption that the intracellular and extracellular media are fluids whose elasticity is negligible. The energy penalty associated with the thickness deformation and the stretching is used to describe the elastic behavior of the membrane:

$$U^{\text{elast}}[\mathbf{y}] = \int_{\partial\Omega} \left[\frac{\kappa_t}{2} \left(\frac{t}{t_0} - 1 \right)^2 \right] + \frac{\kappa_s}{2} \frac{(|\partial\Omega| - |\partial\Omega_0|)^2}{|\partial\Omega_0|}, \quad (140)$$

where $\partial\Omega = \mathbf{y}(\partial\Omega_0)$, κ_t is the modulus associated with thickness changes in units of energy per unit area, κ_s is the stretch modulus, t_0 is the thickness in the reference configuration, and t is the thickness of the deformed membrane. The change in the bending energy is negligible in this context and hence ignored. In addition, since the biological membrane is essentially a fluid membrane, we assume that it is effectively incompressible. Therefore, we have

$$\mathcal{I}_1[\mathbf{y}] = \int_{\partial\Omega} t - \int_{\partial\Omega_0} t_0 = 0. \quad (141)$$

Furthermore, we assume that the cell volume remains constant during the deformation, and hence we have

$$\mathcal{I}_2[\mathbf{y}] = \Delta\Omega = 0. \quad (142)$$

In addition, the electric contribution to the free energy is identified as (Liu, 2013a, 2014a)

$$\mathcal{E}^{\text{elect}}[\mathbf{y}, \mathbf{p}; V_0] + \int_{\mathcal{M}} \frac{|\mathbf{p}|^2}{2\varepsilon_0(\varepsilon_r - 1)}$$
$$+ \int_{\partial\mathcal{M}} \varphi(-\varepsilon_0\nabla\varphi + \mathbf{p}) \cdot \mathbf{n}, \qquad (143)$$

where $\mathcal{E}^{\text{elect}}$ is given by Eq. (6) and the electric potential $\varphi: \mathcal{M} \to \mathbb{R}$ is determined as follows by the Maxwell equation:

$$\nabla \cdot (-\varepsilon_0\nabla\varphi + \mathbf{p}) = 0 \quad \text{in } \mathcal{M}, \quad \varphi|_{\text{interior}} = 0,$$
$$\varphi|_{\text{exterior}} = V_0. \qquad (144)$$

Finally, using the Landau's theory of micromagnetics, the magnetic contribution to the free energy can be written as

$$\mathcal{E}^{\text{mag}}[\mathbf{y}, \mathbf{m}; \mathbf{h}^e] + \int_{\Omega} \frac{\mu_0}{2(\mu_r - 1)} |\mathbf{m}|^2 - \int_{\mathbb{R}^3} [\mu_0\mathbf{h}^e \cdot \mathbf{m}], \qquad (145)$$

where $\mathcal{E}^{\text{mag}}[\mathbf{y}, \mathbf{m}; \mathbf{h}^e] = \int_{\mathbb{R}^3}(\mu_0/2)|\nabla\xi|^2$ and the self magnetic potential $\xi: \mathbb{R}^3 \to \mathbb{R}$ must also satisfy the Maxwell equation:

$$\nabla \cdot (-\nabla\xi + \mathbf{m}\chi_\Omega) = 0 \quad \text{in } \mathbb{R}^3,$$
$$\xi \to 0 \qquad \text{as } |\mathbf{x}| \to +\infty. \qquad (146)$$

In Eq. (146) $\chi_\Omega = 1$ on Ω and 0 otherwise. The source term $\mathbf{m}\chi_\Omega$ in Eq. (146) reflects the fact that only the intracellular medium is magnetizable because of the enclosed nanoscale magnetic proteins or particles. In conclusion, the principle of minimum free energy asserts that the equilibrium state of the system is such that

$$\min\{\mathcal{F}[\mathbf{y}, \mathbf{p}, \mathbf{m}; V_0, \mathbf{h}^e] : (\mathbf{y}, \mathbf{p}, \mathbf{m}) \in \mathcal{S}\}, \qquad (147)$$

where $\mathcal{S}$ represents the admissible space of the state variables $(\mathbf{y}, \mathbf{p}, \mathbf{m})$.

A change of external magnetic field $\mathbf{h}^e$ does induce a change of polarization $\mathbf{p}$ in the membrane due to a nonlinear coupling via mechanical deformation, as can be discerned using the solution to the minimization problem in Eq. (147). In practice, this must be done numerically.

The main result is shown in Fig. 28. The change in electrical field of the cell when subjected to a magnetic field is plotted as a function of the cell's interior relative magnetic permeability. The key insight is that even if the relative magnetic permeability of the biological cell is only slightly greater than vacuum, the cell behaves like a magnetoelectric material and can convert magnetic signals into electrical ones within the detectable range of biological cells. Thus, the magnetoreception ability is universal but perhaps exceedingly weak on some animals, including humans.

A relative permeability of the cell interior that is greater than that of vacuum may be explained by the presence of magnetites (iron oxides) within the cytoplasm or any number of other reasons. The key point is that, as long as the relative magnetic permeability of the biological cell is larger than that of vacuum, the cell behaves like a magnetoelectric material, and its ability to convert magnetic signals into electrical ones depends on both the precise value of the permeability and the strength of the applied field. The proposed aforementioned
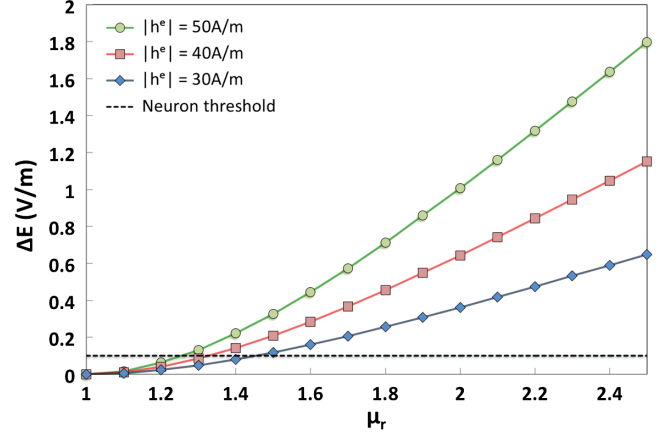

FIG. 28. Variation of the electric field within a cell membrane with respect to the relative permeability for different magnitudes of Earth's magnetic field. To make quantitative estimates, we consider a cell subjected to a magnetic field and plot the ensuing change in the electrical field (ΔE) as a function of the magnetic permeability of its interior. For example, a neuron can sense a variation in the electric field as low as 0.1 V/m: the dashed line shows this threshold. These calculations are done under the assumption that the thickness across the membrane remains uniform. From Krichen, Liu, and Sharma, 2017.

mechanism is complementary with various experimental works (Walker *et al.*, 1997; Diebel *et al.*, 2000; Winklhofer *et al.*, 2001; Fleissner *et al.*, 2003) that detected magnetites in the cells of certain animals. Just a small amount of magnetites will lead to an appreciable permeability contrast.

The described model is able to explain the "magnetic compass" ability, as well the "inclination compass" ability allowing them to be sensitive to the field's axis but not to its polarity (Wiltschko and Wiltschko, 1972). A small subset of magnetosensitive animals (including lobsters, salamanders, and mole rats) can also detect the polarity of Earth's magnetic field and thus distinguish between north and south (Johnsen and Lohmann, 2008). The model cannot explain this ability or further developments and they remain open questions.

VII. CONCLUSIONS AND OUTLOOK

Against a backdrop of what we hope is a unifying theoretical framework, we have provided a perspective on both the ubiquity and the importance of coupling mechanical deformation with electromagnetism in the context of biological cells. There are many implications of this coupling, some that we have reviewed and others that arguably remain to be discovered or investigated. We have attempted to build a connection between seemingly disparate subtopics that are often treated with models that superficially seem different. As an example, we have showed that, using the notion of electrostatic Maxwell stress, both electroporation and dielectrophoresis can be treated within a single setting.

In what follows, we remark on some of the key issues that remain relatively unexplored, and thus could potentially be avenues for future work. We emphasize that our viewpoint is unabashedly from the vantage point of theoretical physics, as opposed to biology, but hope that our perspective has

implications for a better understanding of significant biological phenomena from the perspective of a cell.

(1) We have presented a unifying electromechanics and magnetomechanics framework in Sec. II and VI, respectively. Although we alluded to dissipative effects in Sec. II, a comprehensive framework that incorporates electrodynamics, both electrical and mechanical dissipation (such as membrane viscous effects), and ion transport is missing. In principle, such a framework would not be difficult to establish and literature that highlights one or more of these aspects could be combined together to achieve this. The work of Arroyo and DeSimone (2009) and Arroyo et al. (2018) may be useful for incorporating dissipation. Computational methods go hand in hand with the development of mathematical theories. While significant advancements have been made in the solids area in terms of using multiscale methods [see Yang and Dayal (2011) and Marshall and Dayal (2014)] for coupled electrical and mechanical problems, similar efforts in the context of biological cells would be a welcome development.

(2) The upscaling of electromechanical or magnetomechanical coupling from the level of a cell to the tissue level appears to be a daunting challenge. In the context of coupled mechanical and electromagnetic phenomena, this issue remains unresolved.

(3) A significant literature exists on developing theories of biological membranes from a dimensional reduction of three-dimensional solid or liquid crystal theories; see Friesecke, James, and Müller (2006), Deseri, Piccioni, and Zurlo (2008), Steigmann (2009, 2013, 2018), Edmiston and Steigmann (2011), Ogden and Steigmann (2011), Barham, Steigmann, and White (2012), and Roohbakhshan, Duong, and Sauer (2016). This line of work seems far from being exhausted, however. Specifically, electromagnetomechanical theories of cells that account for the various electromechanical couplings, dissipative effects, presence of proteins, and active "motors" would seem to be a promising future direction. In a somewhat reverse direction, there also appear to be some effort in extracting usually mechanical theories of membranes from microscopic models; see Seguin and Fried (2014). We are unaware of any similar efforts to obtain electromechanical coupling as viewed from a continuum viewpoint by microscopic considerations. Arguably, approaches such as those outlined by Grasinger and Dayal (2020) could be adapted for such an endeavor.

(4) An example of the advantage of unifying the treatment of different biological phenomena using a single theory pertains to the problem of electrofusion of biological cells. It has often been suggested in the literature that electrofusion of the cells requires different steps (Hu et al., 2013). First, it is necessary to expose the cells and vesicles to a nonuniform electric field to sort the cell and bring those into proximity using the resulting kinetic effects (dielectrophoresis and electrorotation). Next, upon application of a dc field, electrodeformation and electroporation of the cell occcur. Finally, the cells that are porated and also close to each other begin to fuse at the pore site, undergo a necking mechanism, and transform into a single body. It is possible to describe the complete process of the electrofusion using a unified framework, as suggested in this review. While mechanical theories of electrofusion abound, to our knowledge the use of a unified framework to describe electrofusion has not occurred.

(5) The study of ion channels in the literature often involves three main topics: ion transport, the gating mechanism, and selectivity (Maffeo et al., 2012).While the effect of mechanical deformation on the operation of mechanosensitive ion channels is extensive, the coupling of ion transport, deformation, and electrostatics in the behavior of voltage-gated channels is conspicuously absent. Coupling effects such as flexoelectricity (Ahmadpoor and Sharma, 2015) and Maxwell stress can potentially affect the function of ion channels. Petrov et al. (1993)) provided plausible experimental evidence that flexoelectricity likely couples with ion transport, but a clear model is still missing. We highlight the experimental evidence supporting the idea that morphological change of the cell membrane and biomolecule as a result of interaction with the electric field can play a significant role in the main aspects of ion-channel function. From a computational perspective, the continuum models that study such conformational changes are limited (Reeves et al., 2008). The biological implications for sensory mechanisms seem to be rich from such a modeling effort.

(6) An electromechanical-diffusion model that can simultaneously couple ion transport, the gating mechanism, and selectivity is still missing. This arguably requires a curation of various insights from experiments and microscopic models, such as atomistics, and then the formulation of a minimal model that ties everything together.

(7) In our review, we have not discussed the role of temperature in the context of the coupling of deformation and electromagnetic fields at the cellular level. The literature is somewhat sparse in this regard, although we do believe there are some avenues for future research pertaining to this topic. In a recent work (Darbaniyan et al., 2021), it was shown that a biological cell is an electret and that (when temperature is considered) the cell behaves like a weak pyroelectric material; i.e., small changes in temperature can be converted into electricity. There are some intriguing implications for this observation. Pit-bearing snakes (such as pythons) are able to see their prey in total darkness, an ability that emanates from being able to detect infrared radiation of objects that are warmer than the ambient medium to form a thermal image. Darbaniyan et al. (2021) argued that the mechanism underpinning the conversion of infrared heat to electrical signals is related to the pyroelectric effect of the cells (in addition to other aspects of the snake physiology, like the morphology of the pit organ).

(8) A definitive explanation for magnetoreception in animals is still absent. Work, much of which we have reviewed, has been conducted on this topic. Perhaps there is no universal mechanism that can be used to explain magnetoreception, and different sets of magnetosensitive animals have their own idiosyncratic mechanisms. We have reviewed a model that explains much of the phenomenology (Krichen, Liu, and Sharma, 2017), but not all of it (such as the ability of some animals to distinguish between north and south and not just the direction). Furthermore, there is no experimental evidence of such a universal model. The discovery of magnetoreceptors would ideally provide an explanation, but this has remained elusive.

ACKNOWLEDGMENTS

REFERENCES

Abidor, I. G., V. B. Arakelyan, L. V. Chernomordik, Yu. A. Chizmadzhev, V. F. Pastushenko, and M. P. Tarasevich, 1979, "Electric breakdown of bilayer lipid membranes: I. The main experimental facts and their qualitative discussion," J. Electroanal. Chem. Interfacial Electrochem. **104**, 37–52.

Abou-Dakka, Milad, E. E. Herrera-Valencia, and Alejandro D. Rey, 2012, "Linear oscillatory dynamics of flexoelectric membranes embedded in viscoelastic media with applications to outer hair cells," J. Non-Newtonian Fluid Mech. **185–186**, 1–17.

Adair, Robert K., 2000, "Static and low-frequency magnetic field effects: Health risks and therapies," Rep. Prog. Phys. **63**, 415.

Adar, Ram M., Samuel A. Safran, Haim Diamant, and David Andelman, 2019, "Screening length for finite-size ions in concentrated electrolytes," Phys. Rev. E **100**, 042615.

Adekanmbi, Ezekiel O., and Soumya K. Srivastava, 2016, "Dielectrophoretic applications for disease diagnostics using lab-on-a-chip platforms," Lab Chip **16**, 2148–2167.

Adžić, Nataša, and Rudolf Podgornik, 2016, "Titratable macroions in multivalent electrolyte solutions: Strong coupling dressed ion approach," J. Chem. Phys. **144**, 214901.

Aggarwal, Sanjay Kumar, and Roderick MacKinnon, 1996, "Contribution of the S4 segment to gating charge in the Shaker K^+ channel," Neuron **16**, 1169–1177.

Ahmadpoor, F., Q. Deng, L. P. Liu, and P. Sharma, 2013, "Apparent flexoelectricity in lipid bilayer membranes due to external charge and dipolar distributions," Phys. Rev. E **88**, 050701.

Ahmadpoor, Fatemeh, and Pradeep Sharma, 2015, "Flexoelectricity in two-dimensional crystalline and biological membranes," Nanoscale **7**, 16555–16570.

Ahuja, Shivani, et al., 2015, "Structural basis of Nav1. 7 inhibition by an isoform-selective small-molecule antagonist," Science **350**, 6267.

Ai, Ye, and Shizhi Qian, 2010, "DC dielectrophoretic particle-particle interactions and their relative motions," J. Colloid Interface Sci. **346**, 448–454.

Ai, Ye, Zhenping Zeng, and Shizhi Qian, 2014, "Direct numerical simulation of AC dielectrophoretic particle-particle interactive motions," J. Colloid Interface Sci. **417**, 72–79.

Alberts, Bruce, 2018, Molecular Biology of the Cell (Garland Science, New York).

Al-Jarro, A., J. Paul, D. W. P. Thomas, J. Crowe, N. Sawyer, F. R. A. Rose, and K. M. Shakesheff, 2007, "Direct calculation of maxwell stress tensor for accurate trajectory prediction during DEP for 2D and 3D structures," J. Phys. D **40**, 71.

Allahyarov, E., H Löwen, A. A. Louis, and J. P. Hansen, 2002, "Discrete charge patterns, Coulomb correlations and interactions in protein solutions," Europhys. Lett. **57**, 731.

Allen, T. W., Andrei Bliznyuk, A. P. Rendell, Serdar Kuyucak, and S.-H. Chung, 2000, "The potassium channel: Structure, selectivity and diffusion," J. Chem. Phys. **112**, 8191–8204.

Anand, Lallit, 2012, "A Cahn-Hilliard-type theory for species diffusion coupled with large elastic-plastic deformations," J. Mech. Phys. Solids **60**, 1983–2002.

Anand, Lallit, and Sanjay Govindjee, 2020, Continuum Mechanics of Solids (Oxford University Press, New York).

Apte, Amey, et al., 2020, "2D electrets of ultrathin MoO_2 with apparent piezoelectricity," Adv. Mater. **32**, 2000006.

Åqvist, Johan, and Victor Luzhkov, 2000, "Ion permeation mechanism of the potassium channel," Nature (London) **404**, 881–884.

Aranda, Said, Karin A. Riske, Reinhard Lipowsky, and Rumiana Dimova, 2008, "Morphological transitions of vesicles induced by alternating electric fields," Biophys. J. **95**, L19–L21.

Argudo, David, Neville P. Bethel, Frank V. Marcoline, and Michael Grabe, 2016, "Continuum descriptions of membranes and their interaction with proteins: Towards chemically accurate models," Biochim. Biophys. Acta Biomembr. **1858**, 1619–1634.

Arroyo, Marino, and Antonio DeSimone, 2009, "Relaxation dynamics of fluid membranes," Phys. Rev. E **79**, 031915.

Arroyo, Marino, Nikhil Walani, Alejandro Torres-Sánchez, and Dimitri Kaurin, 2018, "Onsager's variational principle in soft matter: Introduction and application to the dynamics of adsorption of proteins onto fluid membranes," in The Role of Mechanics in the Study of Lipid Bilayers, CISM International Centre for Mechanical Sciences Vol. 577, edited by David J. Steigmann (Springer, New York), pp. 287–332.

Ashcroft, Frances M., 1999, Ion Channels and Disease (Academic Press, New York).

Ashmore, J., et al., 2010, "The remarkable cochlear amplifier," Hear. Res. **266**, 1–17.

Aubry, N., and P. Singh, 2006, "Control of electrostatic particle-particle interactions in dielectrophoresis," Europhys. Lett. **74**, 623.

Baker, P. F., and D. E. Knight, 1978, "A high-voltage technique for gaining rapid access to the interior of secretory cells [proceedings]," J. Physiol. **284**, 30P.

Bar-Cohen, Yoseph, 2004, Electroactive Polymer (EAP) Actuators as Artificial Muscles: Reality, Potential, and Challenges, SPIE Press Monograph Vol. 136 (SPIE Press, Bellingham, WA).

Barham, Matthew, D. J. Steigmann, and Dan White, 2012, "Magnetoelasticity of highly deformable thin films: Theory and simulation," Int. J. Non-Linear Mech. **47**, 185–196.

Barnett, Alan, and James C. Weaver, 1991, "Electroporation: A unified, quantitative theory of reversible electrical breakdown and mechanical rupture in artificial planar bilayer membranes," Bioelectrochem. Bioenerg. **25**, 163–182.

Barreto, Jose, and Lenard M. Lichtenberger, 1992, "Vesicle acidification driven by a millionfold proton gradient: A model for acid influx through gastric cell membranes," Am. J. Physiol. Gastrointest. Liver Physiol. **262**, G30–G34.

Bartoletti, David C., Gail I. Harrison, and James C. Weaver, 1989, "The number of molecules taken up by electroporated cells: Quantitative determination," FEBS Lett. **256**, 4–10.

Batulan, Zarah, Georges A. Haddad, and Rikard Blunck, 2010, "An intersubunit interaction between S4-S5 linker and S6 is responsible for the slow off-gating component in Shaker K$^+$ channels," J. Biol. Chem. 285, 14005–14019.

Bauer, Siegfried, Reimund Gerhard-Multhaupt, and Gerhard M. Sessler, 2004, "Ferroelectrets: Soft electroactive foams for transducers," Phys. Today 57, No. 2, 37.

Bean, Bruce P., 2007, "The action potential in mammalian central neurons," Nat. Rev. Neurosci. 8, 451–465.

Beaugnon, E., and R. Tournier, 1991, "Levitation of water and organic substances in high static magnetic fields," J. Phys. III (France) 1, 1423–1428.

Beckstein, Oliver, Philip C. Biggin, Peter Bond, Joanne N. Bright, Carmen Domene, Alessandro Grottesi, John Holyoake, and Mark S. P. Sansom, 2003, "Ion channel gating: Insights via molecular simulations," FEBS Lett. 555, 85–90.

Begall, Sabine, E. Pascal Malkemper, Jaroslav Červený, Pavel Němec, and Hynek Burda, 2013, "Magnetic alignment in mammals and other animals," Mamm. Biol. 78, 10–20.

Ben-Yaakov, Dan, David Andelman, Daniel Harries, and Rudi Podgornik, 2009, "Beyond standard Poisson-Boltzmann theory: Ion-specific interactions in aqueous solutions," J. Phys. Condens. Matter 21, 424106.

Benz, R., F. Beckers, and U. Zimmermann, 1979, "Reversible electrical breakdown of lipid bilayer membranes: A charge-pulse relaxation study," J. Membr. Biol. 48, 181–204.

Berneche, Simon, and Benoit Roux, 2001, "Energetics of ion conduction through the K$^+$ channel," Nature (London) 414, 73–77.

Bezanilla, Francisco, 2000, "The voltage sensor in voltage-dependent ion channels," Physiol. Rev. 80, 555–592.

Bezlyepkina, N., R. S. Gracià, P. Shchelokovskyy, Reinhard Lipowsky, and R. Dimova, 2013, "Phase diagram and tie-line determination for the ternary mixture DOPC/eSM/cholesterol," Biophys. J. 104, 1456–1464.

Bhagat, Ali Asgar S., Hansen Bow, Han Wei Hou, Swee Jin Tan, Jongyoon Han, and Chwee Teck Lim, 2010, "Microfluidics for cell separation," Med. Biol. Eng. Comput. 48, 999–1014.

Bhushan, Bharat, 2017, Springer Handbook of Nanotechnology (Springer, New York).

Bingham, Richard J., Peter D. Olmsted, and Stephen W. Smye, 2010, "Undulation instability in a bilayer lipid membrane due to electric field interaction with lipid dipoles," Phys. Rev. E 81, 051909.

Binhi, Vladimir N., 2002, Magnetobiology: Underlying Physical Problems (Academic Press, New York).

Binhi, Vladimir N., and Aleksandr V. Savin, 2003, "Effects of weak magnetic fields on biological systems: Physical aspects," Phys. Usp. 46, 259.

Biria, Aisa, Mohsen Maleki, and Eliot Fried, 2013, "Continuum theory for the edge of an open lipid bilayer," in Advances in Applied Mechanics, Vol. 46, edited by Stéphane P. A. Bordas (Elsevier, New York), pp. 1–68.

Bitbol, Anne-Florence, Doru Constantin, and Jean-Baptiste Fournier, 2012, "Bilayer elasticity at the nanoscale: The need for new terms," PLoS One 7, e48306.

Bivas, I., and Yu. A. Ermakov, 2006, "Elasticity and electrostatics of amphiphilic layers: Current state of the theory and the experiment," Adv. Planar Lipid Bilayers Liposomes 5, 313–343.

Blakemore, Richard, 1975, "Magnetotactic bacteria," Science 190, 377–379.

Boal, David, 2001, Mechanics of the Cell (Cambridge University Press, Cambridge, England), p. 420.

Böckmann, Rainer A., Bert L. De Groot, Sergej Kakorin, Eberhard Neumann, and Helmut Grubmüller, 2008, "Kinetics, statistics, and energetics of lipid membrane electroporation studied by molecular dynamics simulations," Biophys. J. 95, 1837–1850.

Boonnoy, Phansiri, Viwan Jarerattanachat, Mikko Karttunen, and Jirasak Wong-Ekkabut, 2015, "Bilayer deformation, pores, and micellation induced by oxidized lipids," J. Phys. Chem. Lett. 6, 4884–4888.

Boroske, E., and W. Helfrich, 1978, "Magnetic anisotropy of egg lecithin membranes," Biophys. J. 24, 863–868.

Breneman, Kathryn D., William E. Brownell, and Richard D. Rabbitt, 2009, "Hair cell bundles: Flexoelectric motors of the inner ear," PLoS One 4, e5201.

Breneman, Kathryn D., and Richard D. Rabbitt, 2009, "Piezo- and flexoelectric membrane materials underlie fast biological motors in the ear," MRS Online Proc. Libr. 1186, 1186-JJ06-04.

Brown, William Fuller, 1966, Magnetoelastic Interactions, Vol. 9 (Springer, New York).

Brownell, W. E., A. A. Spector, R. M. Raphael, and Aleksander S. Popel, 2001, "Micro- and nanomechanics of the cochlear outer hair cell," Annu. Rev. Biomed. Eng. 3, 169–194.

Brownell, William E., Feng Qian, and Bahman Anvari, 2010, "Cell membrane tethers generate mechanical force in response to electrical stimulation," Biophys. J. 99, 845–852.

Bryant, Gary, and Joe Wolfe, 1987, "Electromechanical stresses produced in the plasma membranes of suspended cells by applied electric fields," J. Membr. Biol. 96, 129–139.

Buyukdagli, Sahin, 2020, "Nanofluidic charge transport under strong electrostatic coupling conditions," J. Phys. Chem. B 124, 11299–11309.

Buyukdagli, Sahin, and Tapio Ala-Nissila, 2017, "Multivalent cation induced attraction of anionic polymers by like-charged pores," J. Chem. Phys. 147, 144901.

Buyukdagli, Sahin, Manoel Manghi, and John Palmeri, 2011, "Ionic exclusion phase transition in neutral and weakly charged cylindrical nanopores," J. Chem. Phys. 134, 074706.

Buyukdagli, Sahin, and Rudolf Podgornik, 2019, "Orientational transition and complexation of DNA with anionic membranes: Weak and intermediate electrostatic coupling," Phys. Rev. E 99, 062501.

Buyukdagli, Sahin, and Rudolf Podgornik, 2021, "Contribution of dipolar bridging to phospholipid membrane interactions: A mean-field analysis," J. Chem. Phys. 154, 224902.

Calabrese, Barbara, Iustin V. Tabarean, Peter Juranka, and Catherine E. Morris, 2002, "Mechanosensitivity of N-type calcium channel currents," Biophys. J. 83, 2560–2574.

Camalet, Sébastien, Thomas Duke, Frank Jülicher, and Jacques Prost, 2000, "Auditory sensitivity provided by self-tuned critical oscillations of hair cells," Proc. Natl. Acad. Sci. U.S.A. 97, 3183–3188.

Cao, Jianshu, et al., 2020, "Quantum biology revisited," Sci. Adv. 6, eaaz4888.

Carle, Georges F., Mark Frank, and Maynard V. Olson, 1986, "Electrophoretic separations of large DNA molecules by periodic inversion of the electric field," Science 232, 65–68.

Carlsson, Fredrik, Martin Malmsten, and Per Linse, 2001, "Monte Carlo simulations of lysozyme self-association in aqueous solution," J. Phys. Chem. B 105, 12189–12195.

Chafai, Djamel Eddine, Vadym Sulimenko, Daniel Havelka, Lucie Kubínová, Pavel Dráber, and Michal Cifra, 2019, "Reversible and irreversible modulation of tubulin self-assembly by intense nanosecond pulsed electric fields," Adv. Mater. 31, 1903636.

Chan, Dylan K., and A. J. Hudspeth, 2005, "Ca^{2+} current–driven nonlinear amplification by the mammalian cochlea in vitro," Nat. Neurosci. 8, 149–155.

Chan, Jun Yuan, *et al.*, 2018, "Dielectrophoresis-based micro-fluidic platforms for cancer diagnostics, Biomicrofluidics **12**, 011503.

Chavanis, Pierre-Henri, 2019, "The generalized stochastic Smoluchowski equation," Entropy **21**, 1006.

Chen, Jian, Mohamed Abdelgawad, Liming Yu, Nika Shakiba, Wei-Yin Chien, Zhe Lu, William R. Geddie, Michael A. S. Jewett, and Yu Sun, 2011, "Electrodeformation for single cell mechanical characterization," J. Micromech. Microeng. **21**, 054012.

Chen, Pu, Xiaojun Feng, Wei Du, and Bi-Feng Liu, 2008, "Microfluidic chips for cell sorting," Front. Biosci. **13**, 2464–2483.

Cheng, I.-Fang, Victoria E. Froude, Yingxi Zhu, Hsueh-Chia Chang, and Hsien-Chang Chang, 2009, "A continuous high-throughput bioparticle sorter based on 3D traveling-wave dielectrophoresis," Lab Chip **9**, 3193–3201.

Chernomordik, Leonid V., and Michael M. Kozlov, 2008, "Mechanics of membrane fusion, Nat. Struct. Mol. Biol. **15**, 675.

Chernomordik, Leonid V., Alexander V. Sokolov, and Vladimir G. Budker, 1990, "Electrostimulated uptake of DNA by liposomes," Biochim. Biophys. Acta Biomembr. **1024**, 179–183.

Choe, Seungho, Karen A. Hecht, and Michael Grabe, 2008, "A continuum method for determining membrane protein insertion energies and the problem of charged residues," J. Gen. Physiol. **131**, 563–573.

Choe, Yong, Marcelo O. Magnasco, and A. J. Hudspeth, 1998, "A model for amplification of hair-bundle motion by cyclical binding of Ca^{2+} to mechanoelectrical-transduction channels," Proc. Natl. Acad. Sci. U.S.A. **95**, 15321–15326.

Chowdhury, Sandipan, and Baron Chanda, 2012, "Thermodynamics of electromechanical coupling in voltage-gated ion channels," J. Gen. Physiol. **140**, 613–623.

Coalson, Rob D., and Maria G. Kurnikova, 2005, "Poisson-Nernst-Planck theory approach to the calculation of current through biological ion channels," IEEE Trans. Nanobioscience **4**, 81–93.

Cohen, Fredric S., Myles H. Akabas, and Alan Finkelstein, 1982, "Osmotic swelling of phospholipid vesicles causes them to fuse with a planar phospholipid bilayer membrane," Science **217**, 458–460.

Corchero, José Luis, and Antonio Villaverde, 2009, "Biomedical applications of distally controlled magnetic nanoparticles," Trends Biotechnol. **27**, 468–476.

Crowley, Joseph M., 1973, "Electrical breakdown of bimolecular lipid membranes as an electromechanical instability," Biophys. J. **13**, 711–724.

Darbaniyan, Faezeh, Kosar Mozaffari, Liping Liu, and Pradeep Sharma, 2021, "Soft matter mechanics and the mechanisms underpinning the infrared vision of snakes," Matter Radiat. Extremes **4**, 241–252.

Dean, D. S., and R. R. Horgan, 2006, "Renormalization of membrane rigidity by long-range interactions," Phys. Rev. E **73**, 011906.

de Groot, Bert L., and Helmut Grubmüller, 2001, "Water permeation across biological membranes: Mechanism and dynamics of aquaporin-1 and GlpF," Science **294**, 2353–2357.

Delemotte, Lucie, and Mounir Tarek, 2012, "Molecular dynamics simulations of lipid membrane electroporation," J. Membr. Biol. **245**, 531–543.

Deng, Qian, Fatemeh Ahmadpoor, William E. Brownell, and Pradeep Sharma, 2019, "The collusion of flexoelectricity and Hopf bifurcation in the hearing mechanism," J. Mech. Phys. Solids **130**, 245–261.

Deng, Qian, Liping Liu, and Pradeep Sharma, 2014a, "Electrets in soft materials: Nonlinearity, size effects, and giant electromechanical coupling," Phys. Rev. E **90**, 012603.

Deng, Qian, Liping Liu, and Pradeep Sharma, 2014b, "Flexoelectricity in soft materials and biological membranes," J. Mech. Phys. Solids **62**, 209–227.

Deseri, Luca, Mario D. Piccioni, and Giuseppe Zurlo, 2008, "Derivation of a new free energy for biological membranes," Continuum Mech. Thermodyn. **20**, 255.

Deserno, Markus, 2015, "Fluid lipid membranes: From differential geometry to curvature stresses," Chem. Phys. Lipids **185**, 11–45.

Devi, U. Vidhya, Paridhi Puri, N. N. Sharma, and M. Ananthasubramanian, 2014, "Electrokinetics of cells in dielectrophoretic separation: A biological perspective," BioNanoScience **4**, 276–287.

Diebel, Carol E., Roger Proksch, Colin R. Green, Peter Neilson, and Michael M. Walker, 2000, "Magnetite defines a vertebrate magnetoreceptor," Nature (London) **406**, 299–302.

Di Leo, V. Claudio, Elisha Rejovitzky, and Lallit Anand, 2014, "A Cahn-Hilliard-type phase-field theory for species diffusion coupled with large elastic deformations: Application to phase-separating Li-ion electrode materials," J. Mech. Phys. Solids **70**, 1–29.

Dimova, Rumiana, Natalya Bezlyepkina, Marie Domange Jordö, Roland L. Knorr, Karin A. Riske, Margarita Staykova, Petia M. Vlahovska, Tetsuya Yamamoto, Peng Yang, and Reinhard Lipowsky, 2009, "Vesicles in electric fields: Some novel aspects of membrane behavior," Soft Matter **5**, 3201–3212.

Dimova, Rumiana, Karin A. Riske, Said Aranda, Natalya Bezlyepkina, Roland L. Knorr, and Reinhard Lipowsky, 2007, "Giant vesicles in electric fields," Soft Matter **3**, 817–827.

Dimova, Rumiana, Karin A. Riske, and M. Damijan, 2016, "Electrodeformation, electroporation, and electrofusion of giant unilamellar vesicles," in *Handbook of Electroporation*, edited by M. Damijan (Springer, New York).

Dini, Luciana, and Luigi Abbro, 2005, "Bioeffects of moderate-intensity static magnetic fields on cell cultures," Micron **36**, 195–217.

Djuzenova, Cholpon S., Ulrich Zimmermann, Hermann Frank, Vladimir L. Sukhorukov, Ekkehard Richter, and Günter Fuhr, 1996, "Effect of medium conductivity and composition on the uptake of propidium iodide into electropermeabilized myeloma cells," Biochim. Biophys. Acta Biomembr. **1284**, 143–152.

Doyle, Declan A., Joao Morais Cabral, Richard A. Pfuetzner, Anling Kuo, Jacqueline M. Gulbis, Steven L. Cohen, Brian T. Chait, and Roderick MacKinnon, 1998, "The structure of the potassium channel: Molecular basis of K^+ conduction and selectivity," Science **280**, 69–77.

Dror, Ron O., Robert M. Dirks, J. P. Grossman, Huafeng Xu, and David E. Shaw, 2012, "Biomolecular simulation: A computational microscope for molecular biology," Annu. Rev. Biophys. **41**, 429–452.

Dutta, Sumana, and Deb Shankar Ray, 2007, "Magnetic field induced pattern formation in reactive membranes," Phys. Rev. E **75**, 016205.

Edmiston, John, and David Steigmann, 2011, "Analysis of nonlinear electrostatic membranes," in *Mechanics and Electrodynamics of Magneto- and Electro-elastic Materials*, CISM International Centre for Mechanical Sciences Vol. 527, edited by Ray W. Ogden and David J. Steigmann (Springer, New York), pp. 153–180.

Edmonds, Donald T., 1996, "A sensitive optically detected magnetic compass for animals," Proc. R. Soc. B **263**, 295–298.

Eguíluz, Víctor M., Mark Ospeck, Y. Choe, A. J. Hudspeth, and Marcelo O. Magnasco, 2000, "Essential Nonlinearities in Hearing," Phys. Rev. Lett. **84**, 5232.

Engelhardt, H., H. Gaub, and E. Sackmann, 1984, "Viscoelastic properties of erythrocyte membranes in high-frequency electric fields," Nature (London) **307**, 378–380.

Engelhardt, H., and E. Sackmann, 1988, "On the measurement of shear elastic moduli and viscosities of erythrocyte plasma membranes by transient deformation in high frequency electric fields," Biophys. J. **54**, 495–508.

English, Niall J., and Damian A. Mooney, 2007, "Denaturation of hen egg white lysozyme in electromagnetic fields: A molecular dynamics study," J. Chem. Phys. **126**, 091105.

English, Niall J., Gleb Y. Solomentsev, and Paul O'Brien, 2009, "Nonequilibrium molecular dynamics study of electric and low-frequency microwave fields on hen egg white lysozyme," J. Chem. Phys. **131**, 035106.

Engstrom, S., 2004, "Physical mechanisms of non-thermal extremely-low-frequency magnetic-field effects," Radio Sci. Bull. **2004**, 95–106, https://ieeexplore.ieee.org/document/7909638.

Faizi, Hammad A., Rumiana Dimova, and Petia M. Vlahovska, 2021, "Electromechanical characterization of biomimetic membranes using electrodeformation of vesicles," Electrophoresis **42**, 2027–2032.

Faizi, Hammad A., Shelli L. Frey, Jan Steinkühler, Rumiana Dimova, and Petia M. Vlahovska, 2019, "Bending rigidity of charged lipid bilayer membranes," Soft Matter **15**, 6006–6013.

Fantoni, Riccardo, 2019, "From the Liouville to the Smoluchowski equation for a colloidal solute particle in a solvent," Physica (Amsterdam) **515A**, 682–692.

Faure, Élise, Greg Starek, Hugo McGuire, Simon Bernèche, and Rikard Blunck, 2012, "A limited 4 Å radial displacement of the S4-S5 linker is sufficient for internal gate closing in K_v channels," J. Biol. Chem. **287**, 40091–40098.

Fettiplace, Robert, and Kyunghee X. Kim, 2014, "The physiology of mechanoelectrical transduction channels in hearing," Physiol. Rev. **94**, 951–986.

Fleissner, Gerta, Elke Holtkamp-Rötzler, Marianne Hanzlik, Michael Winklhofer, Günther Fleissner, Nikolai Petersen, and Wolfgang Wiltschko, 2003, "Ultrastructural analysis of a putative magneto-receptor in the beak of homing pigeons," J. Comp. Neurol. **458**, 350–360.

Flood, Emelie, Celine Boiteux, Bogdan Lev, Igor Vorobyov, and Toby W. Allen, 2019, "Atomistic simulations of membrane ion channel conduction, gating, and modulation," Chem. Rev. **119**, 7737–7832.

Frandsen, Stine K., Mille Vissing, and Julie Gehl, 2020, "A comprehensive review of calcium electroporation—A novel cancer treatment modality," Cancers **12**, 290.

Freeman, Scott A., Michele A. Wang, and James C. Weaver, 1994, "Theory of electroporation of planar bilayer membranes: Predictions of the aqueous area, change in capacitance, and pore-pore separation," Biophys. J. **67**, 42–56.

Freer, Erik M., Oleg Grachev, Xiangfeng Duan, Samuel Martin, and David P. Stumbo, 2010, "High-yield self-limiting single-nanowire assembly with dielectrophoresis," Nat. Nanotechnol. **5**, 525.

Friesecke, Gero, Richard D. James, and Stefan Müller, 2006, "A hierarchy of plate models derived from nonlinear elasticity by gamma-convergence," Arch. Ration. Mech. Anal. **180**, 183–236.

Fromm, Michael E., Loverine P. Taylor, and Virginia Walbot, 1986, "Stable transformation of maize after gene transfer by electro-poration," Nature (London) **319**, 791.

Fu, Anne Y., Charles Spence, Axel Scherer, Frances H. Arnold, and Stephen R. Quake, 1999, "A microfabricated fluorescence-activated cell sorter," Nat. Biotechnol. **17**, 1109–1111.

Fukada, E., and I. Yasuda, 1957, "On the piezoelectric effect of bone," J. Phys. Soc. Jpn. **12**, 1158–1162.

Funk, Richard H. W., Thomas Monsees, and Nurdan Özkucur, 2009, "Electromagnetic effects—From cell biology to medicine," Prog. Histochem. Cytochem. **43**, 177–264.

Furuike, Shou, Victor G. Levadny, Shu Jie Li, and Masahito Yamazaki, 1999, "Low pH induces an interdigitated gel to bilayer gel phase transition in dihexadecylphosphatidylcholine membrane," Biophys. J. **77**, 2015–2023.

Gabriel, Bruno, and Justin Teissie, 1994, "Generation of reactive-oxygen species induced by electropermeabilization of Chinese hamster ovary cells and their consequence on cell viability," Eur. J. Biochem. **223**, 25–33.

Gadsby, David C., 2009, "Ion channels versus ion pumps: The principal difference, in principle," Nat. Rev. Mol. Cell Biol. **10**, 344–352.

Gagnon, Zachary R., 2011, "Cellular dielectrophoresis: Applications to the characterization, manipulation, separation and patterning of cells," Electrophoresis **32**, 2466–2487.

Gamper, Nikita, Yang Li, and Mark S. Shapiro, 2005, "Structural requirements for differential sensitivity of KCNQ K^+ channels to modulation by Ca^{2+}/calmodulin," Mol. Biol. Cell **16**, 3538–3551.

Gao, Ling-Tian, Xi-Qiao Feng, and Huajian Gao, 2009, "A phase field method for simulating morphological evolution of vesicles in electric fields," J. Comput. Phys. **228**, 4162–4181.

Gao, Ling-Tian, Xi-Qiao Feng, Ya-Jun Yin, and Huajian Gao, 2008, "An electromechanical liquid crystal model of vesicles," J. Mech. Phys. Solids **56**, 2844–2862.

Gauger, Bruno, and Friedrich W. Bentrup, 1979, "A study of dielectric membrane breakdown in the *Fucus* egg," J. Membr. Biol. **48**, 249–264.

Geboers, Bart, *et al.*, 2020, "High-voltage electrical pulses in oncology: Irreversible electroporation, electrochemotherapy, gene electrotransfer, electrofusion, and electroimmunotherapy," Radiology **295**, 254–272.

Gehl, J., 2003, "Electroporation: Theory and methods, perspectives for drug delivery, gene therapy and research," Acta Physiol. Scand. **177**, 437–447.

Gehl, Julie, and Lluis M. Mir, 1999, "Determination of optimal parameters for *in vivo* gene transfer by electroporation, using a rapid *in vivo* test for cell permeabilization," Biochem. Biophys. Res. Commun. **261**, 377–380.

Gilson, Michael K., Malcolm E. Davis, Brock A. Luty, and J. Andrew McCammon, 1993, "Computation of electrostatic forces on solvated molecules using the Poisson-Boltzmann equation," J. Phys. Chem. **97**, 3591–3600.

Glaser, Ralf W., Sergei L. Leikin, Leonid V. Chernomordik, Vasili F. Pastushenko, and Artjom I. Sokirko, 1988, "Reversible electrical breakdown of lipid bilayers: Formation and evolution of pores," Biochim. Biophys. Acta Biomembr. **940**, 275–287.

Gold, Thomas, 1948, "Hearing. II. The physical basis of the action of the cochlea," Proc. R. Soc. B **135**, 492–498.

Gothelf, Anita, Lluis M. Mir, and Julie Gehl, 2003, "Electrochemo-therapy: Results of cancer treatment using enhanced delivery of bleomycin by electroporation," Cancer Treat. Rev. **29**, 371–387.

Goulian, M., O. N. Mesquita, D. K. Fygenson, C. Nielsen, O. S. Andersen, and A. Libchaber, 1998, "Gramicidin channel kinetics under tension," Biophys. J. **74**, 328–337.

Gracia, Ruben Serral, Natalya Bezlyepkina, Roland L. Knorr, Reinhard Lipowsky, and Rumiana Dimova, 2010, "Effect of cholesterol on the rigidity of saturated and unsaturated membranes: Fluctuation and electrodeformation analysis of giant vesicles," Soft Matter **6**, 1472–1482.

Grasinger, Matthew, and Kaushik Dayal, 2020, "Statistical mechanical analysis of the electromechanical coupling in an electrically-responsive polymer chain," Soft Matter 16, 6265–6284.

Grasinger, Matthew, Kosar Mozaffari, and Pradeep Sharma, 2021, "Flexoelectricity in soft elastomers and the molecular mechanisms underpinning the design and emergence of giant flexoelectricity," Proc. Natl. Acad. Sci. U.S.A. 118, e2102477118.

Gray, Darren S., John L. Tan, Joel Voldman, and Christopher S. Chen, 2004, "Dielectrophoretic registration of living cells to a microelectrode array," Biosens. Bioelectron. 19, 1765–1774.

Graybill, Philip M., and Rafael V. Davalos, 2020, "Cytoskeletal disruption after electroporation and its significance to pulsed electric field therapies," Cancers 12, 1132.

Grazioli, Davide, Osvalds Verners, Vahur Zadin, Daniel Brandell, and Angelo Simone, 2019, "Electrochemical-mechanical modeling of solid polymer electrolytes: Impact of mechanical stresses on Li-ion battery performance," Electrochim. Acta 296, 1122–1141.

Green, Nicolas G., and Thomas B. Jones, 2007, "Numerical determination of the effective moments of non-spherical particles," J. Phys. D 40, 78.

Green, Nicolas G., and Hywel Morgan, 1999, "Dielectrophoresis of submicrometer latex spheres. 1. Experimental results," J. Phys. Chem. B 103, 41–50.

Grosse, Constantino, and Herman P. Schwan, 1992, "Cellular membrane potentials induced by alternating fields," Biophys. J. 63, 1632–1642.

Gu, Cicely X., Peter F. Juranka, and Catherine E. Morris, 2001, "Stretch-activation and stretch-inactivation of Shaker-IR, a voltage-gated K^+ channel," Biophys. J. 80, 2678–2693.

Guido, I., M. S. Jaeger, and C. Duschl, 2009, "Cell deformation by dielectrophoretic fields," in World Congress on Medical Physics and Biomedical Engineering, September 7–12, 2009, Munich, Germany, IFMBE Proceedings Vol. 25/2, edited by Olaf Dössel and Wolfgang C. Schlegel (Springer, New York), pp. 21–24.

Guidoni, Leonardo, Vincent Torre, and Paolo Carloni, 2000, "Water and potassium dynamics inside the KcsA K^+ channel," FEBS Lett. 477, 37–42.

Gullingsrud, Justin, and Klaus Schulten, 2004, "Lipid bilayer pressure profiles and mechanosensitive channel gating," Biophys. J. 86, 3496–3509.

Gurtovenko, Andrey A., and Ilpo Vattulainen, 2005, "Pore formation coupled to ion transport through lipid membranes as induced by transmembrane ionic charge imbalance: Atomistic molecular dynamics study," J. Am. Chem. Soc. 127, 17570–17571.

Hakizimana, Pierre, William E. Brownell, Stefan Jacob, and Anders Fridberger, 2012, "Sound-induced length changes in outer hair cell stereocilia," Nat. Commun. 3, 1094.

Haluska, Christopher K., Karin A. Riske, Valérie Marchi-Artzner, Jean-Marie Lehn, Reinhard Lipowsky, and Rumiana Dimova, 2006, "Time scales of membrane fusion revealed by direct imaging of vesicle fusion with high temporal resolution," Proc. Natl. Acad. Sci. U.S.A. 103, 15841–15846.

Harbich, W., and W. Helfrich, 1979, "Alignment and opening of giant lecithin vesicles by electric fields," Z. Naturforsch. 34A, 1063–1065.

Harland, Ben, William E. Brownell, Alexander A. Spector, and Sean X. Sun, 2010, "Voltage-induced bending and electromechanical coupling in lipid bilayers," Phys. Rev. E 81, 031907.

Harlos, Karl, Jürgen Stümpel, and Hansjörg Eibl, 1979, "Influence of pH on phosphatidic acid multilayers a rippled structure at high pH values," Biochim. Biophys. Acta Biomembr. 555, 409–416.

Harris, H., 1970, Cell Fusion (Harvard University Press, Cambridge, MA).

Heginbotham, Lise, Ludmila Kolmakova-Partensky, and Christopher Miller, 1998, "Functional reconstitution of a prokaryotic K^+ channel," J. Gen. Physiol. 111, 741–749.

Helfrich, W., 1973a, "Lipid bilayer spheres: Deformation and birefringence in magnetic fields," Phys. Lett. 43A, 409–410.

Helfrich, W., 1973b, "Elastic properties of lipid bilayers: Theory and possible experiments," Z. Naturforsch. 28C, 693–703.

Helfrich, W., 1974, "Deformation of lipid bilayer spheres by electric fields," Z. Naturforsch. C 29, 182–183.

Hellman, Lance M., and Michael G. Fried, 2007, "Electrophoretic mobility shift assay (EMSA) for detecting protein–nucleic acid interactions," Nat. Protoc. 2, 1849.

Heng, Jiunn B., Aleksei Aksimentiev, Chuen Ho, Patrick Marks, Yelena V. Grinkova, Steve Sligar, Klaus Schulten, and Gregory Timp, 2005, "Stretching DNA using the electric field in a synthetic nanopore," Nano Lett. 5, 1883–1888.

Hibino, Masahiro, Masaya Shigemori, Hiroyasu Itoh, Kuniaki Nagayama, and Kazuhiko Kinosita, Jr., 1991, "Membrane conductance of an electroporated cell analyzed by submicrosecond imaging of transmembrane potential," Biophys. J. 59, 209–220.

Hilgemann, Donald W., Siyi Feng, and Cem Nasuhoglu, 2001, "The complex and intriguing lives of PIP_2 with ion channels and transporters," Science's STKE 2001, re19–re19.

Hille, Bertil, 2001, Ion Channels of Excitable Membranes (Sinauer, Sunderland, MA).

Hite, Richard K., Joel A. Butterwick, and Roderick MacKinnon, 2014, "Phosphatidic acid modulation of K_v channel voltage sensor function," eLife 3, e04366.

Hodgkin, Alan L., and Andrew F. Huxley, 1952, "A quantitative description of membrane current and its application to conduction and excitation in nerve," J. Physiol. 117, 500.

Holst, Michael J., 1994, "The Poisson-Boltzmann equation: Analysis and multilevel numerical solution," Ph.D. thesis (University of Illinois, Urbana–Champaign), https://ccom.ucsd.edu/~mholst/pubs/dist/Hols94d.pdf.

Honegger, Thibault, K. Berton, E. Picard, and D. Peyrade, 2011, "Determination of Clausius-Mossotti factors and surface capacitances for colloidal particles," Appl. Phys. Lett. 98, 181906.

Hong, Wei, Xuanhe Zhao, Jinxiong Zhou, and Zhigang Suo, 2008, "A theory of coupled diffusion and large deformation in polymeric gels," J. Mech. Phys. Solids 56, 1779–1793.

Hore, P. J., 2012, "Are biochemical reactions affected by weak magnetic fields?," Proc. Natl. Acad. Sci. U.S.A. 109, 1357–1358.

Hore, P. J., and H. Mouritsen, 2016, "The radical-pair mechanism of magnetoreception," Annu. Rev. Biophys. 45, 299–344.

Hossan, Mohammad Robiul, Robert Dillon, Ajit K. Roy, and Prashanta Dutta, 2013, "Modeling and simulation of dielectrophoretic particle-particle interactions and assembly," J. Colloid Interface Sci. 394, 619–629.

Hou, Xiaowei, Leanne Pedi, Melinda M. Diver, and Stephen B. Long, 2012, "Crystal structure of the calcium release–activated calcium channel Orai," Science 338, 1308–1313.

House, Dustin L., Haoxiang Luo, and Siyuan Chang, 2012, "Numerical study on dielectrophoretic chaining of two ellipsoidal particles," J. Colloid Interface Sci. 374, 141–149.

Hu, Ning, Jun Yang, Sang W. Joo, Arghya Narayan Banerjee, and Shizhi Qian, 2013, "Cell electrofusion in microfluidic devices: A review," Sens. Actuators B 178, 63–85.

Hu, Q., R. P. Joshi, and A. Beskok, 2009, "Model study of electroporation effects on the dielectrophoretic response of spheroidal cells," J. Appl. Phys. 106, 024701.

Huang, Yuran, Sha He, Weipeng Cao, Kaiyong Cai, and Xing-Jie Liang, 2012, "Biomedical nanomaterials for imaging-guided cancer therapy," Nanoscale **4**, 6135–6149.

Huang, Zheyong, *et al.*, 2010, "Deep magnetic capture of magnetically loaded cells for spatially targeted therapeutics," Biomaterials **31**, 2130–2140.

Hudspeth, A. J., 2005, "How the ear's works work: Mechanoelectrical transduction and amplification by hair cells," C.R. Biol. **328**, 155–162.

Hudspeth, A. J., 2014, "Integrating the active process of hair cells with cochlear function," Nat. Rev. Neurosci. **15**, 600–614.

Hudspeth, A. J., Frank Jülicher, and Pascal Martin, 2010, "A critique of the critical cochlea: Hopf—a bifurcation—is better than none," J. Neurophysiol. **104**, 1219–1229.

Hudspeth, A. James, 1989, "How the ear's works work," Nature (London) **341**, 397–404.

Hudspeth, A. James, 1997, "Mechanical amplification of stimuli by hair cells," Curr. Opin. Neurobiol. **7**, 480–486.

Hughes, Michael P., 2016, "Fifty years of dielectrophoretic cell separation technology," Biomicrofluidics **10**, 032801.

Hughes, Michael Pycraft, 2000, "AC electrokinetics: Applications for nanotechnology," Nanotechnology **11**, 124.

Hughes, Steven, Alicia J. El Haj, Jon Dobson, and Boris Martinac, 2005, "The influence of static magnetic fields on mechanosensitive ion channel activity in artificial liposomes," Eur. Biophys. J. **34**, 461–468.

Iwamoto, Mitsumasa, and Zhong-can Ou-Yang, 2013, "Anharmonic magnetic deformation of spherical vesicle: Field-induced tension and swelling effects," Chem. Phys. Lett. **590**, 183–186.

Jackson, J. D., 1962, "Magnetostatics," in *Classical Electrodynamics* (John Wiley & Sons, New York).

Jensen, Morten Ø., and Ole G. Mouritsen, 2004, "Lipids do influence protein function—The hydrophobic matching hypothesis revisited," Biochim. Biophys. Acta Biomembr. **1666**, 205–226.

Jia, Lili, Samira G. Moorjani, Thomas N. Jackson, and William O. Hancock, 2004, "Microscale transport and sorting by kinesin molecular motors," Biomed. Microdevices **6**, 67–74.

Jiang, Youxing, Alice Lee, Jiayun Chen, Martine Cadene, Brian T. Chait, and Roderick MacKinnon, 2002, "Crystal structure and mechanism of a calcium-gated potassium channel," Nature (London) **417**, 515–522.

Jiang, Youxing, Alice Lee, Jiayun Chen, Vanessa Ruta, Martine Cadene, Brian T. Chait, and Roderick MacKinnon, 2003, "X-ray structure of a voltage-dependent K^+ channel," Nature (London) **423**, 33–41.

Jiang, Youxing, Vanessa Ruta, Jiayun Chen, Alice Lee, and Roderick MacKinnon, 2003, "The principle of gating charge movement in a voltage-dependent K^+ channel," Nature (London) **423**, 42–48.

Jogini, Vishwanath, and Benoît Roux, 2005, "Electrostatics of the intracellular vestibule of K^+ channels," J. Mol. Biol. **354**, 272–288.

Johnsen, S., and K. J. Lohmann, 2008, "Magnetoreception in animals," Phys. Today **61**, No. 3, 29–35.

Johnsen, Sönke, and Kenneth J. Lohmann, 2005a, "The physics and neurobiology of magnetoreception," Nat. Rev. Neurosci. **6**, 703–712.

Johnsen, Sönke, and Kenneth J. Lohmann, 2005b, "The physics and neurobiology of magnetoreception," Nat. Rev. Neurosci. **6**, 703–712.

Jones, T., 1995, *Electromechanics of Particles* (Cambridge University Press, Cambridge, England).

Jones, Thomas B., 1979, "Dielectrophoretic force calculation," J. Electrost. **6**, 69–82.

Jones, Thomas B., 2003, "Basic theory of dielectrophoresis and electrorotation," IEEE Eng. Med. Biol. Mag. **22**, 33–42.

Jones, Thomas B., and Masao Washizu, 1996, "Multipolar dielectrophoretic and electrorotation theory," J. Electrost. **37**, 121–134.

Kadaksham, John, Pushpendra Singh, and Nadine Aubry, 2005, "Dielectrophoresis induced clustering regimes of viable yeast cells," Electrophoresis **26**, 3738–3744.

Kagan, Daniel, Rawiwan Laocharoensuk, Maria Zimmerman, Corbin Clawson, Shankar Balasubramanian, Dae Kang, Daniel Bishop, Sirilak Sattayasamitsathit, Liangfang Zhang, and Joseph Wang, 2010, "Rapid delivery of drug carriers propelled and navigated by catalytic nanoshuttles," Small **6**, 2741–2747.

Kaji, Noritada, Yojiro Tezuka, Yuzuru Takamura, Masanori Ueda, Takahiro Nishimoto, Hiroaki Nakanishi, Yasuhiro Horiike, and Yoshinobu Baba, 2004, "Separation of long DNA molecules by quartz nanopillar chips under a direct current electric field," Anal. Chem. **76**, 15–22.

Kakorin, Sergej, Thomas Liese, and Eberhard Neumann, 2003, "Membrane curvature and high-field electroporation of lipid bilayer vesicles," J. Phys. Chem. B **107**, 10243–10251.

Kakorin, Sergej, and Eberhard Neumann, 2002, "Ionic conductivity of electroporated lipid bilayer membranes," Bioelectrochem. Bioenerg. **56**, 163–166.

Kalmijn, Ad. J., 1974, "The detection of electric fields from inanimate and animate sources other than electric organs," in *Electroreceptors and Other Specialized Receptors in Lower Vertrebrates*, Handbook of Sensory Physiology Vol. III/3, edited by A. Fessard (Springer, New York), pp. 147–200.

Kalstrup, Tanja, and Rikard Blunck, 2018, "S4-S5 linker movement during activation and inactivation in voltage-gated K^+ channels," Proc. Natl. Acad. Sci. U.S.A. **115**, E6751–E6759.

Kandušer, Maša, and Marko Ušaj, 2014, "Cell electrofusion: Past and future perspectives for antibody production and cancer cell vaccines," Expert Opin. Drug Delivery **11**, 1885–1898.

Kang, Kwan Hyoung, and Dongqing Li, 2006, "Dielectric force and relative motion between two spherical particles in electrophoresis," Langmuir **22**, 1602–1608.

Kang, Sangmo, 2015, "Dielectrophoretic motions of a single particle in the vicinity of a planar wall under a direct-current electric field," J. Electrost. **76**, 159–170.

Kar, Srabani, Mohan Loganathan, Koyel Dey, Pallavi Shinde, Hwan-You Chang, Moeto Nagai, and Tuhin Subhra Santra, 2018, "Single-cell electroporation: Current trends, applications and future prospects," J. Micromech. Microeng. **28**, 123002.

Karle, Marc, Sandeep Kumar Vashist, Roland Zengerle, and Felix von Stetten, 2016, "Microfluidic solutions enabling continuous processing and monitoring of biological samples: A review," Anal. Chim. Acta **929**, 1–22.

Kasimova, Marina A., Debanjan Tewari, John B. Cowgill, Willy Carrasquel Ursuleaz, Jenna L. Lin, Lucie Delemotte, and Baron Chanda, 2019, "Helix breaking transition in the S4 of HCN channel is critical for hyperpolarization-dependent gating," eLife **8**, e53400.

Kasson, Peter M., Erik Lindahl, and Vijay S. Pande, 2010, "Atomic-resolution simulations predict a transition state for vesicle fusion defined by contact of a few lipid tails," PLoS Comput. Biol. **6**, e1000829.

Kennedy, H. J., A. C. Crawford, and R. Fettiplace, 2005, "Force generation by mammalian hair bundles supports a role in cochlear amplification," Nature (London) **433**, 880–883.

Kern, A., and R. Stoop, 2003, "Essential Role of Couplings between Hearing Nonlinearities," Phys. Rev. Lett. **91**, 128101.

Khoshmanesh, Khashayar, Saeid Nahavandi, Sara Baratchi, Arnan Mitchell, and Kourosh Kalantar-zadeh, 2011, "Dielectrophoretic platforms for bio-microfluidic systems," Biosens. Bioelectron. **26**, 1800–1814.

Kim, J. G., D. J. Im, Y. M. Jung, and I. S. Kang, 2007, "Deformation and motion of a charged conducting drop in a dielectric liquid under a nonuniform electric field," J. Colloid Interface Sci. 310, 599–606.

Kim, Kisoo, and Won Gu Lee, 2017, "Electroporation for nanomedicine: A review," J. Mater. Chem. B 5, 2726–2738.

Kim, Kwang J., and Satoshi Tadokoro, 2007, Eds., Electroactive Polymers for Robotic Applications, Artificial Muscles and Sensors Vol. 23 (Springer, New York), p. 291.

Kim, Yoonho, Hyunwoo Yuk, Ruike Zhao, Shawn A. Chester, and Xuanhe Zhao, 2018, "Printing ferromagnetic domains for untethered fast-transforming soft materials," Nature (London) 558, 274–279.

Kinosita, Jr., Kazuhiko, Ikuo Ashikawa, Nobuyuki Saita, Hideyuki Yoshimura, Hiroyasu Itoh, Kuniaki Nagayama, and Akira Ikegami, 1988, "Electroporation of cell membrane visualized under a pulsed-laser fluorescence microscope," Biophys. J. 53, 1015–1019.

Kirschvink, J., and J. Gould, 1981, "Biogenic magnetite as a basis for magnetic field detection in animals," BioSystems 13, 181–201.

Kirson, Eilon D., Zoya Gurvich, Rosa Schneiderman, Erez Dekel, Aviran Itzhaki, Yoram Wasserman, Rachel Schatzberger, and Yoram Palti, 2004, "Disruption of cancer cell replication by alternating electric fields," Cancer Res. 64, 3288–3295.

Kittel, Charles, and Herbert Kroemer, 1970, Thermal Physics (Wiley, New York).

Klara, Steven S., Patrick O. Saboe, Ian T. Sines, Mahnoush Babaei, Po-Lin Chiu, Rita DeZorzi, Kaushik Dayal, Thomas Walz, Manish Kumar, and Meagan S. Mauter, 2016, "Magnetically directed two-dimensional crystallization of OmpF membrane proteins in block copolymers," J. Am. Chem. Soc. 138, 28–31.

Kotnik, Tadej, 2013, "Lightning-triggered electroporation and electrofusion as possible contributors to natural horizontal gene transfer," Phys. Life Rev. 10, 351–370.

Kotnik, Tadej, Lea Rems, Mounir Tarek, and Damijan Miklavčič, 2019, "Membrane electroporation and electropermeabilization: Mechanisms and models," Annu. Rev. Biophys. 48, 63–91.

Kranjc Brezar, Simona, Matej Kranjc, Maja Čemažar, Simon Buček, Gregor Serša, and Damijan Miklavčič, 2020, "Electrotransfer of siRNA to silence enhanced green fluorescent protein in tumor mediated by a high intensity pulsed electromagnetic field," Vaccines 8, 49.

Krassowska, Wanda, and Petar D. Filev, 2007, "Modeling electroporation in a single cell," Biophys. J. 92, 404–417.

Kremser, Leopold, Dieter Blaas, and Ernst Kenndler, 2004, "Capillary electrophoresis of biological particles: Viruses, bacteria, and eukaryotic cells," Electrophoresis 25, 2282–2291.

Krichen, S., Liping Liu, and P. Sharma, 2017, "Biological cell as a soft magnetoelectric material: Elucidating the physical mechanisms underpinning the detection of magnetic fields by animals," Phys. Rev. E 96, 042404.

Krichen, Sana, and Pradeep Sharma, 2016, "Flexoelectricity: A perspective on an unusual electromechanical coupling," J. Appl. Mech. 83, 030801.

Krishnan, Kannan M., 2010, "Biomedical nanomagnetics: A spin through possibilities in imaging, diagnostics, and therapy," IEEE Trans. Magn. 46, 2523–2558.

Kumaran, V., 2001, "Effect of surface charges on the curvature moduli of a membrane," Phys. Rev. E 64, 051922.

Kummrow, M., and W. Helfrich, 1991, "Deformation of giant lipid vesicles by electric fields," Phys. Rev. A 44, 8356.

Lagarde, Marcia M. Mellado, Markus Drexl, Victoria A. Lukashkina, Andrei N. Lukashkin, and Ian J. Russell, 2008, "Outer hair cell somatic, not hair bundle, motility is the basis of the cochlear amplifier," Nat. Neurosci. 11, 746–748.

Lambert, Neill, Yueh-Nan Chen, Yuan-Chung Cheng, Che-Ming Li, Guang-Yin Chen, and Franco Nori, 2013, "Quantum biology," Nat. Phys. 9, 10–18.

Lang, Sidney B., 2000, "Piezoelectricity, pyroelectricity and ferro-electricity in biomaterials: Speculation on their biological significance," IEEE Trans. Dielectr. Electr. Insul. 7, 466–473.

Larche, F. C., and J. W. Cahn, 1978, "Thermochemical equilibrium of multiphase solids under stress," Acta Metall. 26, 1579–1589.

Larcht'e, F. C., and J. L. Cahn, 1982, "The effect of self-stress on diffusion in solids," Acta Metall. 30, 1835–1845.

Laurence, Jocelyn A., Peter W. French, Robyn A. Lindner, and David R. Mckenzie, 2000, "Biological effects of electromagnetic fields—Mechanisms for the effects of pulsed microwave radiation on protein conformation," J. Theor. Biol. 206, 291–298.

Le Duc, Vinh, Carlos Rosales, Boo Cheong Khoo, and Jaime Peraire, 2008, "Numerical design of electrical-mechanical traps," Lab Chip 8, 755–763.

Lee, Edward W., Susan Thai, and Stephen T. Kee, 2010, "Irreversible electroporation: A novel image-guided cancer therapy," Gut Liver 4, S99.

Lekkerkerker, H. N. W., 1990, "The electric contribution to the curvature elastic moduli of charged fluid interfaces," Physica (Amsterdam) 167A, 384–394.

Levitt, David G., 1986, "Interpretation of biological ion channel flux data—Reaction-rate versus continuum theory," Annu. Rev. Biophys. Biophys. Chem. 15, 29–57.

Levy, Amir, David Andelman, and Henri Orland, 2013, "Dipolar Poisson-Boltzmann approach to ionic solutions: A mean field and loop expansion analysis," J. Chem. Phys. 139, 164909.

Li, Qufei, et al., 2014, "Structural mechanism of voltage-dependent gating in an isolated voltage-sensing domain," Nat. Struct. Mol. Biol. 21, 244.

Liang, Rong, Sheng Cheng, and Xiuying Wang, 2018, "Secondary structure changes induced by pulsed electric field affect antioxidant activity of pentapeptides from pine nut (pinus koraiensis) protein," Food Chem. 254, 170–184.

Liburdy, R. P., T. S. Tenforde, and R. L. Magin, 1986, "Magnetic field-induced drug permeability in liposome vesicles," Radiat. Res. 108, 102–111.

Litster, J. D., 1975, "Stability of lipid bilayers and red blood cell membranes," Phys. Lett. 53A, 193–194.

Liu, L. P., 2008, "Solutions to the Eshelby conjectures," Proc. R. Soc. A 464, 573–594.

Liu, L. P., and P. Sharma, 2013, "Flexoelectricity and thermal fluctuations of lipid bilayer membranes: Renormalization of flexoelectric, dielectric, and elastic properties," Phys. Rev. E 87, 032715.

Liu, Liping, 2013a, "On energy formulations of electrostatics for continuum media," J. Mech. Phys. Solids 61, 968–990.

Liu, Liping, 2013b, "On energy formulations of electrostatics for continuum media," J. Mech. Phys. Solids 61, 968–990.

Liu, Liping, 2014a, "An energy formulation of continuum magneto-electro-elasticity with applications," J. Mech. Phys. Solids 63, 451–480.

Liu, Liping, 2014b, "An energy formulation of continuum magneto-electro-elasticity with applications," J. Mech. Phys. Solids 63, 451–480.

Liu, Liping, Miao Yu, Hao Lin, and Ramsey Foty, 2017, "Deformation and relaxation of an incompressible viscoelastic body with surface viscoelasticity," J. Mech. Phys. Solids 98, 309–329.

Liu, Yuanming, Yanhang Zhang, Ming-Jay Chow, Qian Nataly Chen, and Jiangyu Li, 2012, "Biological Ferroelectricity Uncovered in Aortic Walls by Piezoresponse Force Microscopy," Phys. Rev. Lett. 108, 078103.

Liu, Yuanming, *et al.*, 2014, "Ferroelectric switching of elastin," Proc. Natl. Acad. Sci. U.S.A. **111**, E2780–E2786.

Lohmann, Kenneth J., 1991, "Magnetic orientation by hatchling loggerhead sea turtles (*Caretta caretta*)," J. Exp. Biol. **155**, 37–49.

Lohmann, Kenneth J., 2010, "Q&A: Animal behaviour—Magnetic-field perception," Nature (London) **464**, 1140–1142.

Lohmann, Kenneth J., and Sönke Johnsen, 2000, "The neurobiology of magnetoreception in vertebrate animals," Trends Neurosci. **23**, 153–159.

Lohmann, Kenneth J., and Catherine M. F. Lohmann, 2006, "Sea turtles, lobsters, and oceanic magnetic maps," Mar. Freshwater Behav. Physiol. **39**, 49–64.

Lohmann, Kenneth J., and Catherine M. F. Lohmann, 2019, "There and back again: Natal homing by magnetic navigation in sea turtles and salmon," J. Exp. Biol. **222**, jeb184077.

Lohmann, Kenneth J., Catherine M F. Lohmann, and Nathan F. Putman, 2007, "Magnetic maps in animals: Nature's GPS," J. Exp. Biol. **210**, 3697–3705.

Long, Stephen B., Ernest B. Campbell, and Roderick MacKinnon, 2005, "Voltage sensor of Kv1. 2: Structural basis of electromechanical coupling," Science **309**, 903–908.

Lopez, A., M. P. Rols, and J. Teissie, 1988, "Phosphorus-31 NMR analysis of membrane phospholipid organization in viable, reversibly electropermeabilized Chinese hamster ovary cells," Biochemistry **27**, 1222–1228.

Lorrain, Paul, and Dale R. Corson, 1970, *Electromagnetic Fields and Waves* (Freeman, San Francisco).

Loubet, Bastien, Per Lyngs Hansen, and Michael Andersen Lomholt, 2013, "Electromechanics of a membrane with spatially distributed fixed charges: Flexoelectricity and elastic parameters," Phys. Rev. E **88**, 062715.

Lu, Zhe, Angela M. Klem, and Yajamana Ramu, 2002, "Coupling between voltage sensors and activation gate in voltage-gated K^+ channels," J. Gen. Physiol. **120**, 663–676.

Lund, Mikael, and Bo Jönsson, 2005, "On the charge regulation of proteins," Biochemistry **44**, 5722–5727.

Lundbæk, J. A., P. Birn, S. E. Tape, Gilman E. S. Toombes, R Søgaard, Roger E. Koeppe, Sol M. Gruner, Anker J. Hansen, and Olaf S. Andersen, 2005, "Capsaicin regulates voltage-dependent sodium channels by altering lipid bilayer elasticity," Mol. Pharmacol. **68**, 680–689.

Lundbæk, Jens A., *et al.*, 2004, "Regulation of sodium channel function by bilayer elasticity: The importance of hydrophobic coupling. Effects of micelle-forming amphiphiles and cholesterol," J. Gen. Physiol. **123**, 599–621.

MacQueen, Luke A., Marc Thibault, Michael D. Buschmann, and Michael R. Wertheimer, 2012, "Electromechanical deformation of mammalian cells in suspension depends on their cortical actin thicknesses," J. Biomech. **45**, 2797–2803.

Maeda, K., K. B. Henbest, F. Cintolesi, I. Kuprov, C. T. Rodgers, P. A. Liddell, D. Gust, C. R. Timmel, and P. J. Hore, 2008, "Chemical compass model of avian magnetoreception," Nature (London) **453**, 387–390.

Maffeo, Christopher, Swati Bhattacharya, Jejoong Yoo, David Wells, and Aleksei Aksimentiev, 2012, "Modeling and simulation of ion channels," Chem. Rev. **112**, 6250–6284.

Makinistian, Leonardo, David J. Muehsam, Ferdinando Bersani, and Igor Belyaev, 2018, "Some recommendations for experimental work in magnetobiology, revisited," Bioelectromagnetics (N.Y.) **39**, 556–564.

Maldarelli, Charles, Rakesh K. Jain, Ivan B. Ivanov, and Eli Ruckenstein, 1980, "Stability of symmetric and unsymmetric thin liquid films to short and long wavelength perturbations," J. Colloid Interface Sci. **78**, 118–143.

Mallouk, Thomas E., and Ayusman Sen, 2009, "Powering nanorobots," Sci. Am. **300**, No. 5, 72–77.

Mancinelli, Fabrizio, Michele Caraglia, Alberto Abbruzzese, Guglielmo d'Ambrosio, Rita Massa, and Ettore Bismuto, 2004, "Non-thermal effects of electromagnetic fields at mobile phone frequency on the refolding of an intracellular protein: Myoglobin," J. Cell. Biochem. **93**, 188–196.

Manyuhina, O. V., J. J. Hetzel, M. I. Katsnelson, and A. Fasolino, 2010, "Non-spherical shapes of capsules within a fourth-order curvature model," Eur. Phys. J. E **32**, 223–228.

Manyuhina, O. V., *et al.*, 2007, "Anharmonic Magnetic Deformation of Self-Assembled Molecular Nanocapsules," Phys. Rev. Lett. **98**, 146101.

Mao, Sheng, and Prashant K. Purohit, 2014, "Insights into flexoelectric solids from strain-gradient elasticity," J. Appl. Mech. **81**, 081004.

Marais, Adriana, *et al.*, 2018, "The future of quantum biology," J. R. Soc. Interface **15**, 20180640.

Marshall, Jason, and Kaushik Dayal, 2014, "Atomistic-to-continuum multiscale modeling with long-range electrostatic interactions in ionic solids," J. Mech. Phys. Solids **62**, 137–162.

Martin, P., and A. J. Hudspeth, 2001, "Compressive nonlinearity in the hair bundle's active response to mechanical stimulation," Proc. Natl. Acad. Sci. U.S.A. **98**, 14386–14391.

Martin, P., A. J. Hudspeth, and F. Jülicher, 2001, "Comparison of a hair bundle's spontaneous oscillations with its response to mechanical stimulation reveals the underlying active process," Proc. Natl. Acad. Sci. U.S.A. **98**, 14380–14385.

Martin, Pascal, and A. J. Hudspeth, 1999, "Active hair-bundle movements can amplify a hair cell's response to oscillatory mechanical stimuli," Proc. Natl. Acad. Sci. U.S.A. **96**, 14306–14311.

Matthes, Ruediger, Paolo Vecchia, Alastair F. McKinlay, Bernard Veyret, and Jürgen H. Bernhardt, 2003, "Exposure to static and low frequency electromagnetic fields, biological effects and health consequences (0–100 kHz). Review of the scientific evidence on dosimetry, biological effects, epidemiological observations and health consequences concerning exposure to static and low frequency electromagnetic fields (0–100 kHz)," International Commission on Non-Ionizing Radiation Protection Report No. ICNIRP-13/2003.

May, Sylvio, 2000, "Protein-induced bilayer deformations: The lipid tilt degree of freedom," Eur. Biophys. J. **29**, 17–28.

Mbarki, R., N. Baccam, Kaushik Dayal, and P. Sharma, 2014, "Piezoelectricity above the Curie temperature? Combining flexoelectricity and functional grading to enable high-temperature electromechanical coupling," Appl. Phys. Lett. **104**, 122904.

McConnell, Lane C., Petia M. Vlahovska, and Michael J. Miksis, 2015, "Vesicle dynamics in uniform electric fields: Squaring and breathing," Soft Matter **11**, 4840–4846.

McFadden, Johnjoe, and Jim Al-Khalili, 2018, "The origins of quantum biology," Proc. R. Soc. A **474**, 20180674.

Mehmet, Toner, and Irimia Daniel, 2005, "Blood-on-a-chip," Annu. Rev. Biomed. Eng. **7**, 77–103.

Mehrishi, Jitendra N., and Johann Bauer, 2002, "Electrophoresis of cells and the biological relevance of surface charge," Electrophoresis **23**, 1984–1994.

Michael, D. H., and M. E. O'Neill, 1970, "Electrohydrodynamic instability in plane layers of fluid," J. Fluid Mech. **41**, 571–580.

Miller, Christopher, 1999, "Ionic hopping defended," J. Gen. Physiol. **113**, 783–787.

Mitkova, Denitsa, Natalia Marukovich, Yury A. Ermakov, and Victoria Vitkova, 2014, "Bending rigidity of phosphatidylserine-containing

lipid bilayers in acidic aqueous solutions," Colloids Surf. A **460**, 71–78.

Miyakoshi, Junji, 2005, "Effects of static magnetic fields at the cellular level," Prog. Biophys. Mol. Biol. **87**, 213–223.

Miyazawa, Atsuo, Yoshinori Fujiyoshi, and Nigel Unwin, 2003, "Structure and gating mechanism of the acetylcholine receptor pore," Nature (London) **423**, 949–955.

Moreau, Adrien, Pascal Gosselin-Badaroudine, and Mohamed Chahine, 2014, "Biophysics, pathophysiology, and pharmacology of ion channel gating pores," Front. Pharmacol. **5**, 53.

Morris, Catherine E., and Peter F. Juranka, 2007, "Nav channel mechanosensitivity: Activation and inactivation accelerate reversibly with stretch," Biophys. J. **93**, 822–833.

Mosbacher, J., M. Langer, J. K. H. Hörber, and F. Sachs, 1998, "Voltage-dependent membrane displacements measured by atomic force microscopy," J. Gen. Physiol. **111**, 65–74.

Mouritsen, Henrik, 2018, "Long-distance navigation and magnetoreception in migratory animals," Nature (London) **558**, 50–59.

Mouritsen, Henrik, and Thorsten Ritz, 2005, "Magnetoreception and its use in bird navigation," Curr. Opin. Neurobiol. **15**, 406–414.

Moy, Glenn, Ben Corry, Serdar Kuyucak, and Shin-Ho Chung, 2000, "Tests of continuum theories as models of ion channels. I. Poisson-Boltzmann theory versus Brownian dynamics," Biophys. J. **78**, 2349–2363.

Mozaffari, Kosar, Fatemeh Ahmadpoor, and Pradeep Sharma, 2021, "Flexoelectricity and the entropic force between fluctuating fluid membranes," arXiv:2103.07430.

Mozaffari, Kosar, Liping Liu, and Pradeep Sharma, 2022, "Theory of soft solid electrolytes: Overall properties of composite electrolytes, effect of deformation and microstructural design for enhanced ionic conductivity," J. Mech. Phys. Solids **158**, 104621.

Mozaffari, Kosar, Shengyou Yang, and Pradeep Sharma, 2020, "Surface energy and nanoscale mechanics," in *Handbook of Materials Modeling—Applications: Current and Emerging Materials*, edited by Wanda Andreoni and Sidney Yip (Springer, New York), pp. 1949–1974.

Müller, T., G. Gradl, S. Howitz, S. Shirley, T. Schnelle, and G. Fuhr, 1999, "A 3-D microelectrode system for handling and caging single cells and particles," Biosens. Bioelectron. **14**, 247–256.

Muralidharan, Aswin, Lea Rems, Michiel T. Kreutzer, and Pouyan E. Boukany, 2021, "Actin networks regulate the cell membrane permeability during electroporation," Biochim. Biophys. Acta Biomembr. **1863**, 183468.

Murray, Richard W., 1974, "The ampullae of Lorenzini," in *Electroreceptors and Other Specialized Receptors in Lower Vertebrates*, edited by A. Fessard (Springer-Verlag, Berlin), pp. 125–146.

Nadrowski, Björn, Pascal Martin, and Frank Jülicher, 2004, "Active hair-bundle motility harnesses noise to operate near an optimum of mechanosensitivity," Proc. Natl. Acad. Sci. U.S.A. **101**, 12195–12200.

Needham, D., and R. M. Hochmuth, 1989, "Electro-mechanical permeabilization of lipid vesicles. role of membrane tension and compressibility," Biophys. J. **55**, 1001–1009.

Neu, John C., and Wanda Krassowska, 1999, "Asymptotic model of electroporation," Phys. Rev. E **59**, 3471.

Neu, John C., Kyle C. Smith, and Wanda Krassowska, 2003, "Electrical energy required to form large conducting pores," Bioelectrochem. Bioenerg. **60**, 107–114.

Neugschwandtner, G. S., R. Schwödiauer, S. Bauer-Gogonea, and S. Bauer, 2000, "Large piezoelectric effects in charged, heterogeneous fluoropolymer electrets," Appl. Phys. A **70**, 1–4.

Nguyen, Thanh D., Nikhil Deshmukh, John M. Nagarah, Tal Kramer, Prashant K. Purohit, Michael J. Berry, and Michael C. McAlpine, 2012, "Piezoelectric nanoribbons for monitoring cellular deformations," Nat. Nanotechnol. **7**, 587–593.

Nguyen, Thanh D., Sheng Mao, Yao-Wen Yeh, Prashant K. Purohit, and Michael C. McAlpine, 2013, "Nanoscale flexoelectricity," Adv. Mater. **25**, 946–974.

Niggemann, G., M. Kummrow, and W. Helfrich, 1995, "The bending rigidity of phosphatidylcholine bilayers: Dependences on experimental method, sample cell sealing and temperature," J. Phys. II (France) **5**, 413–425.

Nili, Hossein, and Nicolas G. Green, 2014, "Higher-order dielectrophoresis of nonspherical particles," Phys. Rev. E **89**, 063302.

Nogueira, Juan J., and Ben Corry, 2019, "Ion channel permeation and selectivity," in *The Oxford Handbook of Neuronal Ion Channels*, edited by Arin Bhattacharjee (Oxford University Press, New York).

Nowick, Arthur S., 2005, *Crystal Properties via Group Theory* (Cambridge University Press, Cambridge, England).

O'Brien, E. Timothy, E. D. Salmon, and Harold P. Erickson, 1997, "How calcium causes microtubule depolymerization," Cell Motil. Cytoskeleton **36**, 125–135.

Ogbi, Abdellah, Laurent Nicolas, Ronan Perrussel, Sheppard J. Salon, and Damien Voyer, 2012, "Numerical identification of effective multipole moments of polarizable particles," IEEE Trans. Magn. **48**, 675–678.

Ogden, Raymond, and David Steigmann, 2011, *Mechanics and Electrodynamics of Magneto- and Electro-elastic Materials*, Vol. 527 (Springer Science+Business Media, New York).

Ó Maoiléidigh, Dáibhid, and A. J. Hudspeth, 2013, "Effects of cochlear loading on the motility of active outer hair cells," Proc. Natl. Acad. Sci. U.S.A. **110**, 5474–5479.

Ó Maoiléidigh, Dáibhid, and Frank Jülicher, 2010, "The interplay between active hair bundle motility and electromotility in the cochlea," J. Acoust. Soc. Am. **128**, 1175–1190.

O'Neill, Paul, 2013, "Magnetoreception and baroreception in birds," Dev. Growth Differ. **55**, 188–197.

Oren-Suissa, Meital, and Benjamin Podbilewicz, 2007, "Cell fusion during development," Trends Cell Biol. **17**, 537–546.

Pakhomov, Andrei G., Juergen F. Kolb, Jody A. White, Ravindra P. Joshi, Shu Xiao, and Karl H. Schoenbach, 2007, "Long-lasting plasma membrane permeabilization in mammalian cells by nanosecond pulsed electric field (NSPEF)," Bioelectromagnetics (N.Y.) **28**, 655–663.

Park, Il-Seok, Kwangmok Jung, Doyeon Kim, Sang-Mun Kim, and Kwang J. Kim, 2008, "Physical principles of ionic polymer–metal composites as electroactive actuators and sensors," MRS Bull. **33**, 190–195.

Pastushenko, V. F., and Yu. A. Chizmadzhev, 1982, "Stabilization of conducting pores in BLM by electric current," Gen. Physiol. Biophys. **1**, 43–52, http://www.gpb.sav.sk/1982/1982_01_43.pdf.

Pastushenko, V. F., Yu. A. Chizmadzhev, and V. B. Arakelyan, 1979, "Electric breakdown of bilayer lipid membranes: II. Calculation of the membrane lifetime in the steady-state diffusion approximation," J. Electroanal. Chem. Interfacial Electrochem. **104**, 53–62.

Pathak, Medha, Lisa Kurtz, Francesco Tombola, and Ehud Isacoff, 2005, "The cooperative voltage sensor motion that gates a potassium channel," J. Gen. Physiol. **125**, 57–69.

Payandeh, Jian, Todd Scheuer, Ning Zheng, and William A. Catterall, 2011, "The crystal structure of a voltage-gated sodium channel," Nature (London) **475**, 353–358.

Peng, Anthony W., and Anthony J. Ricci, 2011, "Somatic motility and hair bundle mechanics, are both necessary for cochlear amplification?," Hear. Res. **273**, 109–122.

Perilla, Juan R., Boon Chong Goh, C. Keith Cassidy, Bo Liu, Rafael C. Bernardi, Till Rudack, Hang Yu, Zhe Wu, and Klaus Schulten,

2015, "Molecular dynamics simulations of large macromolecular complexes," Curr. Opin. Struct. Biol. **31**, 64–74.

Perrier, Dayinta L., Afshin Vahid, Vaishnavi Kathavi, Lotte Stam, Lea Rems, Yuval Mulla, Aswin Muralidharan, Gijsje H. Koenderink, Michiel T. Kreutzer, and Pouyan E. Boukany, 2019, "Response of an actin network in vesicles under electric pulses," Sci. Rep. **9**, 8151.

Petelska, Aneta D., and Zbigniew A. Figaszewski, 2002, "Effect of *p*H on the interfacial tension of bilayer lipid membrane formed from phosphatidylcholine or phosphatidylserine," Biochim. Biophys. Acta Biomembr. **1561**, 135–146.

Peter, Christine, and Gerhard Hummer, 2005, "Ion transport through membrane-spanning nanopores studied by molecular dynamics simulations and continuum electrostatics calculations," Biophys. J. **89**, 2222–2234.

Peterlin, Primož, 2010, "Frequency-dependent electrodeformation of giant phospholipid vesicles in AC electric field," J. Biol. Phys. **36**, 339–354.

Pethig, R., 2010, "Review article—Dielectrophoresis: Status of the theory," Biomicrofluidics **4**, 022811.

Pethig, Ronald, Anoop Menachery, Steve Pells, and Paul De Sousa, 2010, "Dielectrophoresis: A review of applications for stem cell research," BioMed Res. Int. **2010**, 182581.

Petrov, A. G., 1975, "Flexoelectric model for active transport," in *Physical and Chemical Basis of Information Transfer*, edited by Julia G. Vassileva-Popova (Springer, New York), pp. 111–125.

Petrov, A. G., and L. Mircevova, 1986, "Is flexoelectricity the coupling factor between chemical energy and osmotic work in the pump? A model of pump," Gen. Physiol. Biophys. **5**, 391–403, https://eurekamag.com/research/005/756/005756937.php.

Petrov, A. G., and V. S. Sokolov, 1986, "Curvature-electric effect in black lipid membranes," Eur. Biophys. J. **13**, 139–155.

Petrov, Alexander G., 2002, "Flexoelectricity of model and living membranes," Biochim. Biophys. Acta Biomembr. **1561**, 1–25.

Petrov, Alexander G., 2006, "Electricity and mechanics of biomembrane systems: Flexoelectricity in living membranes," Anal. Chim. Acta **568**, 70–83.

Petrov, Alexander G., Barbara A. Miller, Kalina Hristova, and Peter N. R. Usherwood, 1993, "Flexoelectric effects in model and native membranes containing ion channels," Eur. Biophys. J. **22**, 289–300.

Phillips, Rob, Jane Kondev, Julie Theriot, and Hernan Garcia, 2012, *Physical Biology of the Cell* (Garland Science, New York).

Plonsey, Robert, and Kenneth W. Altman, 1988, "Electrical stimulation of excitable cells—A model approach," Proc. IEEE **76**, 1122–1129.

Pohl, Herbert A., 1951, "The motion and precipitation of suspensoids in divergent electric fields," J. Appl. Phys. **22**, 869–871.

Pohl, Herbert A., and Joe S. Crane, 1972, "Dielectrophoretic force," J. Theor. Biol. **37**, 1–13.

Pohl, Herbert A., and Ira Hawk, 1966, "Separation of living and dead cells by dielectrophoresis," Science **152**, 647–649.

Pohl, Herbert Ackland, 1958, "Some effects of nonuniform fields on dielectrics," J. Appl. Phys. **29**, 1182–1188.

Pohl, Herbert Ackland, 1978, *Dielectrophoresis: The Behavior of Neutral Matter in Nonuniform Electric Fields*, Cambridge Monographs on Physics (Cambridge University Press, Cambridge, England).

Prigogine, Ilya, 2017, *Non-equilibrium Statistical Mechanics* (Courier Dover Publications, Mineola, NY).

Pujar, Narahari S., and Andrew L. Zydney, 1997, "Charge regulation and electrostatic interactions for a spherical particle in a cylindrical pore," J. Colloid Interface Sci. **192**, 338–349.

Qiang, Yuhao, Jia Liu, Fan Yang, Darryl Dieujuste, and E. Du, 2018, "Modeling erythrocyte electrodeformation in response to amplitude modulated electric waveforms," Sci. Rep. **8**, 10224.

Rahmati, Amir Hossein, Siegfried Bauer, and Pradeep Sharma, 2019, "Nonlinear bending deformation of soft electrets and prospects for engineering flexoelectricity and transverse (d_{31}) piezoelectricity," Soft Matter **15**, 127–148.

Rangamani, P., and D. J. Steigmann, 2014, "Variable tilt on lipid membranes," Proc. R. Soc. A **470**, 20140463.

Raphael, Robert M., Aleksander S. Popel, and William E. Brownell, 2000, "A membrane bending model of outer hair cell electromotility," Biophys. J. **78**, 2844–2862.

Reeves, Daniel, Tristan Ursell, Pierre Sens, Jane Kondev, and Rob Phillips, 2008, "Membrane mechanics as a probe of ion-channel gating mechanisms," Phys. Rev. E **78**, 041901.

Rems, Lea, Marina A. Kasimova, Ilaria Testa, and Lucie Delemotte, 2020, "Pulsed electric fields can create pores in the voltage sensors of voltage-gated ion channels," Biophys. J. **119**, 190–205.

Rey, Alejandro D., 2006, "Liquid crystal model of membrane flexoelectricity," Phys. Rev. E **74**, 011710.

Riske, Karin A., Natalya Bezlyepkina, Reinhard Lipowsky, and Rumiana Dimova, 2006, "Electrofusion of model lipid membranes viewed with high temporal resolution," Biophys. Rev. Lett. **01**, 387–400.

Riske, Karin A., and Rumiana Dimova, 2005, "Electro-deformation and poration of giant vesicles viewed with high temporal resolution," Biophys. J. **88**, 1143–1155.

Riske, Karin A., and Rumiana Dimova, 2006, "Electric pulses induce cylindrical deformations on giant vesicles in salt solutions," Biophys. J. **91**, 1778–1786.

Ritz, T., S. Adem, and K. Schulten, 2000, "A model for photoreceptor-based magnetoreception in birds," Biophys. J. **78**, 707–718.

Ritz, T., M. Ahmad, H. Mouritsen, R. Wiltschko, and W. Wiltschko, 2010, "Photoreceptor-based magnetoreception: Optimal design of receptor molecules, cells, and neuronal processing," J. R. Soc. Interface **7**, 135–146.

Ritz, T., D. H. Dommer, and J. B. Phillips, 2002, "Shedding light on vertebrate magnetoreception," Neuron **34**, 503–506.

Ritz, T., R. Wiltschko, P. J. Hore, C. T. Rodgers, K. Stapput, P. Thalau, C. R. Timmel, and W. Wiltschko, 2009, "Magnetic compass of birds is based on a molecule with optimal directional sensitivity," Biophys. J. **96**, 3451–3457.

Riveline, Daniel, Albrecht Ott, Frank Jülicher, Donald A. Winkelmann, Olivier Cardoso, Jean-Jacques Lacapère, Soffia Magnúsdóttir, Jean-Louis Viovy, Laurence Gorre-Talini, and Jacques Prost, 1998, "Acting on actin: The electric motility assay," Eur. Biophys. J. **27**, 403–408.

Rizo, Josep, and Christian Rosenmund, 2008, "Synaptic vesicle fusion," Nat. Struct. Mol. Biol. **15**, 665.

Rodgers, C. T., and P. J. Hore, 2009, "Chemical magnetoreception in birds: The radical pair mechanism, Proc. Natl. Acad. Sci. U.S.A. **106**, 353–360.

Romeo, Stefania, Anna Sannino, Maria Rosaria Scarfì, Rita Massa, Raffaele d'Angelo, and Olga Zeni, 2016, "Lack of effects on key cellular parameters of MRC-5 human lung fibroblasts exposed to 370 mT static magnetic field," Sci. Rep. **6**, 19398.

Roohbakhshan, Farshad, Thang X. Duong, and Roger A. Sauer, 2016, "A projection method to extract biological membrane models from 3D material models," J. Mech. Behav. Biomed. Mater. **58**, 90–104.

Rosales, Carlos, and Kian Meng Lim, 2005, "Numerical comparison between Maxwell stress method and equivalent multipole approach

for calculation of the dielectrophoretic force in single-cell traps," Electrophoresis **26**, 2057–2065.

Rosazza, Christelle, Sasa Haberl Meglic, Andreas Zumbusch, Marie-Pierre Rols, and Damijan Miklavcic, 2016, "Gene electrotransfer: A mechanistic perspective," Curr. Gene Ther. **16**, 98–129.

Rosen, Arthur D., 1992, "Magnetic field influence on acetylcholine release at the neuromuscular junction," Am. J. Physiol. Cell Physiol. **262**, C1418–C1422.

Rosen, Arthur D., 1993, "A proposed mechanism for the action of strong static magnetic fields on biomembranes," Int. J. Neurosci. **73**, 115–119.

Rosen, Arthur D., 1996, "Inhibition of calcium channel activation in GH3 cells by static magnetic fields," Biochim. Biophys. Acta Biomembr. **1282**, 149–155.

Rosen, Arthur D., 2003, "Mechanism of action of moderate-intensity static magnetic fields on biological systems," Cell Biochem. Biophys. **39**, 163–173.

Rosen, Arthur D., and Jack Lubowsky, 1987, "Magnetic field influence on central nervous system function," Exp. Neurol. **95**, 679–687.

Ross, Christina L., 2017, "The use of electric, magnetic, and electromagnetic field for directed cell migration and adhesion in regenerative medicine," Biotechnol. Prog. **33**, 5–16.

Roux, Benoit, Toby Allen, Simon Berneche, and Wonpil Im, 2004, "Theoretical and computational models of biological ion channels," Q. Rev. Biophys. **37**, 15–103.

Rowat, Amy C., Per Lyngs Hansen, and John Hjort Ipsen, 2004, "Experimental evidence of the electrostatic contribution to membrane bending rigidity," Europhys. Lett. **67**, 144.

Ruzgys, Paulius, Vitalij Novickij, Jurij Novickij, and Saulius Šatkauskas, 2018, "Nanosecond range electric pulse application as a non-viral gene delivery method: Proof of concept," Sci. Rep. **8**, 15502.

Sachdev, Shaurya, Sara Feijoo Moreira, Yasmine Keehnen, Lea Rems, Michiel T. Kreutzer, and Pouyan E. Boukany, 2020, "DNA-membrane complex formation during electroporation is DNA size-dependent," Biochim. Biophys. Acta Biomembr. **1862**, 183089.

Sachs, F., W. E. Brownell, and A. G. Petrov, 2009, "Membrane electromechanics in biology, with a focus on hearing," MRS Bull. **34**, 665.

Sadik, Mohamed M., Jianbo Li, Jerry W. Shan, David I. Shreiber, and Hao Lin, 2011, "Vesicle deformation and poration under strong dc electric fields," Phys. Rev. E **83**, 066316.

Salac, David, 2016, "Vesicles in magnetic fields," arXiv:1608.05587.

Salipante, Paul F., and Petia M. Vlahovska, 2014, "Vesicle deformation in DC electric pulses," Soft Matter **10**, 3386–3393.

Sampath, Srihari C., Srinath C. Sampath, and Douglas P. Millay, 2018, "Myoblast fusion confusion: The resolution begins," Skeletal Muscle **8**, 3.

Sato, Hironobu, Hirokazu Matsumura, Satoshi Keino, and Shuichi Shoji, 2006, "An all SU-8 microfluidic chip with built-in 3D fine microstructures," J. Micromech. Microeng. **16**, 2318.

Saunders, Richard, 2005, "Static magnetic fields: Animal studies," Prog. Biophys. Mol. Biol. **87**, 225–239.

Schlick, Tamar, Rosana Collepardo-Guevara, Leif Arthur Halvorsen, Segun Jung, and Xia Xiao, 2011, "Biomolecular modeling and simulation: A field coming of age," Q. Rev. Biophys. **44**, 191–228.

Schmidt, Daniel, Qiu-Xing Jiang, and Roderick MacKinnon, 2006, "Phospholipids and the origin of cationic gating charges in voltage sensors," Nature (London) **444**, 775–779.

Schmidt, Daniel, and Roderick MacKinnon, 2008, "Voltage-dependent K^+ channel gating and voltage sensor toxin sensitivity depend on the mechanical state of the lipid membrane," Proc. Natl. Acad. Sci. U.S.A. **105**, 19276–19281.

Schneider, Hans-Jörg, 2015, *Chemoresponsive Materials: Stimulation by Chemical and Biological Signals* (Royal Society of Chemistry, London).

Schnelle, Thomas, Torsten Müller, Stefan Fiedler, and Günter Fuhr, 1999, "The influence of higher moments on particle behaviour in dielectrophoretic field cages," J. Electrost. **46**, 13–28.

Schoeman, Rogier M., Wesley T. E. Van Den Beld, Evelien W. M. Kemna, Floor Wolbers, Jan C. T. Eijkel, and Albert Van Den Berg, 2018, "Electrofusion of single cells in picoliter droplets," Sci. Rep. **8**, 3714.

Scott-Taylor, T. H., R. Pettengell, I. Clarke, G. Stuhler, M. C. La Barthe, P. Walden, and A. G. Dalgleish, 2000, "Human tumour and dendritic cell hybrids generated by electrofusion: Potential for cancer vaccines," Biochim. Biophys. Acta Mol. Basis Dis. **1500**, 265–279.

Seguin, Brian, and Eliot Fried, 2014, "Microphysical derivation of the Canham-Helfrich free-energy density," J. Math. Biol. **68**, 647–665.

Sencia, Mitsugi, Junko Takeda, Shunnosuke Abe, and Takeshi Nakamura, 1979, "Induction of cell fusion of plant protoplasts by electrical stimulation," Plant Cell Physiol. **20**, 1441–1443.

Sengel, Jason T., and Mark I. Wallace, 2016, "Imaging the dynamics of individual electropores," Proc. Natl. Acad. Sci. U.S.A. **113**, 5281–5286.

Sens, Pierre, and Hervé Isambert, 2002, "Undulation Instability of Lipid Membranes under an Electric Field," Phys. Rev. Lett. **88**, 128102.

Shahinpoor, M., 1999, "Ionic polymer-metal composites (IPMC) as biomimetic sensors and actuators," in *Field Responsive Polymers: Electroresponsive, Photoresponsive, and Responsive Polymers in Chemistry and Biology*, ACS Symposium Series Vol. 726, edited by Ishrat M. Khan and Joycelyn S. Harrison (American Chemical Society, Washington, DC), pp. 25–50.

Shamoon, D., J. Dermol-Černe, L. Rems, M Reberšek, T. Kotnik, S. Lasquellec, C. Brosseau, and D Miklavčič, 2019, "Assessing the electro-deformation and electro-poration of biological cells using a three-dimensional finite element model," Appl. Phys. Lett. **114**, 063701.

Sharma, Amarnath, and Uma S. Sharma, 1997, "Liposomes in drug delivery: Progress and limitations," Int. J. Pharm. **154**, 123–140.

Sharp, Kim A., and Barry Honig, 1990, "Electrostatic interactions in macromolecules: Theory and applications," Annu. Rev. Biophys. Biophys. Chem. **19**, 301–332.

Shcherbakov, V. P., and M. Winklhofer, 1999, "The osmotic magnetometer: A new model for a magnetite-based magnetoreceptor in animals," Eur. Biophys. J. **28**, 380–392.

Shillcock, Julian C., and Reinhard Lipowsky, 2005, "Tension-induced fusion of bilayer membranes and vesicles," Nat. Mater. **4**, 225–228.

Shillcock, Julian C., and Reinhard Lipowsky, 2006, "The computational route from bilayer membranes to vesicle fusion," J. Phys. Condens. Matter **18**, S1191.

Shklyarevskiy, Igor O., *et al.*, 2005, "Magnetic deformation of self-assembled sexithiophene spherical nanocapsules," J. Am. Chem. Soc. **127**, 1112–1113.

Shrivastava, Indira H., and Mark S. P. Sansom, 2000, "Simulations of ion permeation through a potassium channel: Molecular dynamics of KcsA in a phospholipid bilayer," Biophys. J. **78**, 557–570.

Sigworth, Fred J., 1994, "Voltage gating of ion channels," Q. Rev. Biophys. **27**, 1–40.

Singh, Pushpendra, and Nadine Aubry, 2007, "Transport and deformation of droplets in a microdevice using dielectrophoresis," Electrophoresis **28**, 644–657.

Sitkoff, Doree, Nir Ben-Tal, and Barry Honig, 1996, "Calculation of alkane to water solvation free energies using continuum solvent models," J. Phys. Chem. **100**, 2744–2752.

Skiles, D. D., 1985, *Magnetite Biomineralization and Magneto-reception in Organisms* (Springer New York), pp. 43–102.

Smaby, Janice M., Jean M. Muderhwa, and Howard L. Brockman, 1994, "Is lateral phase separation required for fatty acid to stimulate lipases in a phosphatidylcholine interface?," Biochemistry **33**, 1915–1922.

Smith, Kyle C., John C. Neu, and Wanda Krassowska, 2004, "Model of creation and evolution of stable electropores for DNA delivery," Biophys. J. **86**, 2813–2826.

Smith, Kyle Christopher, 2011, "A unified model of electroporation and molecular transport," Ph.D. thesis (Massachusetts Institute of Technology).

Solovev, Alexander A., Samuel Sanchez, Martin Pumera, Yong Feng Mei, and Oliver G. Schmidt, 2010, "Magnetic control of tubular catalytic microbots for the transport, assembly, and delivery of micro-objects," Adv. Funct. Mater. **20**, 2430–2435.

Solov'yov, I. A., T. Domratcheva, and K. Schulten, 2014, "Separation of photo-induced radical pair in cryptochrome to a functionally critical distance," Sci. Rep. **4**, 3845.

Solov'yov, I. A., and W. Greiner, 2009, "Micromagnetic insight into a magnetoreceptor in birds: Existence of magnetic field amplifiers in the beak," Phys. Rev. E **80**, 041919.

Solov'yov, I. A., P. J. Hore, T. Ritz, and K. Schulten, 2014, "A chemical compass for bird navigation," in *Quantum Effects in Biology*, edited by Masoud Mohseni, Yasser Omar, Gregory S. Engel, and Martin B. Plenio (Cambridge University Press, Cambridge, England), pp. 218–236).

Solov'yov, I. A., H. Mouritsen, and K. Schulten, 2010, "Acuity of a cryptochrome and vision based magnetoreception system in birds," Biophys. J. **99**, 40–49.

Solov'yov, Ilia A., and Walter Greiner, 2009, "Micromagnetic insight into a magnetoreceptor in birds: Existence of magnetic field amplifiers in the beak," Phys. Rev. E **80**, 041919.

Son, Reuben S., Thiruvallur R. Gowrishankar, Kyle C. Smith, and James C. Weaver, 2016, "Modeling a conventional electroporation pulse train: Decreased pore number, cumulative calcium transport and an example of electrosensitization," IEEE Trans. Biomed. Eng. **63**, 571–580.

Spector, A. A., N. Deo, K. Grosh, J. T. Ratnanather, and R. M. Raphael, 2006, "Electromechanical models of the outer hair cell composite membrane," J. Membr. Biol. **209**, 135–152.

Spiegel, Murray F., and Charles S. Watson, 1984, "Performance on frequency-discrimination tasks by musicians and nonmusicians," J. Acoust. Soc. Am. **76**, 1690–1695.

Stampfli, R., 1958, "Reversible electrical breakdown of the excitable membrane of a Ranvier node," An. Acad. Bras. Cienc. **30**, 57–61, https://eurekamag.com/research/025/402/025402612.php.

Steigmann, David, 1999, "Fluid films with curvature elasticity," Arch. Ration. Mech. Anal. **150**, 127–152.

Steigmann, David J., 2009, "A concise derivation of membrane theory from three-dimensional nonlinear elasticity," J. Elast. **97**, 97–101.

Steigmann, David J., 2013, "A well-posed finite-strain model for thin elastic sheets with bending stiffness," Math. Mech. Solids **18**, 103–112.

Steigmann, David J., 2018, "Mechanics and physics of lipid bilayers," in *The Role of Mechanics in the Study of Lipid Bilayers*, CISM International Centre for Mechanical Sciences Vol. 577, edited by David J. Steigmann (Springer, New York), pp. 1–61.

Steinchen, Annie, Dominique Gallez, and Albert Sanfeld, 1982, "A viscoelastic approach to the hydrodynamic stability of membranes," J. Colloid Interface Sci. **85**, 5–15.

Steiner, Ulrich E., and Thomas Ulrich, 1989, "Magnetic field effects in chemical kinetics and related phenomena," Chem. Rev. **89**, 51–147.

Stracke, R., K. J. Böhm, L. Wollweber, J. A. Tuszynski, and E. Unger, 2002, "Analysis of the migration behaviour of single microtubules in electric fields," Biochem. Biophys. Res. Commun. **293**, 602–609.

Stratton, Julius A., 1941, *Electromagnetic Theory* (McGraw-Hill, New York).

Stratton, Julius Adams, 2007, *Electromagnetic Theory*, Vol. 33 (John Wiley & Sons, New York).

Strömberg, Anette, Frida Ryttsén, Daniel T. Chiu, Max Davidson, Peter S. Eriksson, Clyde F. Wilson, Owe Orwar, and Richard N. Zare, 2000, "Manipulating the genetic identity and biochemical surface properties of individual cells with electric-field-induced fusion," Proc. Natl. Acad. Sci. U.S.A. **97**, 7–11.

Sukharev, S. I., V. A. Klenchin, S. M. Serov, L. V. Chernomordik, and Yu. A. Chizmadzhev, 1992, "Electroporation and electrophoretic DNA transfer into cells: The effect of DNA interaction with electropores," Biophys. J. **63**, 1320–1327.

Sukhorukov, Vladimir L., Gustav Meedt, Markus Kürschner, and Ulrich Zimmermann, 2001, "A single-shell model for biological cells extended to account for the dielectric anisotropy of the plasma membrane," J. Electrost. **50**, 191–204.

Sullivan, Stephen, and Kevin Eggan, 2006, "The potential of cell fusion for human therapy," Stem Cell Rev. **2**, 341–349.

Sun, Yinghua, P. Thomas Vernier, Matthew Behrend, Jingjing Wang, Mya Mya Thu, Martin A. Gundersen, and Laura Marcu, 2006, "Fluorescence microscopy imaging of electroperturbation in mammalian cells," J. Biomed. Opt. **11**, 024010.

Suzuki, Yui, Ken H. Nagai, Anatoly Zinchenko, and Tsutomu Hamada, 2017, "Photoinduced fusion of lipid bilayer membranes," Langmuir **33**, 2671–2676.

Tagantsev, A. K., 1986, "Piezoelectricity and flexoelectricity in crystalline dielectrics," Phys. Rev. B **34**, 5883.

Takashima, S., and H. P. Schwan, 1985, "Alignment of microscopic particles in electric fields and its biological implications," Biophys. J. **47**, 513–518.

Taupin, Christiane, Maya Dvolaitzky, and Claude Sauterey, 1975, "Osmotic pressure-induced pores in phospholipid vesicles," Biochemistry **14**, 4771–4775.

Taylor, G. I., and D. H. Michael, 1973, "On making holes in a sheet of fluid," J. Fluid Mech. **58**, 625–639.

Tekle, Ephrem, R. Dean Astumian, and P. Boon Chock, 1991, "Electroporation by using bipolar oscillating electric field: An improved method for DNA transfection of NIH 3T3 cells," Proc. Natl. Acad. Sci. U.S.A. **88**, 4230–4234.

Tenforde, Tom S., 1985, "Mechanisms for biological effects of magnetic fields," in *Biological Effects and Dosimetry of Static and ELF Electromagnetic Fields*, Ettore Majorana International Science Series: Life Sciences Vol. 19, edited by Martino Gandolfo, S. M. Michaelson, and A. Rindi (Springer, New York), pp. 71–92.

Terzi, M. Mert, and Markus Deserno, 2017, "Novel tilt-curvature coupling in lipid membranes," J. Chem. Phys. **147**, 084702.

Thomson, Kenneth, 2010, "Human experience with irreversible electroporation," in *Irreversible Electroporation*, Series in Biomedical Engineering, edited by Boris Rubinsky (Springer, New York), pp. 249–254.

Tian, L., L. Tevet-Deree, G. DeBotton, and K. Bhattacharya, 2012, "Dielectric elastomer composites," J. Mech. Phys. Solids **60**, 181–198.

Tian, Lixiu, 2008, "Effective behavior of dielectric elastomer composites," Ph.D. thesis (California Institute of Technology).

Tieleman, D. Peter, Phil C. Biggin, Graham R. Smith, and Mark S. P. Sansom, 2001, "Simulation approaches to ion channel structure-function relationships," Q. Rev. Biophys. **34**, 473.

Tinevez, Jean-Yves, Frank Jülicher, and Pascal Martin, 2007, "Unifying the various incarnations of active hair-bundle motility by the vertebrate hair cell," Biophys. J. **93**, 4053–4067.

Todorova, Nevena, Alan Bentvelzen, Niall J. English, and Irene Yarovsky, 2016, "Electromagnetic-field effects on structure and dynamics of amyloidogenic peptides," J. Chem. Phys. **144**, 085101.

Toschi, Francesca, Francesca Lugli, Fabio Biscarini, and Francesco Zerbetto, 2009, "Effects of electric field stress on a β-amyloid peptide," J. Phys. Chem. B **113**, 369–376.

Tran, Nhiem, and Thomas J. Webster, 2010, "Magnetic nanoparticles: Biomedical applications and challenges," J. Mater. Chem. **20**, 8760–8767.

Trapani, Josef G., and Stephen J. Korn, 2003, "Effect of external pH on activation of the Kv1. 5 potassium channel," Biophys. J. **84**, 195–204.

Treiber, Christoph Daniel, Marion Salzer, Martin Breuss, Lyubov Ushakova, Mattias Lauwers, Nathaniel Edelman, and David Anthony Keays, 2013, "High resolution anatomical mapping confirms the absence of a magnetic sense system in the rostral upper beak of pigeons," Commun. Int. Biol. **6**, e24859.

Treiber, Christoph Daniel, *et al.*, 2012, "Clusters of iron-rich cells in the upper beak of pigeons are macrophages not magnetosensitive neurons," Nature (London) **484**, 367–370.

Tsong, Tian Yow, 1989, "Electroporation of cell membranes," in *Electroporation and Electrofusion in Cell Biology*, edited by Eberhard Neumann, Arthur E. Sowers, and Carol A. Jordan (Springer, New York), pp. 149–163.

Tukmachev, Dmitry, Oleg Lunov, Vitalii Zablotskii, Alexandr Dejneka, Michal Babic, Eva Syková, and Šárka Kubinová, 2015, "An effective strategy of magnetic stem cell delivery for spinal cord injury therapy," Nanoscale **7**, 3954–3958.

Vacher, Helene, and James S. Trimmer, 2011, "Diverse roles for auxiliary subunits in phosphorylation-dependent regulation of mammalian brain voltage-gated potassium channels," Pfluegers Arch. **462**, 631.

Valles, Jr., James M., M. James, Kevin Lin, James M. Denegre, and Kimberly L. Mowry, 1997, "Stable magnetic field gradient levitation of Xenopus laevis: Toward low-gravity simulation," Biophys. J. **73**, 1130–1133.

Vanbever, Rita, Uwe F. Pliquett, Veronique Preat, and James C. Weaver, 1999, "Comparison of the effects of short, high-voltage and long, medium-voltage pulses on skin electrical and transport properties," J. Controlled Release **60**, 35–47.

Van den, Heuvel, G. L. Martin, Martijn P. De Graaff, and Cees Dekker, 2006, "Molecular sorting by electrical steering of microtubules in kinesin-coated channels," Science **312**, 910–914.

Vaněček, Václav, Vitalii Zablotskii, Serhiy Forostyak, Jiří Růžička, Vít Herynek, Michal Babič, Pavla Jendelová, Šárka Kubinová, Alexandr Dejneka, and Eva Syková, 2012, "Highly efficient magnetic targeting of mesenchymal stem cells in spinal cord injury," Int. J. Nanomed. **7**, 3719.

Vargas, Ernesto, Francisco Bezanilla, and Benoît Roux, 2011, "In search of a consensus model of the resting state of a voltage-sensing domain," Neuron **72**, 713–720.

Velev, Orlin D., Sumit Gangwal, and Dimiter N. Petsev, 2009, "Particle-localized AC and DC manipulation and electrokinetics," Annu. Rep. Prog. Chem., Sect. C: Phys. Chem. **105**, 213–246.

Vernier, P. Thomas, Yinghua Sun, Laura Marcu, Cheryl M. Craft, and Martin A. Gundersen, 2004, "Nanoelectropulse-induced phosphatidylserine translocation," Biophys. J. **86**, 4040–4048.

Vitkova, V., J. Cenova, O. Finogenova, M. D. Mitov, Yu. Ermakov, and I. Bivas, 2004, "Surface charge effect on the bending elasticity of lipid bilayers," C.R. Acad. Bulg. Sci. **57**, 11–25, https://adsabs.harvard.edu/full/2004CRABS..57k..25V.

Vlahovska, Petia M., Ruben Serral Gracia, Said Aranda-Espinoza, and Rumiana Dimova, 2009, "Electrohydrodynamic model of vesicle deformation in alternating electric fields," Biophys. J. **96**, 4789–4803.

Voldman, Joel, Rebecca A. Braff, Mehmet Toner, Martha L. Gray, and Martin A. Schmidt, 2001, "Holding forces of single-particle dielectrophoretic traps," Biophys. J. **80**, 531–542.

Walker, Michael M., Carol E. Diebel, Cordula V. Haugh, Patricia M. Pankhurst, John C. Montgomery, and Colin R. Green, 1997b, "Structure and function of the vertebrate magnetic sense," Nature (London) **390**, 371–376.

Wang, Connie X., Isaac A. Hilburn, Daw-An Wu, Yuki Mizuhara, Christopher P Cousté, Jacob N. H. Abrahams, Sam E. Bernstein, Ayumu Matani, Shinsuke Shimojo, and Joseph L. Kirschvink, 2019, "Transduction of the geomagnetic field as evidenced from alpha-band activity in the human brain," eNeuro **6**, PMC6494972.

Wang, K., E. Mattern, and T. Ritz, 2006, "On the use of magnets to disrupt the physiological compass of birds," Phys. Biol. **3**, 220–231.

Wang, X.-B., Y. Huang, F. F. Becker, and P. R. C. Gascoyne, 1994, "A unified theory of dielectrophoresis and travelling wave dielectrophoresis," J. Phys. D **27**, 1571.

Wang, Xujing, Xiao-Bo Wang, and Peter R. C. Gascoyne, 1997, "General expressions for dielectrophoretic force and electrorotational torque derived using the Maxwell stress tensor method," J. Electrost. **39**, 277–295.

Weaver, James C., and Yu. A. Chizmadzhev, 1996, "Theory of electroporation: A review," Bioelectrochem. Bioenerg. **41**, 135–160.

Weaver, James C., and Robert A. Mintzer, 1981, "Decreased bilayer stability due to transmembrane potentials," Phys. Lett. **86A**, 57–59.

Wei, Guo-Wei, 2010, "Differential geometry based multiscale models," Bull. Math. Biol. **72**, 1562–1622.

Wei, Ming-Tzo, Joseph Junio, and H. Daniel Ou-Yang, 2009, "Direct measurements of the frequency-dependent dielectrophoresis force," Biomicrofluidics **3**, 012003.

Weng, Ping-You, I-An Chen, Che-Kai Yeh, Pin-Yi Chen, and Jia-Yang Juang, 2016, "Size-dependent dielectrophoretic crossover frequency of spherical particles," Biomicrofluidics **10**, 011909.

Wertheimer, Nancy, and E. D. Leeper, 1979, "Electrical wiring configurations and childhood cancer," Am. J. Epidemiol. **109**, 273–284.

Wiltschko, R., and W. Wiltschko, 1995, *Magnetic Orientation in Animals* (Springer-Verlag, Berlin).

Wiltschko, Roswitha, 2012, *Magnetic Orientation in Animals*, Vol. 33 (Springer Science+Business Media, New York).

Wiltschko, Roswitha, and Wolfgang Wiltschko, 2003, "Avian navigation: From historical to modern concepts," Anim. Behav. **65**, 257–272.

Wiltschko, Wolfgang, and Roswitha Wiltschko, 1972, "Magnetic compass of European robins," Science **176**, 62–64.

Wiltschko, Wolfgang, and Roswitha Wiltschko, 2005, "Magnetic orientation and magnetoreception in birds and other animals," J. Comp. Physiol. A **191**, 675–693.

Winklhofer, M., and J. L. Kirschvink, 2010, "A quantitative assessment of torque-transducer models for magnetoreception," J. R. Soc. Interface **7**, 273–289.

Winklhofer, Michael, Elke Holtkamp-Rötzler, Marianne Hanzlik, Gerta Fleissner, and Nikolai Petersen, 2001, "Clusters of superparamagnetic magnetite particles in the upper-beak skin of homing pigeons: Evidence of a magnetoreceptor?," Eur. J. Mineral. **13**, 659–669.

Winterhalter, M., and W. Helfrich, 1988a, "Deformation of spherical vesicles by electric fields," J. Colloid Interface Sci. **122**, 583–586.

Winterhalter, M., and Wolfgang Helfrich, 1988b, "Effect of surface charge on the curvature elasticity of membranes," J. Phys. Chem. **92**, 6865–6867.

Wong, Tai-Kin, and Eberhard Neumann, 1982, "Electric field mediated gene transfer," Biochem. Biophys. Res. Commun. **107**, 584–587.

Wu, Le-Qing, and J. David Dickman, 2012, "Neural correlates of a magnetic sense," Science **336**, 1054–1057.

Xia, Nan, Tom P. Hunt, Brian T. Mayers, Eben Alsberg, George M. Whitesides, Robert M. Westervelt, and Donald E. Ingber, 2006, "Combined microfluidic-micromagnetic separation of living cells in continuous flow," Biomed. Microdevices **8**, 299.

Xie, Xi, Alexander M. Xu, Sergio Leal-Ortiz, Yuhong Cao, Craig C. Garner, and Nicholas A. Melosh, 2013, "Nanostraw-electroporation system for highly efficient intracellular delivery and transfection," ACS Nano **7**, 4351–4358.

Yamamoto, Tetsuya, Said Aranda-Espinoza, Rumiana Dimova, and Reinhard Lipowsky, 2010, "Stability of spherical vesicles in electric fields," Langmuir **26**, 12390–12407.

Yang, C. Y., and U. Lei, 2007, "Dielectrophoretic force and torque on an ellipsoid in an arbitrary time varying electric field," Appl. Phys. Lett. **90**, 153901.

Yang, Liju, 2012, "A review of multifunctions of dielectrophoresis in biosensors and biochips for bacteria detection," Anal. Lett. **45**, 187–201.

Yang, Lun, and Kaushik Dayal, 2011, "A completely iterative method for the infinite domain electrostatic problem with nonlinear dielectric media," J. Comput. Phys. **230**, 7821–7829.

Yang, Peng, Reinhard Lipowsky, and Rumiana Dimova, 2009, "Nanoparticle formation in giant vesicles: Synthesis in biomimetic compartments," Small **5**, 2033–2037.

Ye, Hui, and Austen Curcuru, 2015, "Vesicle biomechanics in a time-varying magnetic field," BMC Biophys. **8**, 2.

Ye, Ting, Hua Li, and Khin Yong Lam, 2011, "Motion, deformation and aggregation of two cells in a microchannel by dielectrophoresis," Electrophoresis **32**, 3147–3156.

Yellen, Gary, 2002, "The voltage-gated potassium channels and their relatives," Nature (London) **419**, 35–42.

Yellin, Florence, Yizeng Li, Varun K. A. Sreenivasan, Brenda Farrell, Manu B. Johny, David Yue, and Sean X. Sun, 2018, "Electromechanics and volume dynamics in nonexcitable tissue cells," Biophys. J. **114**, 2231–2242.

Zablotskii, V., O. Lunov, S. Kubinova, T. Polyakova, E. Sykova, and A. Dejneka, 2016, "Effects of high-gradient magnetic fields on living cell machinery," J. Phys. D **49**, 493003.

Zablotskii, Vitalii, Alexandr Dejneka, Šárka Kubinová, Damien Le-Roy, Frédéric Dumas-Bouchiat, Dominique Givord, Nora M. Dempsey, and Eva Syková, 2013, "Life on magnets: Stem cell networking on micro-magnet arrays," PLoS One **8**, e70416.

Zablotskii, Vitalii, Tatyana Polyakova, and Alexandr Dejneka, 2018, "Cells in the non-uniform magnetic world: How cells respond to high-gradient magnetic fields," BioEssays **40**, 1800017.

Zagnoni, Michele, and Jonathan M. Cooper, 2009, "On-chip electro-coalescence of microdroplets as a function of voltage, frequency and droplet size," Lab Chip **9**, 2652–2658.

Ze, Qiji, Xiao Kuang, Shuai Wu, Janet Wong, S. Macrae Montgomery, Rundong Zhang, Joshua M. Kovitz, Fengyuan Yang, H. Jerry Qi, and Ruike Zhao, 2020, "Magnetic shape memory polymers with integrated multifunctional shape manipulation," Adv. Mater. **32**, 1906657.

Zhadin, Mikhail N., 2001, "Review of Russian literature on biological action of DC and low-frequency AC magnetic fields," Bioelectromagnetics (N.Y.) **22**, 27–45.

Zhang, Junyan, Zhenyu Song, Qinxin Liu, and Yongxin Song, 2020, "Recent advances in dielectrophoresis-based cell viability assessment," Electrophoresis **41**, 917–932.

Zhang, Ping-Cheng, Asbed M. Keleshian, and Frederick Sachs, 2001, "Voltage-induced membrane movement," Nature (London) **413**, 428–432.

Zhang, Xin, Kevin Yarema, and An Xu, 2017, *Biological Effects of Static Magnetic Fields* (Springer, New York).

Zhao, Ruike, Yoonho Kim, Shawn A. Chester, Pradeep Sharma, and Xuanhe Zhao, 2019, "Mechanics of hard-magnetic soft materials," J. Mech. Phys. Solids **124**, 244–263.

Zhao, Wei, and Ruijin Yang, 2010, "Experimental study on conformational changes of lysozyme in solution induced by pulsed electric field and thermal stresses," J. Phys. Chem. B **114**, 503–510.

Zhao, Xuanhe, and Zhigang Suo, 2008, "Electrostriction in elastic dielectrics undergoing large deformation," J. Appl. Phys. **104**, 123530.

Zheng, Jie, and Matthew C. Trudeau, 2015, *Handbook of Ion Channels* (CRC Press, Boca Raton).

Zhou, Qiangjun, Peng Zhou, Austin L. Wang, Dick Wu, Minglei Zhao, Thomas C. Südhof, and Axel T. Brunger, 2017, "The primed SNARE-complexin-synaptotagmin complex for neuronal exocytosis," Nature (London) **548**, 420–425.

Zhou, Yong, and Robert M. Raphael, 2007, "Solution *p*H alters mechanical and electrical properties of phosphatidylcholine membranes: Relation between interfacial electrostatics, intramembrane potential, and bending elasticity," Biophys. J. **92**, 2451–2462.

Zimmerberg, Joshua, and Michael M. Kozlov, 2006, "How proteins produce cellular membrane curvature," Nat. Rev. Mol. Cell Biol. **7**, 9–19.

Zimmermann, U., 1982, "Electric field-mediated fusion and related electrical phenomena," Biochim. Biophys. Acta Rev. Biomembr. **694**, 227–277.

Zimmermann, U., G. Pilwat, and F. Riemann, 1974, "Dielectric breakdown of cell membranes," Biophys. J. **14**, 881–899.

Zimmermann, U., and P. Scheurich, 1981, "High frequency fusion of plant protoplasts by electric fields," Planta **151**, 26–32.

Zimmermann, U., J. Vienken, and G. Pilwat, 1980, "Development of drug carrier systems: Electrical field induced effects in cell membranes," J. Electroanal. Chem. Interfacial Electrochem. **116**, 553–574.

Zubko, Pavlo, Gustau Catalan, and Alexander K. Tagantsev, 2013, "Flexoelectric effect in solids," Annu. Rev. Mater. Res. **43**, 387–421.